Environmental risk factors in etiologically complex birth defects

By

Tyler G. Beames

A dissertation submitted in partial fulfillment of the requirements for the degree of

Doctor of Philosophy

(Molecular and Environmental Toxicology)

at the

UNIVERSITY OF WISCONSIN-MADISON

2025

Date of final oral examination: 06/25/2025

The dissertation is approved by the following members of the Final Oral Committee:

Robert J. Lipinski, Professor, Comparative Biosciences

Kristen C. Malecki, Professor, Environmental and Occupational Health Sciences

Michael E. Cahill, Assistant Professor, Comparative Biosciences

Chad M. Vezina, Professor, Comparative Biosciences

ACKNOWLEDGMENTS

This work is not only the culmination of my research efforts as a PhD candidate at the University of Wisconsin-Madison; it is also a testament to the unwavering support I have received from family, friends, colleagues, and mentors, year after year, which has been the foundation for all of my successes, and the impetus for every second, third, fourth, fifth, and hundredth attempt. I am eternally grateful, just not good at showing it.

I thank my parents, Burt and Liz, for getting me here, and for a great deal of advice that I probably should have taken. I appreciate how easy it has been to talk with both of you about my research and my experience as a graduate student, given that you have been through it all yourselves. I thank my brother, Arthur, and my sister-in-law, Erika, for living in Minneapolis, just a stone's throw away, and hosting many family gatherings. The camping trips have also been great for disconnecting and resetting.

I thank the MET program for the opportunity and for bringing together a wonderful group of people who are all very passionate about knowing what's bad for you. As for my cohort—Brenna Walton (and Kayla by extension), Brandon Scharpf, Robbie Manuel, Cyndi Kennedy, and Thomas Peterson—I appreciated the commiserating, but the celebrations were always better. Of course, I thank Mark Marohl for regularly checking in at the height of the pandemic and for continuing to show support for the program by attending just about every defense. I also thank Lindsey Felth Tanaka for being three steps ahead of me—a post-doc with a one-year-old and a house—and for letting me pick your brain about each of those steps.

Jumping back in time, I thank Rebecca Clewell for giving me the opportunity to work in a lab when the only credential I had was a passing grade in Biology 101. I also appreciate the two additional opportunities you gave me to do better work in subsequent years. Also from my Hamner/ScitoVation days, I thank Susan Ross for introducing me to cell culture, Bethany Parks for doing the same with flow cytometry, and Scott Slattery for a great deal of imaging-based guidance (and for always covering the worst timepoint).

I thank Jessica Hartman, especially, for three years of formal mentorship followed by five years (and counting) of informal mentorship. I owe all of my good laboratory habits to you. You not only saw my potential, but helped me realize it. I appreciate your friendship (and your TV recommendations).

I thank my fellow Lipinski Lab members, past and present, for countless interesting conversations, many science-related, many not. In particular, I thank Miranda Sun and Kenneth Rivera González for making me feel welcome and included as the "new kid." I also appreciate having had the opportunity to work with Austin Steward, Matt McLaughlin, Rachel Walkup, Sunil Singh, Megan Stewart, Matthew Nangle, Chris Jabbarpour, and Jacob Kracke-Bock.

I thank Rob for being both an engaging and an engaged advisor, as well as for teaching me how to tell stories through my science. I have improved as a researcher and as a communicator during my time in your lab. I also thank my committee members, Kristen Malecki, Chad Vezina, and Mike Cahill, for their thoughtful contributions to the refinement of my thesis.

Most of all, I thank my wife, Maitlyn, for sticking with me even though you told me not to fall in love with Madison when I came for my interviews. Since I accepted my offer here,

we have traded the humid summers of NC for the frigid winters of WI; we got engaged, we got married, and we had a kid. It isn't possible to adequately thank you for all you have done to make my life better and more meaningful. But I'll keep trying.

Last, but certainly not least, I thank Sean. You made getting to the finish line harder but infinitely more rewarding.

ABSTRACT

Birth defects are among the leading causes of infant mortality, and reducing exposure to environmental hazards is a direct path to disease prevention. The identification of specific environmental hazards, however, is complicated by the multifactorial nature of many non-syndromic birth defects. The objective of this body of work is to investigate environmental risk in birth defect etiology, specifically addressing gene-environment interactions, chemical interactions, and low-dose effects. Investigations were focused through the Sonic hedgehog (Shh) pathway, a key regulator of embryonic development that is sensitive to both genetic and chemical perturbation and is associated with common and etiologically complex birth defects. First, we provide an overview of gene-environment interactions in abnormal development, utilizing Shh-associated malformations as key examples. We then present a novel, cell-based assay of Shh pathway signal transduction that was employed to investigate chemical interactions across this complex signaling cascade. We observed both additive and synergistic disruption of Shh signaling activity following co-exposure to compounds reported to act throughout the Shh pathway. We then leveraged high-throughput screening datasets and our Shh pathway signal transduction assay to prioritize purported Shh pathway inhibitors for in-house characterization. Pathway inhibition was confirmed for a subset of the 44 compounds tested, and additional animal tests were proposed based on potency and efficacy of hits. Finally, we evaluated the impacts of low-dose Shh pathway inhibition during craniofacial morphogenesis on neurodevelopment. No changes in early forebrain patterning or adult behavior were observed in the absence of overt malformations. Taken together, these findings underscore the challenges of characterizing environmental risk in human-relevant contexts and present approaches for overcoming these challenges.

TABLE OF CONTENTS

ABBREVIATIONS

3D, three-dimensional

AC_{50}, half-maximal activity

ATO, arsenic trioxide

BaP, benzo[a]pyrene

CAL2, Constitutively Active Shh-LIGHT2

CBD, cannabidiol

CS, conditioned stimulus

EGCG, epigallocatechin gallate

EPA, Environmental Protection Agency

DMEM, Dulbecco's Modified Eagle Medium

EtOH, ethanol

FASD, fetal alcohol spectrum disorder

FBS, fetal bovine serum

GD, gestational day

GxE, gene-environment

H&E, hematoxylin and eosin

HHAT, Hedgehog acyltransferase

HPE, holoprosencephaly

Hpf, hours post-fertilization

iMEF, immortalized mouse embryonic fibroblast

ISH, in situ hybridization

IOD, interocular distance

LOEL, lowest observed effect level

MGE, medial ganglionic eminence

MPM, microphysiological model

NDD, neurodevelopmental disorder

OFC, orofacial cleft

PBO, piperonyl butoxide

qPCR, quantitative polymerase chain reaction

RLU, relative luminescent unit

Shh, Sonic hedgehog

SMO, smoothened

ULL, upper lip length

US, unconditioned stimulus

USDA, United States Department of Agriculture

INTRODUCTION

Birth defects are a major public health problem that has remained remarkably stable in recent decades (Stallings et al., 2024). Affecting 1 in 33 newborns in the United States and approximately 8 million infants globally each year (Christianson et al., 2006), birth defects are a leading cause of infant mortality and can confer lifelong physical, social, and financial burdens for affected individuals. Efforts to prevent birth defects have produced mixed results, and specific causes cannot be ascertained in up to 80% of non-syndromic birth defect cases (Feldkamp et al., 2017; Toufaily et al., 2018). Despite these challenges, mitigation of environmental risk remains the most direct and practicable approach to prevention.

Embryonic development is a highly dynamic and exquisitely coordinated process during which the foundations for all tissues and structures of the body are laid. Environmental exposures and genetic variants have been shown to cause structural and functional abnormalities by altering these early foundations. In a small proportion of cases, congenital anomalies are caused by exposure to a single chemical, formally called a teratogen, as seen with ethanol and fetal alcohol syndrome (Jones & Smith, 1975), thalidomide and phocomelia (Vargesson, 2015), and valproic acid and fetal valproate syndrome (Ornoy, 2009). More often, however, the multifactorial nature of non-syndromic birth defects complicates the identification of hazards that are not individually causative of the disease. Complex, multifactorial etiologies have been implicated in the development of craniofacial malformations, congenital heart defects, neural tube defects, hypospadias, and neurodevelopmental disorders (Chapman et al., 2019; De Felice et al.,

2015; Everson et al., 2020; Everson et al., 2019; Finnell et al., 2021; Heyne et al., 2016; Kietzman et al., 2014; Moreau et al., 2019; van der Zanden et al., 2012).

Understanding the processes that underlie normal embryonic development is critical for unravelling the etiological mystery at the core of many congenital anomalies. The Sonic hedgehog (Shh) signaling pathway, for instance, is an important regulator of craniofacial morphogenesis. Under typical conditions, craniofacial development proceeds with SHH ligand being secreted from the ectoderm of facial growth centers and interacting with adjacent cranial neural crest-derived mesenchymal cells (Kurosaka, 2015). As a paracrine factor, secreted SHH ligand forms a concentration gradient within the mesenchyme that imparts a corresponding gradient of signaling activity that decreases with increasing distance from sites of SHH production (Hu et al., 2015; Johnson et al., 2021; Kurosaka, 2015; Lan & Jiang, 2009). Activation of the Shh signaling pathway in the craniofacial mesenchyme alters the transcriptional profile of these cells, promoting cellular proliferation and growth of tissues that will form the lip and palate (Everson et al., 2017).

Studies in animal models illustrate the developmental consequences of abnormal Shh signaling. In genetic models, the complete loss of Shh signaling through knockout of the *Shh* gene results in lethal malformations of the face and forebrain. Specifically, *Shh*$^{-/-}$ mice display severe midfacial hypoplasia, resulting in a reduction in the size of the forebrain and midbrain, failure of the optic vesicle to separate and develop into laterally positioned eyes, and failure of the nasal pits to separate to form paired nostrils (Chiang et al., 1996). Notably, this constellation of abnormal traits is present in humans born with holoprosencephaly (HPE), a disorder that was first linked to functionally defective variants in the *SHH* gene in humans (Roessler et al., 1996). Small molecule inhibitors of

Shh signaling have been used to probe the impact of timing on Shh signaling-mediated craniofacial dysmorphogenesis. A study employing the pharmacological Shh pathway inhibitor vismodegib produced HPE-like phenotypes and orofacial clefts (OFCs) in mice in a timing-dependent manner (Heyne, Melberg, et al., 2015), and a naturally occurring plant alkaloid and Shh signaling antagonist, cyclopamine, has been utilized in a robust mouse model of cleft lip and palate (Heyne, Melberg, et al., 2015; Lipinski et al., 2008). Bridging the loss of Shh signaling at the molecular level and deficient growth at the tissue level, cyclopamine administration was demonstrated to decrease cellular proliferation within the cranial neural crest-derived mesenchyme of the facial process that give rise to the upper lip (Everson et al., 2017).

In human populations, both HPE and OFCs exemplify etiological complexity. Over 20 genes have been found to cause HPE, including several factors within the Shh signaling pathway (Tekendo-Ngongang et al., 2020). Most HPE genes are considered to act in an autosomal dominant fashion, though a great deal of phenotypic variation exists even among individuals with similar genetic variants (Solomon et al., 2012). This variability is indicative of a multifactorial etiology in which genetic or environmental risk factors modulate the severity of a disorder that is driven primarily through a known genetic predisposition. However, despite the identification of dozens of HPE genes, only a quarter of all cases are associated with the most common established genetic variants, underscoring the etiological complexity of this disorder (Roessler et al., 2018; Tekendo-Ngongang et al., 2020). In contrast to HPE, extensive investigations into the genetics of OFCs have not revealed causative variants. Instead, dozens of genetic risk factors have been associated with OFCs (Leslie & Marazita, 2013), and these factors are believed to act

in concert with other genetic and environmental influences to disrupt development of the upper lip and palate. Recent years have seen a shift toward elucidating gene-environment interactions in the etiology of HPE and OFCs (Addissie et al., 2021; Everson et al., 2019; Hong & Krauss, 2018; Marazita, 2023). Hypothesis-driven investigations of chemical-chemical interactions in animal models of Shh-mediated craniofacial morphogenesis remain sparse, but work several works in zebrafish have been now been published (Everson et al., 2020; Everson et al., 2023).

An additional challenge to the identification and characterization of environmental risk factors is the potential for low-dose effects. Consideration of adverse outcomes that do not present as overt malformations is especially important for compounds that target craniofacial development. Fetal alcohol spectrum disorder (FASD) illustrates this point. After researchers linked prenatal alcohol exposure to a constellation of craniofacial and limb malformations and neurobehavioral deficits, these atypical traits became the primary diagnostic criteria in fetal alcohol syndrome (Jones & Smith, 1975; Jones et al., 1973). FASD, on the other hand, encompasses individuals with prenatal alcohol exposure who may not display diagnostic features but nonetheless suffer from neurodevelopmental effects (Coles et al., 2020; Hoyme et al., 2016). Based on overlap in the craniofacial phenotypes resulting from prenatal alcohol exposure and Shh pathway disruption, there is the potential for Shh signaling antagonists to similarly alter neurodevelopment without causing overt malformations. Addressing this possibility may reveal pernicious neurobehavioral effects that could be influenced by exposure to environmental Shh pathway antagonists and would be relevant for the diagnosis of Shh signaling-related disorders.

Although mounting evidence points to environmental risk factors as contributors to etiologically complex birth defects, significant knowledge gaps remain regarding the identity of human-relevant environmental risk factors as well as their interactions with additional risk factors and low-dose effects. The purpose of this body of work is to characterize environmental risk in the context of etiologically complex birth defects. Focusing our studies through the lens of the Shh signaling pathway, we present an overview of gene-environment interactions in birth defect etiology, examine chemical interactions among small molecules acting throughout this signaling cascade, prioritize human-relevant environmental Shh pathway inhibitors for characterization in animal models, and investigate the impacts of low-dose prenatal Shh signaling disruption on neurodevelopment in mice. We also provide recommendations for additional studies to continue to address the knowledge gaps we have identified. Not only do the studies described herein advance our understanding of how chemicals can disrupt Shh signaling and impact development, but they provide blueprint for carrying out similar experiments for other developmentally important signaling pathways.

CHAPTER I

This manuscript was published in Development (2020 Jul 17;147(21):dev191064. doi: 10.1242/dev.191064). TGB and RJL wrote the manuscript.

CHAPTER I: GENE-ENVIRONMENT INTERACTIONS: ALIGNING BIRTH DEFECTS RESEARCH WITH COMPLEX ETIOLOGY

Tyler G. Beames[1,2], Robert J. Lipinski[1,2,*]

[1]Department of Comparative Biosciences, School of Veterinary Medicine, University of Wisconsin-Madison, Madison, WI 53706, USA

[2]Molecular and Environmental Toxicology Center, School of Medicine and Public Health, University of Wisconsin-Madison, Madison, WI 53706, USA

[*]Author for correspondence (robert.lipinski@wisc.edu)

ABSTRACT

Developmental biologists rely on genetics-based approaches to understand the origins of congenital abnormalities. Recent advancements in genomics have made it easier than ever to investigate the relationship between genes and disease. However, nonsyndromic birth defects often exhibit non-Mendelian inheritance, incomplete penetrance or variable expressivity. The discordance between genotype and phenotype indicates that extrinsic factors frequently impact the severity of genetic disorders and vice versa. Overlooking gene-environment interactions in birth defect etiology limits our ability to identify and eliminate avoidable risks. We present mouse models of sonic hedgehog signaling and craniofacial malformations to illustrate both the importance of and current challenges in resolving gene-environment interactions in birth defects. We then prescribe approaches for overcoming these challenges, including use of genetically tractable and environmentally responsive *in vitro* systems. Combining emerging technologies with molecular genetics and traditional animal models promises to advance our understanding of birth defect etiology and improve the identification and protection of vulnerable populations.

INTRODUCTION

A multifactorial model of birth defect etiology can be traced back to F. Clarke Fraser's research in the 1950s. At the time, the recent discovery that the uterus was not impervious to the environment led many developmental biologists to pursue the emerging study of mammalian teratogens and teratology at the expense of genetics. Fraser, a geneticist by training, retrospectively described it as a period during which 'the pendulum of opinion was swinging away from the idea that malformations are genetic in origin…to the other extreme – that malformations are mostly caused by environmental factors' (Fraser, 2008). Following this change in momentum, birth defects research diverged. Josef Warkany advanced the nascent field of teratology, while medical genetics found a foothold and flourished under the leadership of Victor McKusick. Fraser, convinced of the importance of both genetic and environmental influences, instead sought to integrate these two approaches for explaining abnormal development.

Having been provided cortisone to investigate its potential to disrupt neural tube development in mice, Fraser unexpectedly discovered that maternal treatment induced cleft palate in the pups (Fraser, 2008). On a hunch, Fraser administered cortisone to each of the mouse strains available to him. Cleft palate was inducible across five strains, but Fraser noted that incidence was strain, and therefore genotype, dependent (Fraser & Fainstat, 1951). This early experiment in teratogenetics, Fraser's term for the study of gene-environment interaction in developmental disorders, illustrated the importance of combinatory insults and risk interactions. Even so, medical genetics and teratology largely progressed independently, each field working on the same puzzle with a different set of pieces.

Although it is true that traditional epidemiological and genetic approaches have resolved the causes of birth defects that are strongly genetic or environmental in nature, it is now widely recognized that complex interactions between genetic and environmental influences shape the nature and severity of most birth defects. In spite of this recognition, it is our opinion that the advent of modern genomics in recent decades has led to another sea change, one in which a genetics-forward approach dominates the study of abnormal development. We believe, as Fraser did, that there is more to the story.

Gene-environment interactions (also abbreviated to GxE) occur when genetic and environmental influences additively or synergistically contribute to a phenotypic effect. Environment, in this context, may broadly refer to any influence that is not genetic in nature, including toxin and toxicant exposure, maternal infection, hypoxia, and macromolecule or micronutrient excesses or deficiencies. A widely recognized example of a gene-environment interaction is phenylketonuria, an autosomal recessive disease caused by mutation in phenylalanine hydroxylase, which is exacerbated as phenylalanine intake exceeds an affected individual's ability to metabolize it. In practice, individuals lacking a functional copy of phenylalanine hydroxylase exhibit phenotypes including intellectual disability, seizures and behavioral problems, the severity of which correlates with phenylalanine intake, whereas a single intact allele is considered protective against phenylketonuria. Although illustrative, this simple type of gene-environment interaction – a homozygous genetic aberration acting in concert with an otherwise innocuous environmental influence – is not universally representative of the phenomenon. Rather, interactions can take several forms (described by Khoury et al., 1988) in which environmental or genetic influences drive a phenotype that is modified by additional

factors. In fetal alcohol spectrum disorder, for instance, prenatal alcohol (ethanol) exposure is sufficient to disrupt development of the brain and face, although certain gene variants appear to exacerbate these outcomes (reviewed by Lovely et al., 2017). Thus, the impact of the primary insult, maternal alcohol exposure, is modified by genotype. Importantly, the phenotypic variability seen in fetal alcohol spectrum disorders highlights the continuous nature of many multifactorial diseases, including some of the most common human structural birth defects.

CRANIOFACIAL BIRTH DEFECTS: A FACE OF GENE-ENVIRONMENT OUTCOMES

Craniofacial birth defects, such as those seen in fetal alcohol spectrum disorders, illustrate both the challenges and opportunities of studying gene-environment interactions. The head and face develop through precisely coordinated expansion and fusion of embryonic growth centers comprising multiple migrating and differentiating cell populations. Consequently, congenital craniofacial abnormalities are relatively common, and the functional and societal importance of the face makes these malformations particularly impactful for patients and their families.

Orofacial clefts (OFCs) of the lip and palate are the most prevalent human craniofacial birth defects and affect approximately 1 in 700 newborns (Leslie & Marazita, 2013). Most OFCs occur in apparent isolation of other malformations and are considered nonsyndromic. The vast majority of these cases do not follow Mendelian inheritance patterns, although genetics undeniably plays a substantial role in modifying risk. For example, OFC incidence varies by background and demonstrates at least some familial heritability (Watkins et al., 2014). Accordingly, OFCs have long been thought to arise from

gene-environment interactions (reviewed by Dixon et al., 2011; Krauss & Hong, 2016; Lovely et al., 2017), although efforts to understand this complex etiology have largely focused on the genetic side of the equation. Dozens of OFC risk loci have been identified by employing complementary genetic approaches, including genome-wide association studies (reviewed by Beaty et al., 2016; Leslie & Marazita, 2013; see also OMIM 119530). Similarly, despite frequent postulation of environmental contributions to clefting, no exogenous factor is known to exhibit strong penetrance, and commonly implicated factors either only slightly increase risk (e.g. maternal exposure to cigarette smoke) (Hackshaw et al., 2011) or have shown mixed results in epidemiological studies (e.g. maternal alcohol exposure) (Bell et al., 2014). In most cases, the functional consequence of identified genetic variants and environmental influences, and how these factors may interact to produce OFCs, remains unknown.

In considering gene-environment interactions in craniofacial malformations, a useful counterpart to OFCs is the related malformation holoprosencephaly (HPE). Defined by deficient development of the median forebrain, HPE frequently co-occurs with facial abnormalities including OFCs. At its most severe, HPE results in cyclopia, characterized by a single central eye. Although relatively rare in newborns, HPE has an estimated prevalence of 1 in 250 conceptuses (Petryk et al., 2015), suggesting that it is among the most common human embryonic malformations. Furthermore, although chromosomal abnormalities account for approximately 1 in 3 HPE cases (Petryk et al., 2015), the remaining cases are considered etiologically heterogeneous with genetics playing an important, but apparently incomplete, role. For example, of the 17 (and counting) genes associated with HPE, mutations in the four most common are detected in only 25% of

cases (Roessler et al., 2018; Tekendo-Ngongang et al., 2020). Even in this subset of gene-associated cases, causative mutations are almost exclusively heterozygous and considered to act as autosomal dominant but with incomplete penetrance and highly variable expressivity. Increasingly, rare gene variants associated with HPE are being identified (Hughes et al., 2020; Kruszka, Berger, Casa, et al., 2019; Kruszka, Berger, Weiss, et al., 2019), which may contribute to the phenotypic variability of this condition and increase the number of potential gene-gene interactions, although documented instances of 'multiple-hit' mutation events are exceedingly rare in HPE (Roessler et al., 2018). As with OFCs, gene-environment interactions are considered central to HPE etiology, with the identification of specific interactions remaining limited and prevention strategies largely unavailable. However, findings spanning decades of research across multiple fields have coalesced to support a model of gene-environment interactions in HPE etiology.

SONIC HEDGEHOG SIGNALING AND HOLOPROSENCEPHALY: A LENS TO VIEW GENE AND ENVIRONMENT

Just 4 years after the historic elucidation of DNA's double helix, ranchers in the western United States observed sheep born with craniofacial malformations including cyclopia, the hallmark phenotype of severe HPE, and alerted the United States Department of Agriculture (USDA). In a now science-famous story, USDA researchers traced these birth defects to maternal grazing on the plant *Veratrum californicum* and a teratogenic alkaloid that they dubbed cyclopamine (Chen, 2016; Keeler, 1978). Without the tools to probe the mechanism of cyclopamine-mediated birth defects, this curiosity of teratology faded into the background. Meanwhile, the modern genetics era dawned. Nobel prize-winning fruit fly studies identified genes now known to be central mediators of

development and disease, including one named hedgehog. Within two decades, a knockout mouse for sonic hedgehog (*Shh*), a mammalian *hedgehog* homolog, was generated and found to have severe craniofacial malformations, including cyclopia (Chiang et al., 1996). Astute developmental biologists reconsidered those one-eyed sheep and subsequently demonstrated in chicks, mice and mammalian cells that cyclopamine-induced birth defects result from the inhibition of the Shh signaling pathway component smoothened during embryonic development (Chen et al., 2002; Incardona et al., 1998; Lipinski et al., 2008). Remarkably – though not entirely serendipitously – human genetic studies published around that time revealed the first gene associated with HPE: sonic hedgehog (Roessler et al., 1996). Collectively, over five decades, these studies in flies, sheep, mice and humans directly linked Shh signaling to craniofacial birth defects and highlighted the sensitivity of the pathway to both genetic and environmental disruption.

Shh signaling is a logical focus for investigations of etiologically heterogeneous craniofacial birth defects; Shh pathway mutations have been linked to human HPE, and both natural and synthetic inhibitors of Shh signaling have been shown to cause HPE and isolated OFCs in mice. Human malformation-associated mutations have been reported in the *SHH* gene itself, the genes encoding the SHH secretory protein (*DISP1*), the SHH receptor (*PTCH1*) and associated membrane proteins (*CDON*, *BOC* and *GAS1*), and *GLI2*, the dominant pathway transcriptional activator (Hong & Krauss, 2018; Roessler et al., 2018). With respect to environmental influences, the Shh pathway is also inherently sensitive to small molecule modulation. Following the discovery of cyclopamine, numerous small molecules have been identified as pathway inhibitors acting through the same smoothened-targeted mechanism (Pietrobono & Stecca, 2018; Rimkus et al., 2016).

Such small molecules include diverse environmental chemicals, such as phytocannabinoids (Khaliullina et al., 2015) and a widely used pesticide synergist, piperonyl butoxide (Everson et al., 2019). Alcohol (ethanol), a known human teratogen, can also be added to this mix and has been suggested to act on multiple factors upstream of and within the Shh signaling cascade to disrupt development of the face and brain (Sulik, 2005). These examples illustrate how a single developmental pathway can be susceptible to a diverse cast of genetic and environmental influences that, individually, may have only subphenotypic impacts but, in combination, produce an additive or synergistic outcome. Teasing apart these interactions is a major research challenge, but one that will be crucial for solving the puzzle of complex birth defects.

Combining genetic tractability with environmental sensitivity, the mouse is a powerful model to examine specific gene-environment interactions (Hong & Krauss, 2018). *SHH* mutations, the first and most commonly identified in human HPE, provide an instructive example. In human pedigrees, *SHH* mutations are heterozygous and display incomplete penetrance and highly variable expressivity (Solomon et al., 2012). In mice, loss of both *Shh* alleles results in severe HPE, whereas heterozygous mice are indistinguishable from wild-type littermates. However, studies have shown that these 'silent' mutations dramatically exacerbate the teratogenicity of environmental chemicals, including ethanol and piperonyl butoxide (Everson et al., 2019; Kietzman et al., 2014). Similar experiments have shown additive or synergistic interactions between additional gene-environment pairs including *Cdon* and ethanol (Hong & Krauss, 2012), *Gli2* and ethanol (Kietzman et al., 2014), and *Gli2* and the synthetic smoothened antagonist vismodegib (Heyne et al., 2016).

Of course, gene-environment interactions during development are not limited to craniofacial malformations or mediated only through the Shh signaling pathway. Specific gene-environment interactions have been described in mouse-based studies of congenital conditions, including heart disease (Chapman et al., 2019; Moreau et al., 2019), scoliosis (Sparrow et al., 2012), hypospadias (van der Zanden et al., 2012), and complex developmental defects and miscarriage (Cuny et al., 2020; Shi et al., 2017). Importantly, several of these examples go beyond chemicals to demonstrate roles for other environmental influences, including maternal hypoxia (Chapman et al., 2019; Moreau et al., 2019; Sparrow et al., 2012) and nutrient deficiency (Cuny et al., 2020; Shi et al., 2017). Collectively, these findings provide crucial proof of concept for gene-environment interactions in diverse etiologically complex birth defects. However, also apparent in these examples is an inherent limitation of this approach: being time and resource intensive, mouse-based experiments are typically limited to a small 'cherry-picked' list of known factors.

NEW APPROACHES TO SOLVING THE GENE-ENVIRONMENT PUZZLE

The primary barrier to investigating gene-environment interactions is the sheer number of possible combinatory permutations between the genome and the growing list of chemicals that comprise the exposome, 'the comprehensive characterization of an individual's lifetime exposure history' (Wild, 2011). Although successfully utilized as proof of concept in multifactorial etiologies, mouse studies are not ideally suited for high-throughput discovery of environmental influences and novel interactions. By contrast, zebrafish, although less representative of human development, are increasingly being used to examine gene-environment interactions in high-throughput systems (Balik-

Meisner et al., 2018), as discussed in the context of abnormal development in recent reviews (Grinblat & Lipinski, 2019; Krauss & Hong, 2016). Traditional mammalian cell culture approaches offer even greater throughput than zebrafish, but such systems frequently lack the physiological relevance to probe the dynamic cellular and molecular interactions that drive tissue and organ development.

Situated between traditional two-dimensional cell monocultures and animal models are advanced *in vitro* approaches, such as organoids and microphysiological models (MPMs, discussed below), that blend genetic tractability and scalability with varying degrees of physiological complexity. The implementation of *in vitro* systems capable of probing disruptions in developmental processes requires the use of representative cell types, appropriate cellular organization, stability and robustness, methods for assessing function and phenotype, and reproducibility. To test gene-environment interactions, these models must also be genetically tractable. Utility of organoids, three-dimensional (3D) aggregates of self-organized cells, has already been demonstrated in research on the brain, eye, gut, reproductive system, kidney, lung and pancreas (Truskey, 2018). For example, one research group recently demonstrated that brain organoids exposed to a gradient of SHH protein show *in vivo*-like gene expression patterns and that these patterns are disrupted, and organoid growth limited, by Shh signaling inhibition (Cederquist et al., 2019). Organoids have also been utilized to simulate fusion of the human embryonic palate and demonstrate that chemical inducers of cleft palate can inhibit palate organoid fusion *in vitro* (Belair et al., 2018; Wolf et al., 2018). Such models, if appropriately sensitive and scalable, may serve as *in vitro* platforms for the discovery of environmental toxicants with the potential to contribute to OFCs and HPE and other

neurodevelopmental abnormalities. Furthermore, utilizing patient-derived cells and leveraging CRISPR/Cas-9 gene-editing technology in developing organoid models expands the utility of this technology in gene-environment interactions research (Truskey, 2018). Organoids should be useful for examining both genetic and environmental disruption of intercellular signaling and tissue organization, at least at the level of the functional unit of an organ. Looking beyond brain and palate, heart and liver organoids have a tendency to resemble embryonic tissue (Takebe et al., 2013; Voges et al., 2017), making them especially promising for mechanistic studies of congenital defects. Organoids have also recently been shown to be amenable to chemical screening approaches (Mills et al., 2019) and efforts are underway to enhance the production and reproducibility of organoids and to develop methods for assessing organoid function (Arora et al., 2017; Kratz et al., 2019).

In contrast to organoids, MPMs, which encompass a broad category of 3D culture models including organ-on-a-chip systems, employ microfabrication and microfluidics to create extracellular structures that aid replication of tissue architecture and physiological forces (Truskey, 2018). One of the goals of MPMs is to simulate a more realistic external environment, for example by providing scaffolding to seed distinct cellular layers (similar to those comprising the cerebral cortex), fluid dynamics to mimic the flow of interstitial fluid within the brain, and microhole structures that simulate the blood-brain barrier (Yi et al., 2015). The use of microfluidics may also produce more realistic exposure scenarios than traditional cell culture models by dynamically controlling the inflow and outflow of treatments or culture components. Furthermore, by combining modular organ-on-a-chip platforms using microfluidics, a degree of xenobiotic metabolism may be incorporated,

though scaling is considerably more difficult in complex arrays (Truskey, 2018). Regardless, as these systems typically mimic only a subset of features of an *in vivo* biological system, they are well suited to screening chemicals and, ideally, complex mixtures. In addition, many of the advantages of organoids also apply to MPMs. Genetic tractability, the use of patient-derived cells and 'organoid-on-a-chip' MPM systems that utilize self-organized 3D structures (Skardal et al., 2020) all demonstrate the flexibility and broad potential of modern *in vitro* techniques to improve the faithful recapitulation of biological and physiological processes. In this way, organoids and MPMs may be ideal for the practical detection of toxicants in the environment using an unbiased approach that moves from demonstration of perturbation to chemical identification to mechanistic studies.

Although organoids and MPMs provide an exciting avenue for discovery of gene-environment interactions, their practical limitations must be taken into consideration. Being more complex than traditional cell culture, advanced *in vitro* models are generally more time and resource intensive, although this gap should narrow as technologies improve. More crucial for the study of birth defects, these advanced cell-based systems do not fully recapitulate dynamic and transient developmental processes or the full physiological complexity of maternal-embryo interfaces, including xenobiotic metabolism and placental transfer. However, advanced *in vitro* systems are not intended to replace all other approaches to birth defects research; instead, organoids and MPMs complement genomics and animal-based models by providing a scalable, human tissue-specific platform for screening gene-environment interactions in complex developmental etiologies.

PERSPECTIVES

As organoid and MPM approaches mature, the barriers to high-throughput gene-environment interaction testing will recede. The immense volume of possible interactions becomes less daunting as animal-free models provide insight into the multifactorial mechanisms of physiological disruption in etiologically complex diseases, isolated in a dish from the uncontrollable confounding factors inherent to *in vivo* studies. Once sufficiently scaled, these advanced *in vitro* approaches will allow for more agnostic environmental toxicant screening on customizable genetic backgrounds and biological platforms. This is the modern path to gene-environment interaction discovery. However, for all their benefits, these emerging *in vitro* technologies are not without important drawbacks. The discoveries made in these *in vitro* systems must still be validated in traditional mammalian animal models.

The introduction of advanced molecular and genetic approaches signaled a momentous shift in developmental biology at the turn of the 21st century. The introduction of advanced cell culture techniques may prove equally momentous. Regardless, organoids and MPMs are tools, just as animal models and molecular techniques are tools. Each possesses potential as well as limitations. One approach need not supersede another; rather, we must use all the tools available to us to best serve the wellbeing of those who entrust us with this important research. F. Clarke Fraser opined that birth defects 'are caused by a little bit of this and a little bit of that' (International Neural Tube Defect Conference, 2009). Our approach to solving them, also, must consist of a little bit of this and a little bit of that.

DECLARATIONS

Funding: This work was supported in part by the National Institute of Environmental Health Sciences of the National Institutes of Health (NIH) (R01ES026819). Deposited in PMC for release after 12 months.

Acknowledgments: The authors thank John C. Carey, Brian P. Johnson and Elizabeth J. Leslie for their critical review of this manuscript.

Competing Interests: The authors declare no competing or financial interests.

CHAPTER II

This manuscript was submitted to *Toxicological Sciences* (July 2025). TGB, JLE, RJL designed studies; TGB, JLE, DAD, KYP, EW conducted experiments and acquired data; TGB and JLE analyzed data; TGB wrote the manuscript; JLE, JKE, RJL reviewed and edited the manuscript; all authors read and approved the final manuscript.

CHAPTER II: A CELL-BASED SONIC HEDGEHOG SIGNALING TRANSDUCTION SYSTEM TO IDENTIFY ADDITIVE AND SYNERGISTIC CHEMICAL INTERACTIONS

Tyler G. Beames[1], Joshua L. Everson[2,3], Dhara A Desai[2], Kayla Y. Perez[2], Elizabeth Wu[2], Johann K. Eberhart[2,3], and Robert J. Lipinski[1,*]

[1]Department of Comparative Biosciences, School of Veterinary Medicine, University of Wisconsin-Madison, Madison, Wisconsin, United States

[2]Department of Molecular Biosciences, School of Natural Sciences, University of Texas at Austin, Austin, TX, United States

[3]Waggoner Center for Alcohol and Addiction Research, School of Pharmacy, University of Texas at Austin, Austin, TX, United States

[*]Author for correspondence (robert.lipinski@wisc.edu)

ABSTRACT

Sonic hedgehog (Shh) signaling is an essential developmental pathway that is sensitive to small molecule disruption and directly linked to common and etiologically complex human birth defects. Numerous mechanistically diverse small molecule Shh pathway antagonists have been identified, but their interactions in pathway disruption have received minimal attention. We established a tractable co-culture model in which autonomous SHH ligand production initiates this complex inter- and intracellular signal transduction cascade and culminates in activation of a GLI-responsive luminescent reporter. Compounds reported to target SHH ligand processing (RU-SKI 43, AY 9944, U18666A), SMO-mediated signal transduction (cyclopamine, vismodegib, piperonyl butoxide, cannabidiol), and GLI transcription factors (GANT 61, arsenic trioxide) reduced Shh pathway-driven reporter activity with AC_{50} values in the low micromolar range or below. We then evaluated chemical interactions among Shh pathway inhibitors using isobolographic analysis. Co-exposure assays revealed additive interactions from combined SMO and GLI inhibition, while disruption of SMO and cholesterol dynamics synergistically decreased Shh pathway activity. Unexpectedly, piperonyl butoxide synergized with other SMO inhibitors, and further characterization of piperonyl butoxide's impacts on Shh signaling supported an additional mechanism of inhibition independent of SMO. In zebrafish embryos, combined exposure to piperonyl butoxide and cyclopamine also produced a greater-than-additive increase in craniofacial dysmorphogenesis. These findings demonstrate the importance of tractable models that recapitulate complex signal transduction pathways to empirically test for additive and synergistic chemical interactions in risk assessment.

INTRODUCTION

Birth defects are a persistent public health concern, affecting approximately one in 33 live births (Christianson et al., 2006). In addition to being a leading cause of infant mortality, birth defects confer lifelong physical, neurodevelopmental, and financial consequences. Most non-syndromic birth defect cases have unknown etiologies and are thought to result from complex gene-environment interactions (Beames & Lipinski, 2020). Advances in genetic and genomic technologies have resolved the genetic landscape of many of these conditions (Innes & Lynch, 2021), but our current knowledge of the prenatal environment during critical periods of development is extremely limited (Lipinski & Krauss, 2023). Defining and characterizing environmental risk factors is a direct path to the development of birth defect prevention strategies.

The Sonic hedgehog (Shh) signaling pathway is a key regulator of embryonic development and a relevant focus for the study of environmental birth defect risk factors due to its sensitivity to small molecule modulation. The plant alkaloid and first known chemical inhibitor of Hedgehog signaling, cyclopamine, was named for its ability to induce cyclopia in sheep (Chen, 2016; Keeler, 1978) and was later revealed to act by inhibiting Smoothened (SMO), the key signal transducer of the Shh pathway (Chen et al., 2002; Incardona et al., 1998). In recent decades, over a dozen SMO inhibitors have been identified (Pietrobono & Stecca, 2018; Rimkus et al., 2016), and additional upstream and downstream pathway components were demonstrated to be susceptible to inhibition.

The sensitivity of the Shh pathway to diverse small molecule antagonists reflects the complexity of this signaling cascade. SHH ligand function requires autoproteolytic cleavage, a process that appends a cholesterol moiety to the C-terminus of the truncated

peptide, followed by palmitoylation of the N-terminus by Hedgehog acyltransferase (HHAT). The mature peptide is then shuttled out of SHH-producing cells by DISP1 and binds its receptor PTCH1 on SHH-responsive cells, thereby relieving the repression of SMO. Once activated, SMO promotes Shh-regulated gene expression through the GLI transcription factors proteins (Choudhry et al., 2014). In addition to SMO inhibition, small molecules are now known to disrupt Shh signaling by reducing cholesterol availability (Cooper et al., 1998; Gofflot et al., 2001) or directly antagonizing HHAT or GLI proteins (Beauchamp et al., 2011; Lauth et al., 2007; Ritzefeld et al., 2024) (Fig. 1).

The critical role of Shh signaling during embryogenesis underscores its importance in the development of etiologically complex malformations. Shh signaling is required for morphogenesis of the face and forebrain (Barratt et al., 2022; Bush & Jiang, 2012; Jiang et al., 2006), digit specification (Tickle & Towers, 2017), and numerous other developmental processes. Disruption of the Shh pathway is associated with congenital conditions, including holoprosencephaly (HPE), orofacial clefts (OFCs) of the lip and palate, hypospadias, and limb malformations. HPE, the most common malformation observed in human embryos (Matsunaga & Shiota, 1977), is characterized by insufficient growth of the medial forebrain and midface and frequently co-occurs with orofacial clefts (Cohen, 2006; Richieri-Costa & Ribeiro, 2010; Tekendo-Ngongang et al., 2020). In humans, HPE and OFCs are associated with genetic variants in genes that encode components of the Shh signaling pathway. In mice, prenatal exposure to SMO antagonists can cause HPE-like phenotypes with associated midfacial malformations or isolated OFCs with the specific outcome dependent upon the timing of exposure (Everson et al., 2017; Heyne, Melberg, et al., 2015). Disrupted Shh signaling is also implicated in hypospadias

(Miyagawa et al., 2011) and limb malformations (Rivera-González et al., 2024). While gene-environment interactions have been a focus for investigating Shh signaling-mediated congenital malformations (Everson et al., 2020; Everson et al., 2019; Heyne et al., 2016; Hong & Krauss, 2012; Kietzman et al., 2014), environment-environment interactions have received little attention. The multi-level sensitivity of the Shh pathway to small molecule modulation creates the opportunity for complex chemical interactions, and characterizing these interactions is important for birth defect risk assessment.

When the actions of multiple chemicals converge on a common adverse outcome, the cumulative result may be additive, synergistic, or antagonistic. Isobolographic analysis is the gold-standard approach for differentiating between types of chemical interactions, taking additivity as its null hypothesis (Huang et al., 2019). However, the resource-intensive nature of isobolographic analysis—requiring multiple concentration-response assays for each endpoint and chemical pairing—limits its practicality in animal models. To prioritize co-exposures for *in vivo* risk assessment, it is important to design assay systems that are biologically relevant and readily scalable. In this study, we developed a sensitive, tractable cell-based assay that recapitulates key steps within the Shh signaling cascade that are susceptible to small molecule disruption. After challenging the system with small molecules purported to target cholesterol modification and palmitoylation of the SHH ligand, signal transduction through SMO, and the GLI transcription factors, we applied isobolographic analysis to investigate chemical interactions. Shh pathway-modified cell lines were then employed to support mechanistic targets among a subset of compounds, and a zebrafish model was utilized to test the impact of interaction between two environmental Shh pathway inhibitors on craniofacial morphogenesis.

MATERIALS AND METHODS

Chemicals/Reagents

The Smoothened inhibitors cyclopamine (CASRN 4449-51-8) and vismodegib (CASRN 879085-55-9) were purchased from LC Laboratories, piperonyl butoxide (PBO; CASRN 51-03-6) was purchased from Toronto Research Chemicals, and cannabidiol (CBD; CASRN 13956-29-1) was purchased from Cayman Chemical. The HHAT inhibitor RU-SKI 43 (CASRN 1043797-53-0), the cholesterol synthesis and transport modifiers U18666A (CASRN 3039-71-2) and AY 9944 (CASRN 366-93-8), and the GLI inhibitor GANT 61 (CASRN 500579-04-4) were purchased from Cayman Chemical. Arsenic trioxide (ATO; CASRN 1327-53-3) was sourced from Sigma-Aldrich.

Cell culture

Shh pathway activity was assessed using Shh-LIGHT2 cells, an immortalized mouse embryonic fibroblast (iMEF) line incorporating a GLI-driven firefly luciferase and constitutive *Renilla* luciferase (Taipale et al., 2000). Constitutively Active Shh-LIGHT2 (CAL2) cells were generated by stably overexpressing full-length human SHH (*hSHH*) and *GFP*. Cells with high *hSHH* expression were isolated via fluorescence-activated cell sorting of cells in the top 40th percentile of GFP intensity and used for subsequent experiments. Shh-LIGHT2 cells and CAL2 cells were cultured in Dulbecco's Modified Eagle Medium (DMEM) with 10% fetal bovine serum (FBS) and 1% penicillin-streptomycin, as well as the selection agents G418 (0.4 mg/mL) and zeocin (0.15 mg/mL). Additional Shh pathway-modified cell lines were employed to support pathway specificity. *Ptch1*$^{-/-}$ mouse embryonic fibroblasts (Taipale et al., 2000) and iMEFs

expressing a constitutively active form of SMO (*SMO*^{M2}) (Lipinski et al., 2008; Taipale et al., 2000) were grown in DMEM containing 10% FBS and 1% penicillin-streptomycin.

Luminescent reporter assay

Shh-LIGHT2 cells and CAL2 cells were expanded separately prior to seeding into 24-well plates. At 90% confluence, cells were counted and resuspended at 5×10^5 cells/mL. CAL2 and Shh-LIGHT2 suspensions were mixed at 1:3 (25% CAL2, 75% Shh-LIGHT2) or 1:9 (10% CAL2, 90% LIGHT2) ratios. Mono-cultures and co-cultures were then seeded at a density of 2×10^5 cells/well (5×10^5 cells/mL in 0.4 mL medium). After 24 h, growth medium was replaced with treatment medium (1% FBS and 1% penicillin/streptomycin) containing 0.1% DMSO to match subsequent vehicle treatment conditions. Following optimization, Shh pathway activity assays were conducted using the optimized 1:9 CAL2:Shh-LIGHT2 model. Cells were seeded in growth media for 24 h then treated with test compounds at the indicated concentrations for 48 h. All compounds were dissolved in 100% DMSO, and the final concentration of DMSO in all wells was 0.1%. After treatment, cells were processed using the Dual-Luciferase® Reporter Assay System (Promega) according to the manufacturer's recommendations. Briefly, cells were washed once with DPBS before adding 1× Passive Lysis Buffer (Promega) and rocking at 100 RPM for 15 min at room temperature. Lysates were collected and stored at -80°C prior to assessing firefly and *Renilla* luciferase activity. Luminescence was measured using a BioTek Synergy HT Multi-Detection Plate Reader (Agilent). Activity is reported either untransformed as the ratio of firefly luciferase to *Renilla* luciferase or as percent reduction with in-plate vehicle (0.1% DMSO) or positive (10 μM cyclopamine) controls defining 0% and 100% reduction in pathway activity, respectively.

Immunofluorescence

CAL2 mono-cultures and 1:3 and 1:9 co-cultures were seeded into 24-well plates as described above. After 48 h of treatment, cells were rinsed with DPBS and fixed in 4% paraformaldehyde at room temperature for 15 min. Fixed cells were permeabilized with 0.5% Triton X-100 in DPBS for 1 h at room temperature, then incubated in 60 nM DAPI for 1 h at room temperature. Fluorescence imaging for DAPI and GFP was performed using a BZ-X700 microscope (Keyence).

RNA extraction, reverse transcription, and qPCR

CAL2 monocultures and 1:3 and 1:9 co-cultures were seeded into 24-well plates as described above. Monocultures of *Ptch1*$^{-/-}$ and *SMO*^{M2} iMEFs were similarly seeded into 24-well plates. After 48 h of treatment, cells were rinsed in DPBS and lysed for RNA extraction using the Amersham RNAspin Mini Kit (Cytiva) according to manufacturer recommendations, including on-column DNase digestion. cDNA was synthesized from 500 ng total RNA using the GoScript reverse transcription system (Promega). Gene expression was evaluated by singleplex quantitative real-time polymerase chain reaction (qPCR) using SSoFast EvaGreen Supermix (Bio-Rad) on a CFX96 Real-Time PCR Detection System (Bio-Rad Laboratories). Primers for *Gapdh*, *hSHH* and *Gli1* were designed using PrimerQuest (IDT) and are listed in Table S1. Analyses were performed using the 2-ΔΔCt method with *Gapdh* serving as the reference gene.

Isobolographic analysis

In vitro co-exposure tests were performed using the 1:9 CAL2:Shh-LIGHT2 co-culture with luminescence as the readout of pathway activity. Half-maximal activity (AC_{50}) values

and slope parameters were estimated for each compound from 8- or 9-point half-log concentration response curves using the Hill equation. For isobolographic analysis, isoboles were constructed based on single-compound AC_{50} values (i.e., x- and y-intercepts on the isobologram) and slopes. Pairs of compounds with significantly different slopes were considered to have a variable potency ratio, and resulting isoboles were curved instead of linear (Grabovsky & Tallarida, 2004). Potency estimates for chemical combinations were derived from five half-log concentration series generated using pairs of Shh inhibitors at AC_{50} ratios of approximately 4:0, 3:1, 2:2, 1:3, and 0:4. Co-cultures were treated for 48 h with a concentration series of each ratio, and luminescence was assessed as a readout of Shh pathway activity. AC_{50} values were estimated for each compound within each binary mixture, and these values were plotted on the isobologram as a visual representation of chemical interactions (Tallarida, 2016). Chemicals for co-exposure testing were assumed to interact according to independent action, and additional characterization was reserved for pairs that deviated from additivity.

Zebrafish husbandry, chemical exposure, and imaging

All experiments were conducted according to the guidelines in *The Zebrafish Book, 5th edition* (Westerfield, 1993) and the National Institutes of Health *Guide for the Care and Use of Laboratory Animals*. Studies were approved by the University of Texas at Austin Institutional Animal Care and Use Committee (protocol number AUP-2023-00297). Wild-type zebrafish derived from the AB strain were utilized, and developmental staging of embryos was determined based on established morphological features (Kimmel et al., 1995).

Stock solutions of cyclopamine and PBO in DMSO were diluted into embryo medium for single-compound and combined exposures and spiked with an appropriate volume of 1% DMSO to reach a final DMSO concentration of 0.1% for all doses. Chorionated embryos were treated with DMSO vehicle or test compounds from gastrulation at 6 hours post-fertilization (hpf) to pharyngula stage at 24 hpf to target the critical window for Shh pathway-mediated craniofacial malformation in zebrafish (Everson et al., 2020; Everson et al., 2023). AC_{50} values were estimated for cyclopamine from an 8-point 2× linear concentration series spanning 0.78-100 μM. At 24 hpf, treatment media were replaced with fresh embryo medium.

At 48 hpf, embryos were fixed in 2% paraformaldehyde and ventrally imaged on an Olympus SZX7 stereomicroscope using an DP22 digital camera (Olympus). Interocular distance was measured as the narrowest point between the eyes using Image J (NIH).

Statistical analysis

Statistical analyses were performed using GraphPad Prism 10. Unpaired t-tests were used to assess differences in luminescence between vehicle-treated and SHH-treated Shh-LIGHT2 monocultures, as well as differences between concentration-response slope parameters for co-exposure studies. Comparisons between mono- and co-culture conditions and between vehicle and experimental treatments were evaluated using one-way ANOVA with Dunnett's post hoc test. For gene expression analyses, log-transformed relative expression data were similarly evaluated using one-way ANOVA. Zebrafish interocular distance measurements were assessed using one-way ANOVA with Tukey's multiple comparisons correction. An alpha value of less than or equal to 0.05 was considered significant.

RESULTS

Development of a cell-based assay of Sonic hedgehog pathway signal transduction

To establish a practical, cell-based model of Shh signal transduction beginning with peptide production and processing, we engineered mouse Shh-LIGHT2 cells to stably overexpress *hSHH* and *GFP*. The resulting Constitutively Active Shh-LIGHT2 (CAL2) cells were isolated using fluorescence-activated cell sorting based on GFP intensity. Unlike previous 2D *in vitro* models that rely on exogenous SHH ligand or genetic modification to activate the pathway at or downstream of SMO (Lauth et al., 2007; Taipale et al., 2000), signaling is initiated with ligand synthesis in this system.

When cultured alone, CAL2 cells produced a modest increase in normalized luminescent reporter activity (firefly/*Renilla*) relative to Shh-LIGHT2 cells stimulated with exogenous SHH ligand. However, treatment of CAL2 cells with the potent SMO antagonist cyclopamine failed to reduce reporter activity down to the level of untreated Shh-LIGHT2 cells (Fig. 2a), suggesting a muted responsiveness due to excessive production of SHH ligand. To optimize sensitivity and dynamic range, we cultured CAL2 cells with Shh-LIGHT2 cells at ratios of 1:3 and 1:9. To confirm the seeding ratio and assess spatial distribution of Shh-LIGHT2 cells and GFP-expressing CAL2 cells, CAL2 mono-cultures and 1:3 and 1:9 co-cultures were fixed and stained with DAPI for imaging (Fig. 2b-d). Reducing the proportion of CAL2 cells produced a corresponding reduction of *hSHH* transcripts and increased the expression of the gold-standard Shh-pathway readout gene *Gli1* (Fig. 2e). Reporter activity was then measured in cyclopamine-treated co-cultures to assess sensitivity to pathway-specific antagonism. While each culture condition exhibited

a higher level of reporter activity than untreated Shh-LIGHT2 cells, the 1:9 co-culture demonstrated the greatest dynamic range when treated with cyclopamine (Fig. 2f). Based on these findings, the 1:9 CAL2:Shh-LIGHT2 co-culture (subsequently referred to as the "optimized co-culture") was selected for downstream experiments.

Sensitivity of a Shh pathway signal transduction assay to mechanistically distinct chemicals

We next assessed whether the co-culture assay recapitulates sensitivity to chemicals acting across the Shh pathway signal transduction cascade. Using the optimized co-culture, we examined inhibition following treatment with a panel of small molecule antagonists reported to act through four distinct mechanisms. SHH ligand is modified by the addition of cholesterol and palmitate moieties prior to secretion, which has been shown to be important for ligand activity (Dawber et al., 2005; Jeong & McMahon, 2002; Pepinsky et al., 1998). Available cholesterol can be reduced using U18666A (Cenedella, 2009) and AY 9944 (Kraml et al., 1964), inhibitors of cholesterol transport and synthesis, respectively, and RU-SKI 43 blocks the activity of HHAT, the enzyme that appends palmitate to the immature SHH ligand (Buglino & Resh, 2008; Petrova et al., 2013). Blocking each of these mechanisms of SHH ligand processing significantly reduced pathway activity at 10 μM (Fig. 3a-b).

Following maturation and secretion, SHH ligand binds PTCH1 to relieve its inhibition of SMO, the primary signal transducer in canonical Shh signaling. Known SMO antagonists include the plant alkaloid cyclopamine (Chen et al., 2002), the pharmacologic drug vismodegib (Robarge et al., 2009), the pesticide synergist PBO (Wang et al., 2012), and the phytocannabinoid CBD (Lo et al., 2021). Similar to the upstream pathway inhibitors,

each of these compounds significantly reduced reporter activity in the co-culture assay, and cyclopamine, vismodegib, and PBO did so at concentrations below 10 μM (Fig. 3c).

Downstream of SMO, the GLI transcription factors mediate pathway-responsive gene expression changes. The pharmacologic compound GANT 61 and the industrial chemical ATO are both reported to inhibit Shh pathway activation at the level of the GLI proteins (Beauchamp et al., 2011; Lauth et al., 2007). Both chemicals significantly reduced Shh pathway activity relative to vehicle controls at or below 10 μM (Fig. 3d).

Together, these data support the fidelity of this co-culture system for the interrogation of mechanistically distinct inhibitors that act throughout the Shh signal transduction cascade. To assess specificity, we tested benzo[a]pyrene and ethanol, compounds that are associated with altered craniofacial development but reported to act independent of or indirectly upon Shh signaling, respectively (Barbieri et al., 1986; Hong et al., 2020; Sidik et al., 2021). Reporter activity was not significantly reduced following exposure to either of these compounds, supporting the specificity of the model (Fig. 3e).

Evaluating interactions between Shh pathway antagonists

To evaluate chemical interactions using isobolographic analysis, potency estimates were derived for each antagonist individually. Following 48 h treatments with a nine-point half-log concentration series for each pathway antagonist, cytotoxicity was assessed visually by a loss of integrity of the cell monolayer as well as quantitatively based on normalized luminescent ratio. Due to reduced viability, the highest concentrations tested for U18666A, AY 9944, and RU-SKI 43 were excluded from curve-fitting (Fig. 4a-c). Potency estimates (AC_{50}) were derived using the Hill equation, where applicable.

Inhibitors reported to target cholesterol transport (U18666A, Fig. 4a) and synthesis (AY 9944, Fig. 4b) and the acyltransferase HHAT (RU-SKI 43, Fig. 4c) all reduced pathway activity with AC_{50} values in the low micromolar range. As expected based on previous reports, purported SMO inhibitors exhibited a wide range of potencies (Fig. 4d-g). Cyclopamine, vismodegib, and PBO produced AC_{50} values from the low nanomolar to the low micromolar range, whereas CBD only partially reduced Shh pathway activity at the highest concentration tested. Both reported GLI antagonists, GANT 61 and ATO, had AC_{50} values in the low or sub-micromolar range (Fig. 4h-i). AY 9944, RU-SKI 43, and CBD were excluded from downstream isobolographic analysis because their concentration response curves did not plateau at approximately 0% reduction (AY 9944) or 100% reduction (RU-SKI 43 and CBD).

To assess chemical interactions, isobolograms were constructed by plotting AC_{50} values for individual compounds on orthogonal axes and connecting these values with an isobole, a line or curve of that represents the additive interaction for any ratio of those compounds (Tallarida, 2016). For mixtures, experimentally derived potency measures falling below the isobole are described as synergistic; conversely, interactions that sit above the isobole are described as antagonistic (Fig. 5a). Initial co-exposure analyses assumed independent action for all compound pairs. Based on the greater number of described SMO inhibitors relative to other Shh pathway targets, co-exposure testing focused on co-inhibition of SMO or simultaneous inhibition of SMO and upstream or downstream targets. As proof of concept, two aliquots of the SMO inhibitor cyclopamine were mixed at fixed ratios to confirm additivity and validate the assay (Fig. 5b). The combination of cyclopamine and the pharmacologic SMO inhibitor vismodegib similarly

produced an additive interaction (Fig. 5c), while cyclopamine and PBO unexpectedly synergized to reduce Shh pathway activity (Fig. 5d). PBO and visomdegib co-treatment induced a similar synergistic response, supporting a broader capacity for PBO to induce super-additive Shh pathway disruption (Fig. 5e).

To examine whether cross-target interactions promote synergy, cells were exposed to cyclopamine and either upstream or downstream Shh pathway antagonists. While co-exposure to cyclopamine and the cholesterol transport inhibitor U18666A produced a synergistic interaction (Fig. 5f), both of the GLI antagonists, GANT 61 and ATO, interacted with cyclopamine additively to reduce pathway activity (Fig. 5g-h).

Sensitivity of Shh pathway-modified cell lines to small molecule antagonists

Next, the mechanism of Shh pathway inhibition among the compounds utilized for co-exposure testing was examined using Shh pathway-modified cell lines. *Ptch1*$^{-/-}$ iMEFs display constitutive pathway activity beginning at the level of SMO and are therefore expected to be resistant to upstream inhibitors. As anticipated, antagonists targeting SMO and GLI reduced the expression of the Shh pathway target gene *Gli1* in these cells (Fig. 6a). However, U18666A was also able to inhibit Shh signaling in *Ptch1*$^{-/-}$ cells, possibly due to the role of cholesterol in SMO activation (Luchetti et al., 2016). *SMO*^{M2} iMEFs express a mutated, constitutively active form of SMO that confers partial resistance to inhibitors such as cyclopamine (Taipale et al., 2000). Indeed, these cells showed greater sensitivity to the GLI antagonist GANT 61 than to the SMO antagonists cyclopamine or vismodegib (Fig. 6b). Notably, PBO exhibited a similar level inhibition as GANT 61, suggesting that PBO may be able to disrupt Shh signaling through a SMO-independent

mechanism not previously described by Wang and colleagues (2012). U18666A did not significantly alter pathway activity in *SMO*^{M2} cells.

Developmental impacts of cyclopamine and PBO co-exposure in zebrafish

Given the unexpected finding of synergy between PBO and both cyclopamine and vismodegib, as well as PBO's ability to disrupt Shh activity downstream of its previously reported binding partner, SMO, we tested whether co-exposure to PBO and cyclopamine super-additively disrupts Shh-dependent developmental processes in a zebrafish model. Changes in craniofacial development following Shh pathway inhibition are readily observed in zebrafish models, including reduced midfacial development measured by interocular distance (Lipinski et al., 2007). Interocular distance was reduced by exposure to cyclopamine alone with an AC_{20} value of 3.25 μM (Fig. 7a). Previous reports in zebrafish indicated that chemical co-exposures can produce greater-than-additive effects of morphogenetic processes. For example, while single exposure to either 25 μM PBO or a 1% dose of ethanol caused only 11% and 9% reductions of midfacial tissue, respectively, co-exposure to these same PBO and ethanol doses caused 43% reduction in midfacial tissue (Everson et al., 2020). To test whether cyclopamine and PBO interact to produce a greater-than-additive effect on craniofacial development, zebrafish embryos were exposed to vehicle, 3.25 μM cyclopamine, 25 μM PBO, or combination treatments from 6 hpf to 24 hpf. Interocular distance, measured at 48 hpf (Fig. 7b-e), demonstrated 14% and 13% reductions following individual treatments with cyclopamine or PBO, respectively, while the combined exposure to cyclopamine and PBO resulted in a much greater 72% reduction (Fig. 7f). The observed increase in midfacial craniofacial malformation exceeds the 27% reduction that would be anticipated from a purely additive interaction.

DISCUSSION

Characterizing environmental risk in the development of etiologically complex birth defects benefits from understanding how chemicals interact to disrupt developmental processes. Given the vast number of potential environmental interactions, experimental models should balance biological relevance with tractability. Focusing our attention on Shh signaling—a critical developmental pathway that is susceptible to environmental modulation—we developed a tractable cell culture model of Shh pathway signal transduction, demonstrated its sensitivity to a broad array of small molecule antagonists, and applied isobolographic analysis to characterize chemical interactions. We observed both additive and synergistic interactions between pairs of Shh pathway inhibitors. In the case of cyclopamine and PBO, the synergistic interaction *in vitro* translated into a potentiation of teratogenicity in a zebrafish model of craniofacial morphogenesis.

Traditional toxicity testing relies on single-compound studies in animal models to estimate human risk. Such studies are time- and resource-intensive, spurring efforts to develop animal-free assays for high-throughput compound screening and mixture testing (Krewski et al., 2010). However, it is critical to carefully balance throughput and biological fidelity to efficiently generate high-quality risk assessments. Numerous cell-based models have been utilized to great effect to probe the molecular machinery comprising Shh signaling (Lauth et al., 2007; Lipinski et al., 2008; Taipale et al., 2000), but our co-culture prioritizes recapitulation of the full Shh signal transduction cascade to assess co-exposures across multiple mechanisms. The fidelity of this model was demonstrated through its sensitivity to small molecule antagonists targeting cholesterol synthesis and transport, palmitoylation of the SHH ligand, signal transduction through

SMO, and GLI transcription factors. Notably, disruption of each of these Shh pathway components results in HPE-like or OFC phenotypes in animal models (Chen et al., 2004; Heyne, Melberg, et al., 2015; Mo et al., 1997; Roux et al., 2000). The evaluation of co-exposure to Shh signaling inhibitors is therefore integral for assessing environmental risk conferred by mechanistically varied pathway antagonists.

Despite growing reliance on *in vitro* chemical screens, chemical interactions are investigated sparingly. The single-compound approach is at odds with the complexity of the human exposome, and research has demonstrated cumulative adverse effects of chemicals on biological processes even below individual no-observed-effect levels (reviewed in Kortenkamp et al., 2007). Furthermore, while additivity is assumed to result from chemicals with sufficiently similar structures and mechanisms, such as dioxin-like compounds or xenoestrogens (Ahlborg & Hanberg, 1994; Payne et al., 2000; Silva et al., 2002), Shh signaling inhibitors exhibit distinct targets, increasing the potential for super-additive interactions. The pesticide synergist PBO illustrates this complexity. Previous reports have demonstrated PBO-SMO binding in cell-free models and the induction of Shh-associated malformations following PBO exposure in mouse and zebrafish models (Everson et al., 2020; Everson et al., 2019; Wang et al., 2012). Unexpectedly, PBO synergized with the SMO inhibitors cyclopamine and vismodegib to reduce Shh pathway activity in our model and inhibited Shh signaling downstream of SMO in *SMO*^{M2} cells. Taken together, these results suggest that PBO may have multiple mechanisms that converge on the Shh signaling pathway. PBO potentiated cyclopamine's developmental toxicity in a zebrafish embryo model, extending the *in vitro* synergy findings to a more complex model and underscoring the potential greater-than-additive impacts that co-

exposures may have on sensitive morphogenetic processes. Further investigation could reveal additional mechanisms and elucidate how they contribute to the observed synergistic interactions.

Several limitations constrain our approach. During development, SHH acts in a concentration-dependent manner, forming a gradient of pathway activity (Dessaud et al., 2007; Stamataki et al., 2005). Given the variable exposure of Shh-responsive cells to this ligand in its native biological context, it is likely that there is a corresponding spatial sensitivity to environmental antagonists. A previously reported microphysiological model of Shh signaling recapitulates this signaling gradient *in vitro* and may be used to clarify whether gradient formation is differentially modulated by additive or synergistic co-exposures (Johnson et al., 2021). In addition, the Shh pathway exists within a broader network of critical developmental pathways, including Wnt, TGFβ, and nodal, that have been shown to regulate Shh signaling activity and may mediate additional chemical-chemical interactions. Similar co-culture approaches combining overexpression of related pathways may help reveal the impacts of cross-pathway interactions and facilitate prioritization for toxicity testing in more biologically faithful but resource-intensive models.

This study demonstrated synergistic chemical interactions among small molecules acting within a complex signaling pathway that is linked to human birth defects. This key finding, supported in a zebrafish embryo model, demonstrates the importance of investigating co-exposures when performing chemical risk assessments. To examine interactions, we developed and validated a tractable assay that recapitulates key mechanisms within the Shh pathway signal transduction cascade. Isobolographic analysis

revealed both additive and synergistic interactions resulting from co-exposure to Shh pathway antagonists. That synergy could not be predicted on the basis of purportedly similar or distinct mechanisms among inhibitors further highlights the necessity for tractable, biologically relevant assays that support the efficient empirical investigation of chemical interactions. Future research will explore the mechanisms by which synergy is produced, as well as leverage this cell culture assay to screen for and characterize environmentally relevant Shh pathway antagonists, extending our understanding of environmental risk in the development of etiologically complex birth defects.

DECLARATIONS

Funding: This work was supported by the National Institutes of Environmental Health Sciences under awards R01ES026819, K99ES034471, F31ES034632, and T32ES007015. Additional support was provided by the National Institute of Dental and Craniofacial Research under award R35DE029086.

Acknowledgments: We thank the fish facility technicians at the University of Texas at Austin, especially Jaden Salganik, for expert husbandry in support of this work. The authors also thank Rachel B. Walkup and Alexandra J. Griffith for careful review of this manuscript.

Conflict of interest: The authors declare that they have no conflict of interest.

Ethical approval: University of Texas at Austin Institutional Animal Care and Use Committee under protocol AUP-2023-00297.

Data Availability Statement: The datasets generated during the current study are available from the corresponding author on reasonable request.

TABLES

Table S1 Primer Sequences for qRT-PCR

Species	**Gene/Direction**	**Sequence**
Mouse	*Gapdh*-forward	AACACTGAGCATCTCCCTCACA
	Gapdh-reverse	GGTGGGTGCAGCGAACTTTATT
Mouse	*Gli1*-forward	CCACCACCCTACCTCTGTCTATTC
	Gli1-reverse	GTTCAGACCATTGCCCATCACA
Human	*SHH*-forward	AAGGACAAGTTGAACGCTTTGG
	SHH-reverse	TCGGTCACCCGCAGTTTC

FIGURES

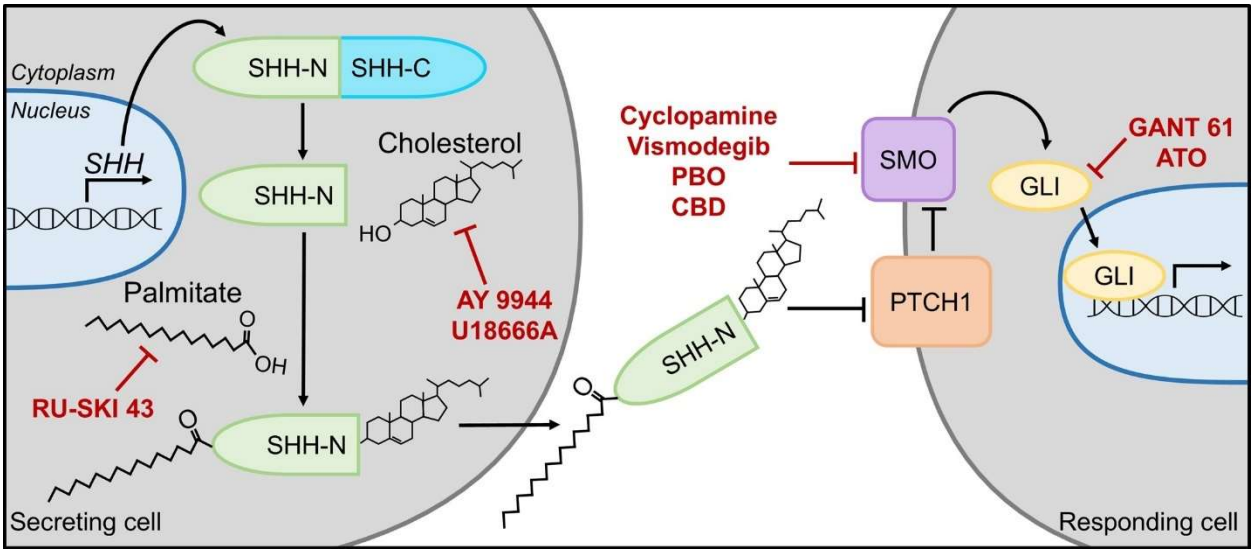

Fig. 1 The Sonic hedgehog (Shh) signaling pathway is sensitive to disruption by mechanistically distinct small molecules. Shh signal transduction proceeds along a multi-step cascade initiated by autoproteolytic cleavage of the full-length SHH protein and followed by cholesterol and palmitate modification of the N-terminal peptide. The mature ligand is secreted and inhibits the cell-surface protein PTCH1, inducing a transduction cascade through SMO that activates downstream GLI transcription factors. Small molecules, shown in red text, disrupt the Shh pathway at multiple levels including cholesterol synthesis and transport, palmitoylation, signal transduction through SMO, and GLI activation. PBO, piperonyl butoxide; CBD, cannabidiol; ATO, arsenic trioxide

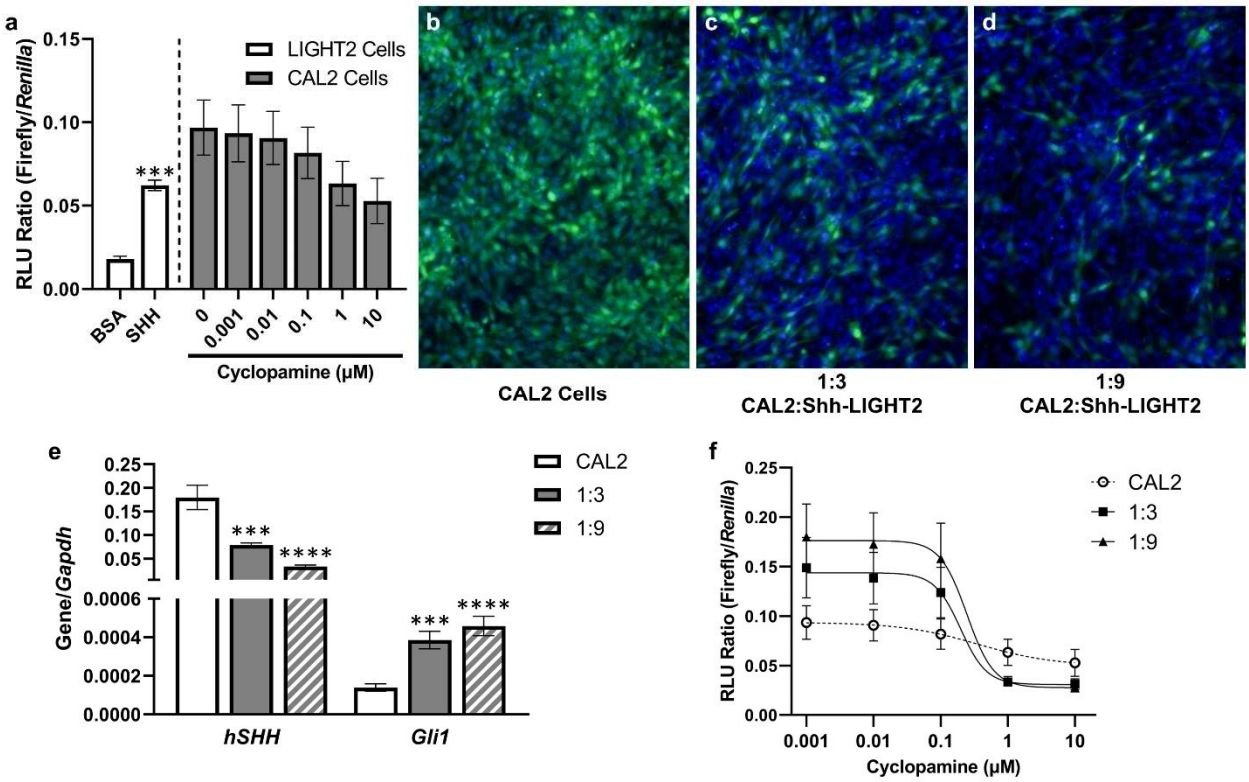

Fig. 2 Optimization of a co-culture assay of Shh pathway signal transduction. (**a**) Luminescent reporter activity was significantly increased in Shh-LIGHT2 cells following treatment with SHH ligand. CAL2 cells exhibited high baseline reporter activity, though treatment with a concentration series of cyclopamine produced a non-significant trend, suggestive of partial pathway inhibition. Bars represent the mean and SEM (n=3). An unpaired t-test was used to evaluate differences between vehicle- (BSA) and SHH-treated Shh-LIGHT2 cells, and a one-way ANOVA with Dunnett's post-hoc test was used to assess the cyclopamine concentration-response. (**b-d**) GFP-expressing CAL2 cells were seeded as monocultures or 1:3 or 1:9 co-cultures with Shh-LIGHT2 cells and fixed for immunostaining. Nuclei (DAPI) are shown in blue and GFP in green. (**e**) Expression of *hSHH* and *Gli1* in monocultures of CAL2 cells and co-cultures of 1:3 and 1:9 CAL2:Shh-LIGHT2 cells. Data represent the mean and SEM (n=5). One-way ANOVA with Dunnett's post-hoc test was used to evaluate differences between the CAL2 monoculture and the co-

culture conditions for each gene. (**f**) Co-cultures of CAL2 and Shh-LIGHT2 cells were treated for 48 h with a concentration series of cyclopamine, and normalized luminescent reporter activity was used to assess Shh pathway activity. The CAL2 monoculture response curve is shown again for reference. Curves were fit using four-parameter nonlinear curve-fitting. Values represent the mean and SEM (n=3). ***p < 0.001, ****p < 0.0001

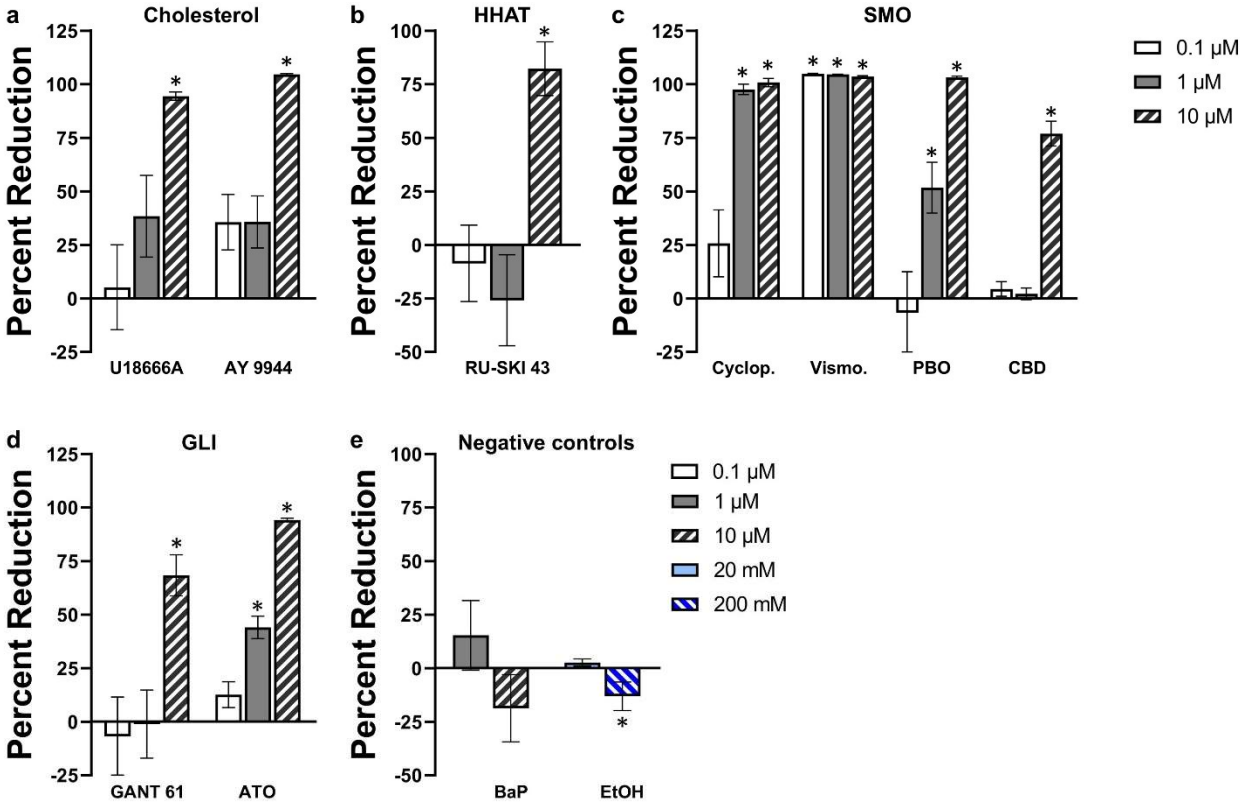

Fig. 3 Mechanistically distinct small molecules reduce Shh pathway activity in a model of whole pathway signal transduction. (**a-d**) The optimized co-culture was treated with graded concentrations of Shh pathway antagonists reported to target cholesterol synthesis and transport (**a**), HHAT (**b**), signal transduction through SMO (**c**), or GLI transcription factors (**d**). (**e**) The negative controls benzo[a]pyrene (BaP) and ethanol (EtOH) were included to support the specificity of the model. Pathway activity was evaluated based on normalized luminescent reporter activity, and percent reduction in reporter activity was defined relative to vehicle (0%) and 10 µM cyclopamine (100%) controls. Bars represent the mean and SEM (n=5). One-way ANOVA with Dunnett's post-hoc test was used to assess significant changes relative to the vehicle. *$p < 0.05$

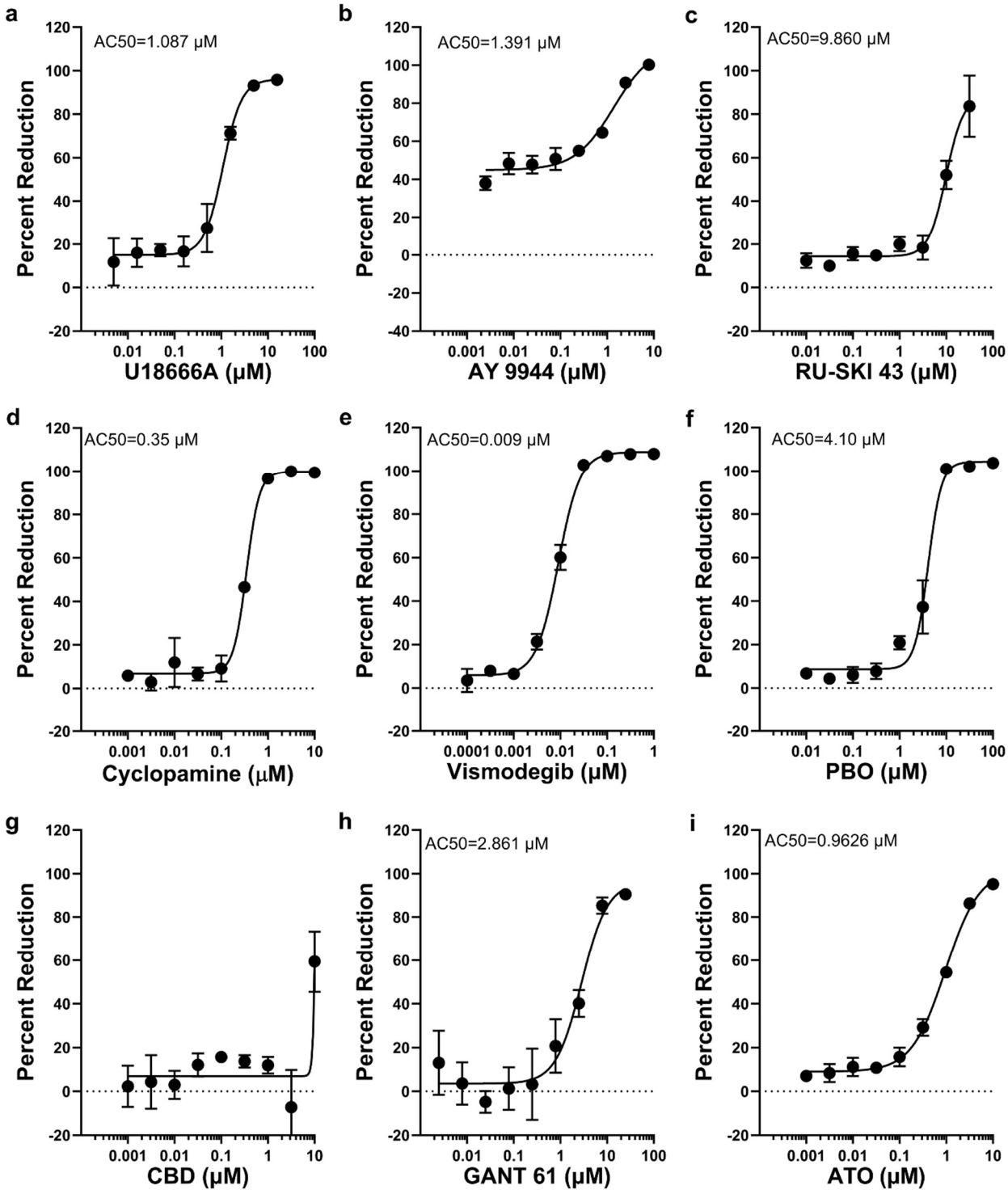

Fig. 4 Shh pathway antagonists generally exhibit similar efficacy with variable potency. (**a-i**) The co-culture model was treated with nine-point, half-log concentration series of pathway inhibitors targeting cholesterol synthesis (**a**) and transport (**b**), HHAT (**c**), the

signal transducer SMO (**d-g**), and GLI transcription factor activation (**h-i**). AC_{50} values, when they could be calculated, are shown in the top left of each plot. Top concentrations were excluded for RU-SKI 43, U18666A, and AY 9944 due to reduced cell viability at the conclusion of the treatment period. Values represent mean and SEM (n=3)

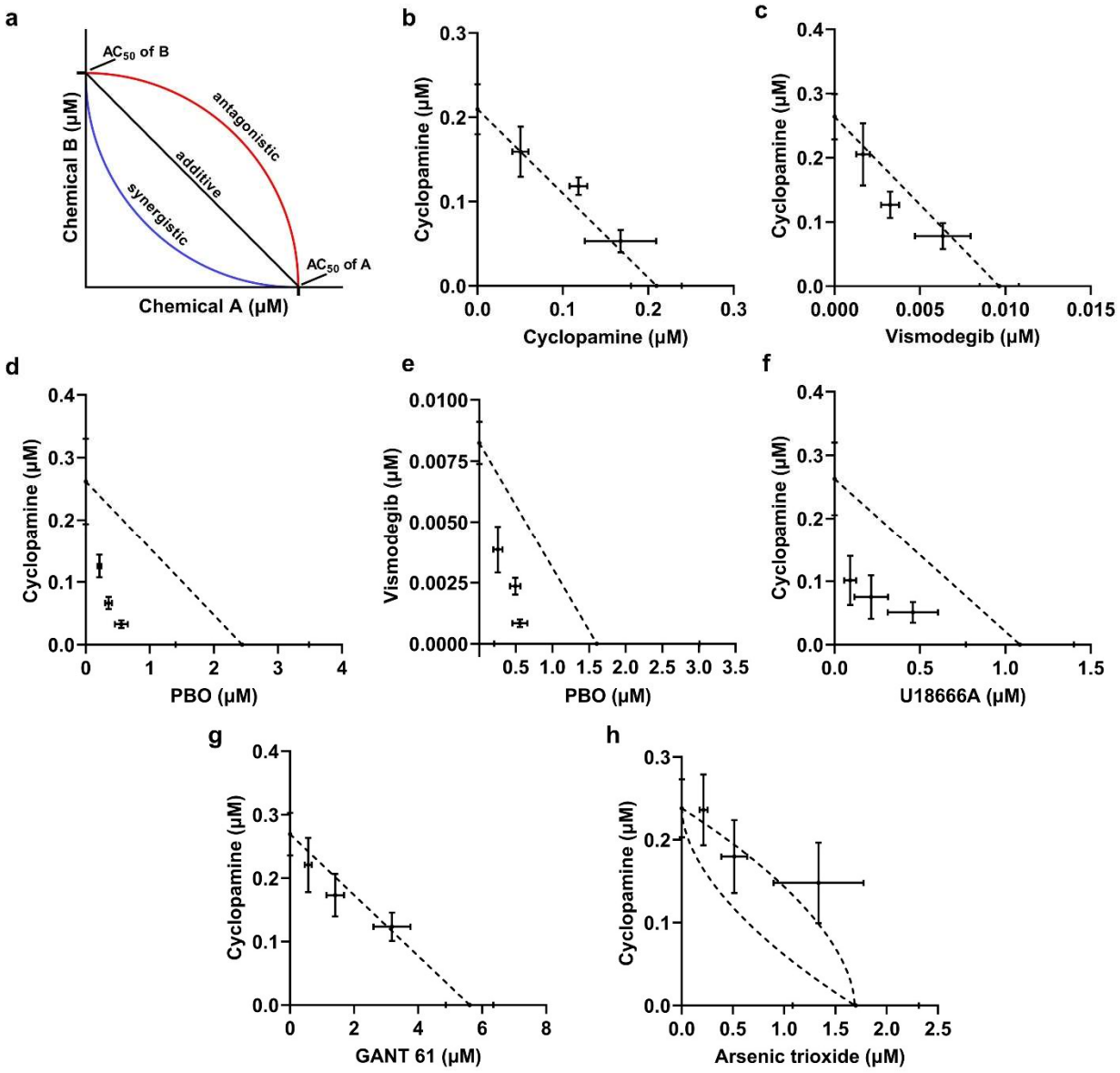

Fig. 5 Co-exposure to Shh pathway antagonists results in additive and synergistic interactions. (**a**) Schematic of an isobologram illustrating a linear isobole (black line) extending between the axes. Potency measures (i.e., AC_{50} values) for individual compounds are plotted on the axes, and the potency of mixtures lie on the isobole for additive combinations, below the isobole for synergistic interactions, and above the isobole for antagonistic interactions. (**b**) Two aliquots of cyclopamine were mixed at ratios of 1:3, 2:2, and 3:1 to assess additivity in a proof-of-concept "mixture" experiment. The

resulting AC_{50} values predictably aligned well with the isobole (dashed line). (**c-d**) Cyclopamine was mixed with other reported SMO inhibitors (vismodegib, PBO) to assess interactions between similarly acting compounds. (**e**) Vismodegib was then mixed with PBO to further characterize the interaction between reported SMO inhibitors. (**f-h**) Cyclopamine was also combined with inhibitors reported to act through distinct mechanistic targets (U18666A, GANT 61, ATO) within the Shh pathway. Dashed lines represent the isobole for each chemical combination, and the dashed curves in panel **h** represent two equally valid non-linear isoboles that describe the interaction between cyclopamine and ATO. Error bars represent 95% confidence intervals (n=3)

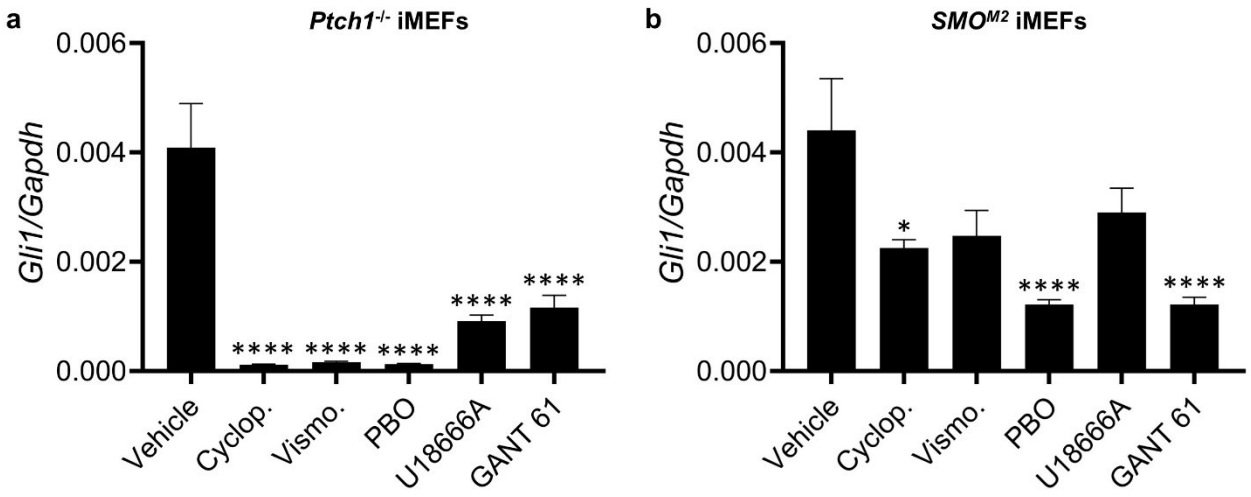

Fig. 6 Shh pathway-modified cell lines exhibit differential sensitivity to Shh antagonists. (**a**) Shh pathway-modified cell lines were treated with vehicle media or 15 μM U18666A, 10 μM cyclopamine, 1 μM vismodegib, 100 μM PBO, or 25 μM GANT61. Shh pathway activity, measured as *Gli1* expression relative to *Gapdh*, was reduced in response to each treatment in *Ptch1*$^{-/-}$ cells. (**b**) In *SMO*^{M2} cells, only cyclopamine, PBO, and GANT61 reduced *Gli1* expression. However, cyclopamine only modestly affected Shh pathway activity in *SMO*^{M2}, whereas cells were strongly antagonized by PBO and GANT 61. Data represent the mean and SEM (n=5). Test compound exposures were compared against vehicle controls using one-way ANOVA with Dunnett's post hoc test. *$p < 0.05$, ****$p < 0.0001$

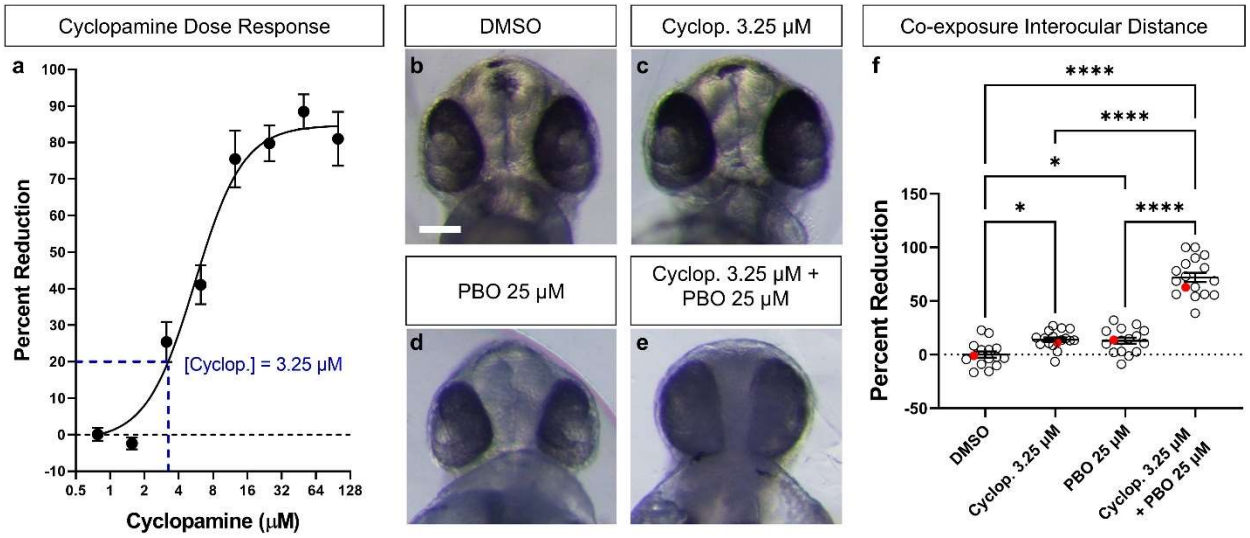

Fig. 7 Co-exposure to cyclopamine and PBO causes greater-than-additive craniofacial malformations in zebrafish embryos. (**a**) Zebrafish embryos were exposed to a cyclopamine dose series from 6 hpf to 24 hpf. Interocular distance measurements were normalized between vehicle (0% reduction) and fully approximated eyes (100% reduction), and the dose-response curve was used to determine the dose of cyclopamine which resulted in a 20% reduction. Sample sizes varied as follows: vehicle, n=15; 0.78 µM, n=15; 1.56 µM, n=15; 3.125 µM, n=15; 6.25 µM, n=11; 12.5 µM, n=8; 25 µM, n=9; 50 µM, n=5; 100 µM, n=7. (**b-e**) Representative embryos treated with vehicle, 3.25 µM cyclopamine, 25 µM PBO, or their combination and imaged ventrally for interocular distance measurement. Scale bar = 100 µm. (**f**) Percent reduction of interocular distance normalized to DMSO control for individual embryos are plotted with red filled circles corresponding to the embryos shown in **b-e**. Co-exposure significantly reduced interocular distance compared to vehicle-treated and single compound-treated embryos. Values represent mean and SEM (vehicle, n=15; cyclopamine, n=16; PBO, n=16; cyclopamine + PBO, n=19). One-way ANOVA with Tukey's multiple comparisons correction was used to compare all treatment conditions. *$p < 0.05$, ****$p < 0.0001$

CHAPTER III

This manuscript was prepared for submission to *Toxicological Sciences*. TGB, RJL designed studies; TGB conducted experiments and acquired data; TGB analyzed data; TGB wrote the manuscript; RJL reviewed and edited the manuscript.

CHAPTER III: A TIERED STRATEGY FOR PRIORITIZING ENVIRONMENTAL SONIC HEDGEHOG SIGNALING DISRUPTORS AS POTENTIAL BIRTH DEFECT RISK FACTORS

Tyler G. Beames[1,2], Robert J. Lipinski[1,2,*]

[1]Department of Comparative Biosciences, School of Veterinary Medicine, University of Wisconsin-Madison, Madison, WI 53706, USA

[2]Molecular and Environmental Toxicology Center, School of Medicine and Public Health, University of Wisconsin-Madison, Madison, WI 53706, USA

[*]Author for correspondence (robert.lipinski@wisc.edu)

ABSTRACT

In animal models, disruption of the Sonic hedgehog (Shh) pathway during embryonic development results in craniofacial malformations that mimic human birth defects, including orofacial clefts and holoprosencephaly. Shh signaling is sensitive to small molecule modulation, but the extent to which environmental chemicals interfere with this pathway during development is unknown. We present an approach to prioritize and evaluate chemicals with the potential to perturb craniofacial development through Shh signaling inhibition. An initial candidate list was identified from a Shh pathway inhibition screen of nearly 8,000 chemicals then refined using the results of a zebrafish developmental toxicity screen, specifically based on altered craniofacial morphogenesis. Additional refinement was made by excluding compounds associated with cellular toxicity, promiscuous activity across assays, or lack of relevant exposure potential. To screen for chemicals acting throughout the Shh pathway, prioritized compounds and a selection of validated antagonists were tested in a cell-based assay that recapitulates inter- and intracellular signal transduction events throughout the Shh pathway. Of the 44 compounds evaluated, 15 reduced Shh pathway activity by ≥20% and were subsequently evaluated at additional concentrations to characterize their potency and efficacy. Despite prioritizing compounds based on bioactivity and phenotypic effects, only 30% of previously defined “inconclusive antagonists” were confirmed in our assay, and “active antagonists” were 57% concordant. Chemicals previously validated in the literature showed 73% concordance with our assay. These results support an integrated strategy for prioritizing potential birth defect risk factors for additional characterization and underscore the importance of validating high-throughput screening results.

INTRODUCTION

Mitigating environmental risk is one of the most feasible approaches for reducing the incidence of birth defects. However, most isolated birth defect cases are believed to arise from multifactorial causes, complicating the identification of specific environmental hazards (Feldkamp et al., 2017; Toufaily et al., 2018). The vast breadth of the exposome, which is comprised of hundreds of thousands of registered chemicals, persistent environmental pollutants, and naturally occurring compounds (Wang et al., 2020; Wild, 2005, 2012), has spurred the development and implementation of high-throughput toxicity screens to reduce reliance on resource intensive animal models and accelerate the generation of toxicological data. Despite these efforts, the majority of chemicals lack adequate toxicity data (Judson et al., 2009), highlighting the need for effective prioritization strategies. Pathway-based *in vitro* assays present one avenue for refining chemical testing.

The Sonic hedgehog (Shh) pathway is a key regulator of embryonic patterning and morphogenesis. Disruption of Shh signaling during early development causes common and significant congenital malformations including cleft lip and palate (Heyne, Melberg, et al., 2015; Lipinski et al., 2008; Rivera-González et al., 2024), holoprosencephaly (Chen, 2016; Chiang et al., 1996; Heyne, Melberg, et al., 2015; Roessler et al., 1996), limb abnormalities (Biesecker, 2011; Rivera-González et al., 2024), and hypospadias (Miyagawa et al., 2011). These disorders are etiologically complex, and the inherent sensitivity of Shh signaling to chemical perturbation makes it a practical focus for the study of environmental birth defect risk factors. Furthermore, while research in cancer biology has focused on characterizing synthetic and naturally occurring Shh signaling

inhibitors as chemotherapeutics (Pietrobono & Stecca, 2018; Rimkus et al., 2016), few reports have explored the potential for environmentally relevant chemicals to contribute to congenital anomalies through Shh pathway interference.

Shh signaling is mediated by a multistep cascade involving several molecular targets that are susceptible to disruption by small molecules (Choudhry et al., 2014). Following the translation of the full-length SHH protein, the carboxy-terminal domain initiates a cholesterol-dependent autoproteolytic cleavage event to produce a truncated SHH-N peptide with a C-terminal cholesterol group. Subsequently, Hedgehog acyltransferase (HHAT) appends a palmitate moiety to the N-terminus of the SHH-N peptide to produce the fully functional SHH ligand. The mature SHH ligand is secreted into the extracellular space and acts in an autocrine and paracrine fashion to bind its receptor, PTCH1. SHH ligand binding relieves PTCH1-mediated inhibition of SMO, and SMO promotes Shh pathway-dependent transcriptional changes by activating GLI transcription factors. Small molecules have been shown to inhibit Shh signaling at multiple points along this cascade, disrupting cholesterol production and transport (Cooper et al., 1998; Gofflot et al., 2001), preventing palmitoylation by HHAT (Ritzefeld et al., 2024), directly inhibiting SMO (Pietrobono & Stecca, 2018; Rimkus et al., 2016), and blocking GLI transcription factor activity (Lauth et al., 2007; Rimkus et al., 2016). We recently developed a simple, cell-based co-culture assay that recapitulates the full Shh signaling cascade and demonstrated its responsiveness to mechanistically diverse pathway antagonists (Beames et al., submitted). This pathway-competent *in vitro* system is well suited for identifying chemicals that disrupt Shh signaling at various mechanistic levels.

As proof of concept, we implemented an approach to prioritize and evaluate chemicals based on their potential to cause Shh signaling-mediated birth defects. To focus our efforts on chemicals with environmental relevance, we leveraged data associated with the U.S. federal Tox21 and Toxicity Forecaster (ToxCast) screening initiatives. Collectively, these datasets contain toxicity estimates for thousands of compounds across hundreds of endpoints. Prioritization began by identifying hits in a Shh antagonism screen conducted under Tox21 that included nearly 8,000 chemicals but has received minimal follow-up. We next integrated the results from a high-throughput zebrafish developmental toxicity screen to focus our efforts on compounds demonstrated to alter craniofacial development and to attempt capture compounds acting upstream of PTCH1 that are difficult to identify with traditional *in vitro* Shh pathway systems. The candidate list was refined by excluding compounds likely to induce cytotoxic or non-specific effects based on Tox21 and ToxCast assays. Active compounds, as well as a selection of validated Shh pathway antagonists, were further characterized in a co-culture model of Shh pathway signal transduction to support future mechanism-driven developmental toxicology studies.

MATERIALS AND METHODS

Chemical selection

The chemical selection workflow is illustrated in Fig. 1. Prioritization began with high-throughput screening data obtained through the US Environmental Protection Agency's (EPA) CompTox Dashboard (https://comptox.epa.gov/dashboard/, Williams et al., 2017). This dashboard hosts assay datasets from a number of sources, including the interagency Tox21 program (Richard et al., 2021). In a Tox21 assay evaluating Shh pathway activity (assay name: TOX21_SHH_3T3_GLI3_Antagonist), NIH/3T3

immortalized mouse embryonic fibroblasts (iMEFs) were used to screen compounds for Shh pathway antagonism. Results of concentration-response assessments were binned as "active antagonist," "inconclusive antagonist," "inconclusive," "inconclusive agonist," "active antagonist," or "inactive." For this prioritization approach, both active antagonists and inconclusive antagonists were considered putative Shh pathway inhibitors and considered for further evaluation.

Chemicals shown to alter morphogenesis in animal models are strong candidates for a mechanism-based screen of teratogens, so we looked to a zebrafish developmental toxicity assay to further refine our compound list (Truong et al., 2014). Based on an established role for Shh signaling in craniofacial morphogenesis and previous evidence that blocking hedgehog signaling during zebrafish embryogenesis results in the loss of anterior craniofacial structures (Eberhart et al., 2006), we selected jaw (assay name: Tanguay_ZF_120hpf_JAW) and snout (assay name: Tanguay_ZF_120hpf_SNOU) morphological endpoints for filtering. Of 1060 compounds screened, 130 altered jaw and/or snout development in the zebrafish screen. While all 1060 compounds included in the zebrafish screen were also included in the Tox21 chemical library, 35 of the craniofacial hits were neither active nor inconclusive antagonists in the Tox21 Shh antagonism screen. These compounds were retained in the prioritization schema to potentially enrich for compounds that act upstream of SHH-PTCH1 binding to disrupt craniofacial morphogenesis but that would not be expected to be identified in traditional *in vitro* Shh pathway antagonism screens that utilize purified ligand or conditioned media.

A series of exclusion criteria were employed to further refine this list. Alongside Shh pathway antagonism, the Tox21 screen assessed changes in cellular viability (assay name: TOX21_SHH_3T3_GLI3_Antagonist_viability). For both Shh pathway antagonism and viability endpoints, half-maximal activity (AC_{50}) concentrations were used to assess potency. To minimize confounding effects due to general cytotoxicity, compounds were excluded if the ratio of *in vitro* viability AC_{50} to Shh antagonism AC50 was <5. Only cell-based endpoints were used for this determination because they more closely align with our *in vitro* screen. This criterion reduced the number of compounds to 97.

Next, we excluded promiscuous compounds—compounds that are active across a wide array of endpoints—by applying a pan-assay activity threshold of 15%. This threshold equated to approximately 150 assays out of up to 1129, the highest number of ToxCast assays in which the remaining compounds had been tested. This criterion reduced the number of compounds to 49.

To assess the accuracy of our prioritization method, 11 additional chemicals identified through a search of the literature as Shh pathway antagonists were included in testing, bringing the total to 60 chemicals. Synthetic chemicals with chemotherapeutic potential were not considered due to their limited potential for unintentional exposure.

The final compound list underwent manual curation. Both carbofuran (CASRN 1563-66-2) and fenamiphos (CASRN 22224-92-6) were excluded for safety reasons. Twelve additional compounds were excluded due to a lack of plausible human exposure sources. Reasons for exclusion at this level included discontinued usage (e.g., benodanil, CASRN 15310-01-7), never having been approved for therapeutic use (e.g. volinanserin, CASRN

139290-91-5), or minimal presence on databases such as PubMed, PubChem, and Google Scholar (e.g. difpas-pyrazole, CASRN 151506-44-4).

Chemicals/Reagents

Cyclopamine was purchased from LC Laboratories. The following compounds were purchased from MilliporeSigma: 2,2,4-Trimethyl-1,3-pentanediol diisobutyrate (CASRN 6846-50-0), 2-naphthalenol (CASRN 135-19-3), 4-hydroxy-3-methoxybenzaldehyde (CASRN 121-33-5), benomyl (CASRN 17804-35-2), butylparaben (CASRN 94-26-8), chlorpropham (CASRN 101-21-3), diisobutyl phthalate (CASRN 84-69-5), diphenylamine (CASRN 122-39-4), esfenvalerate (CASRN 66230-04-4), ethylparaben (CASRN 120-47-8), malaoxon (CASRN 1634-78-2), pentanal (CASRN 110-62-3), propanil (CASRN 709-98-8), propylparaben (CASRN 94-13-3), tert-butylbenzene (CASRN 98-06-6), and thiophanate-methyl (CASRN 23564-05-8). The following compounds were purchased from Cayman Chemical: berberine Cl (CASRN 633-65-8), carbendazim (CASRN 10605-21-7), chlorpyrifos-methyl (CASRN 5598-13-0), curcumin (CASRN 458-37-7), cymoxanil (CASRN 57966-95-7), cypermethrin (CASRN 52315-07-8), cyproconazole (CASRN 94361-06-5), dexamethasone sodium phosphate (CASRN 2392-39-4), dimethomorph (CASRN 110488-70-5), diphenhydramine hydrochloride (CASRN 147-24-0), epigallocatechin gallate (EGCG, CASRN 989-51-5), flutolanil (CASRN 66332-96-5), genistein (CASRN 446-72-0), ipriflavone (35212-22-7), malathion (CASRN 121-75-5), methomyl (CASRN 16752-77-5), paclobutrazol (CASRN 76738-62-0), resveratrol (CASRN 501-36-0), sulforaphane (CASRN 4478-93-7), tomatidine (CASRN 77-59-8), tolnaftate (2398-96-1), triadimefon (CASRN 43121-43-3), triadimenol (CASRN 55219-65-3), triamcinolone (CASRN 124-94-7), vitamin D3 (CASRN 67-97-0), and zerumbone

(CASRN 471-05-6). Carfentrazone-ethyl (CASRN 128639-02-1) and tefluthrin (CASRN 79538-32-2) were purchased from Santa Cruz Biotechnology. All compounds were dissolved at 1000X in 100% DMSO, with the exceptions of 2,2,4-Trimethyl-1,3-pentanediol diisobutyrate, diisobutyl phthalate, pentanal, sulforaphane, and tert-butylbenzene, which were diluted to 1000X stocks in 100% DMSO.

Cell culture

The Shh-LIGHT2 iMEF line possesses a GLI-responsive firefly luciferase reporter as well as a constitutive *Renilla* luciferase reporter (Taipale et al., 2000). CAL2 cells, a modified Shh-LIGHT2 line that stably overexpresses *hSHH*, retain the GLI-responsive luminescent reporter and activate Shh signaling when cultured alone or in combination with Shh-LIGHT2 cells (Beames et al., submitted). Growth medium for both Shh-LIGHT2 cells and CAL2 cells consisted of Dulbecco's Modified Eagle Medium (DMEM) with 10% fetal bovine serum (FBS) and 1% penicillin-streptomycin, as well as the selection agents G418 (0.4 mg/mL) and zeocin (0.15 mg/mL).

Luciferase reporter assay

In vitro experiments were conducted using a previously described co-culture that recapitulates the full Shh signal transduction cascade (Beames et al., submitted). In brief, Shh-LIGHT2 cells and CAL2 cells were expanded separately before being seeded into 24-well plates at a ratio of 9:1 (e.g. 90% Shh-LIGHT2 cells, 10% CAL2 cells) and a density of 2×10^5 cells/well. 24 h after seeding, growth medium was replaced with treatment medium consisting of DMEM with 1% FBS, 1% penicillin-streptomycin, and vehicle (0.1% DMSO) or the indicated treatment in a final concentration of 0.1% DMSO. Following 48 h of treatment, samples were processed using the Dual-Luciferase® Reporter Assay

System (Promega) according to the manufacturer's instructions. Wells were rinsed in DPBS before cells were lysed in Promega's Passive Lysis Buffer. Plates were rocked at room temperature at 100 RPM for 15 min, and lysates were stored -80°C prior to measuring firefly and *Renilla* luciferase activity on a BioTek Synergy HT Multi-Detection Plate Reader (Agilent). Luciferase assay results were normalized by taking the ratio of the firefly luciferase signal relative to the *Renilla* luciferase signal. Data were reported as percent reduction in luminescence, with in-plate vehicle-treated cells defining 0% reduction and cells treated with 10 μM cyclopamine defining 100% reduction.

Scoring compounds by potency and efficacy

Non-linear curve-fitting of concentration-response data was performed using GraphPad Prism. For compounds exhibiting a sigmoidal concentration-response, four-parameter non-linear curve-fitting based on the Hill equation was performed. Biphasic concentration-response profiles were fit using bell-shaped curves. To produce a composite score of activity accounting for both potency and efficacy, the chemical concentration causing 50% Shh pathway reduction—imputed from best-fit curves—and the maximum efficacy achieved were employed.

$$composite\ score = (1/A) * E \qquad (1)$$

where A is the concentration causing 50% pathway reduction and E is the maximum efficacy notated as percent reduction.

RESULTS

Prioritization of chemicals impacting craniofacial development in zebrafish

Compound prioritization is detailed in the Methods and summarized in Fig. 1. The results of a high-throughput cell-based Shh pathway antagonism screen were the focus of initial chemical selection. The Tox21 Shh pathway antagonism screen was used as the foundation for our approach because the results have not previously been validated and because it utilized conditioned media to stimulate Shh signaling, in contrast to our assay that incorporates upstream pathway steps. Of 7,871 screened compounds, 2,333 were either active or inconclusive antagonists.

Next, we considered compounds that altered craniofacial morphogenesis in a zebrafish developmental toxicity screen (Truong et al., 2014). As this screen was not targeted toward Shh pathway inhibition, jaw and snout endpoints were the focus of analysis based on the key role that Shh signaling plays in zebrafish craniofacial development. Jaw and/or snout development was significantly altered in 130 chemicals out of 1060 tested. Cross-referencing these 130 chemicals against the larger Tox21-led screen of Shh pathway antagonism, 98 (75%) were classified as active or inconclusive antagonists. Of the remaining 32 compounds, 26 were classified as inactive (20%) and 6 as putative Shh pathway agonists (5%).

Cell viability was also assessed in the Tox21 screen, and a five-fold potency threshold separating Shh antagonism and reduced viability was set. An additional 33 compounds were excluded to avoid cytotoxicity-based assay interference. Assay promiscuity is a sign of possible non-specific effects. A pan-assay promiscuity threshold of 15% was implemented based on activity across all ToxCast endpoints tested for each compound.

The promiscuity filter removed fifteen more compounds to reduce the number of prioritized chemicals to 49.

The remaining compounds were manually curated to exclude those lacking plausible human exposure routes. Discontinued biocides, investigational drugs, and chemicals lacking use data were not considered for further characterization. To evaluate the utility of this prioritization approach, 11 additional environmentally relevant compounds that were independently shown to antagonize the Shh pathway in peer-reviewed studies were included in the final list. Of these compounds, three (sulforaphane, tomatidine, and zerumbone) were not included in the Tox21 chemical screen, seven (berberine Cl, EGCG, genistein, resveratrol, vitamin D3, tolnaftate, and curcumin) were classified as active or inconclusive antagonists but had been previously excluded because they were not evaluated in the zebrafish screen, and one (ipriflavone) was classified as an active agonist but not included in the zebrafish screen. The Tox21-tested compounds that were initially excluded before being prioritized based on findings in the literature are identified as "literature only" hits in this study to reflect the nature of their inclusion.

The final prioritized list consisted of 46 chemicals (Table 1) and included cyclopamine and piperonyl butoxide, well-characterized Shh pathway inhibitors that cause Shh pathway-mediated malformations in animal models (Everson et al., 2019; Incardona et al., 1998; Lipinski et al., 2008; Rivera-González et al., 2024). In total, 16 (35%) of the compounds were included solely based on altered craniofacial development in zebrafish, nine (20%) were active antagonists in the Tox21 screen and were zebrafish hits, and 10 compounds (22%) were reported as Tox21 inconclusive antagonists and were also zebrafish hits. The remaining 11 (24%) compounds were selected from the literature. This

distribution among the prioritization groups illustrates the complementarity of the morphological, mechanistic, and literature-based approach for compound prioritization (Fig. 2).

Screening prioritized chemicals in a co-culture assay of Shh pathway signal transduction

Each of the prioritized compounds—excluding the well-studied Shh pathway inhibitors cyclopamine and piperonyl butoxide—was screened in a co-culture assay of Shh pathway signal transduction that recapitulates the complete Shh signaling pathway (Beames et al., submitted). While most cell-based screens of Shh pathway disruptors employ purified Shh ligand, conditioned media, or constitutive pathway activation, this co-culture model incorporates SHH ligand production and secretion, ligand-receptor binding at PTCH1, signal transduction through SMO, and downstream transcription factor activation. This system can capture pathway antagonists that act across the Shh signal transduction cascade, including those acting upstream of SMO that are missed in many screening models (Beames et al., submitted).

Fifteen compounds reduced Shh pathway activity by at least 20% at one or more tested concentrations (Fig. 3), meeting the predefined threshold for additional characterization. Results for the remaining compounds are reported in Fig. S1. Of the 10 compounds that were categorized as inconclusive antagonists in the Tox21 Shh antagonism screen, 3 (30%) were confirmed to block Shh signaling in the co-culture system. By contrast, four of seven (57%) chemicals prioritized based on pathway interference and disrupted zebrafish craniofacial development inhibited Shh pathway activity in the co-culture assay. Eight of the 11 compounds identified in a literature search for Shh pathway antagonists

were active in the co-culture assay, yielding a concordance of 73% among independently validated compounds.

Ten compounds were categorized as inconclusive antagonists in the Tox21 screen. Three of these (benomyl, chlorpyrifos-methyl, and triamcinolone) were active in the Shh pathway signal transduction co-culture assay, supporting an elevation in their priority for follow-up testing. In contrast, the remaining inconclusive antagonists were inactive in the co-culture system and did not demonstrate Shh pathway-related teratogenicity in zebrafish.

Finally, the concordance rate among all compounds that altered craniofacial development in zebrafish was lower at just 20%, consistent with the expectation that, as an untargeted assay, the zebrafish screen likely captures a broad range of developmental toxicants acting on multiple mechanisms of action. The overall concordance across all screened compounds was 34% (Table 2).

Characterizing concentration-response profiles to rank-order chemicals for additional validation

Compounds which exceeded the 20% threshold in the initial co-culture screen underwent additional characterization using expanded concentration series. Tomatidine was excluded from this follow-up assessment due to poor solubility. Individual data points were excluded from curve fitting due to reduced viability if visual inspection revealed a loss of monolayer integrity at the end of the treatment period or the *Renilla* luciferase signal fell below a threshold of relative luminescent units (RLU).

The expanded concentration-response curves revealed differences in potency and efficacy among the tested chemical (Fig. 4). Several compounds, including tolnaftate, zerumbone, diphenhydramine HCl, 2-naphthalenol, chlorpyrifos-methyl, vitamin D3, esfenvalerate, and benomyl, showed stronger pathway reduction at concentrations above 10 μM, the upper limit utilized in the threshold-based screen. Triamcinolone, by contrast, showed a similar flat partial antagonistic response despite expanding the concentration range by an order of magnitude higher and lower. Notably, biphasic effects were more apparent from the expanded concentration-response curves for ipriflavone and berberine Cl. Ipriflavone, interestingly, was identified as a Shh pathway agonist in the Tox21 screen, which may reflect difficulties in fitting curves to data with different profiles across large-scale screening efforts.

To rank compounds for additional follow-up testing, a composite score based on potency and efficacy was assigned to each compound. Because AC_{50} values could not be determined for compounds that lacked an inflection point in the fit curve (i.e., 2-naphthalenol and chlorpyrifos-methyl) or for biphasic compounds that did not closely fit a curve described by the Hill equation (i.e., ipriflavone and berberine Cl), the concentration of each chemical reducing Shh pathway activity by 50% was instead used to estimate compound potency. Composite scores are defined by the product of the maximum efficacy and the reciprocal of the estimated 50% inhibitory concentration. Higher scores reflect a higher prioritization. Composite scores could not be calculated for esfenvalerate and EGCG, which did not achieve 50% reduction in activity. Triamcinolone, which did not demonstrate any clear concentration-dependent activity, was excluded

from ranking. The 50% reduction concentrations, maximum efficacies, and composite scores are listed in Table 3.

DISCUSSION

The human exposome is comprised of hundreds of thousands of registered chemicals and mixtures, persistent pollutants, unintentional byproducts, and naturally occurring compounds (Escher et al., 2017; Wang et al., 2020; Wild, 2012). Given the limited developmental toxicity data for most of these environmental factors, efficient prioritization strategies and tractable screening assays are critical for identifying compounds for further testing in biological models of increasing complexity (Knudsen et al., 2011). In this study, we leveraged publicly available high-throughput toxicity screening datasets to produce and refine a list of putative environmental Shh pathway antagonists. We then employed a recently developed cell-based assay of Shh pathway signal transduction to screen this prioritized compound list, as well as additional Shh pathway antagonists described in independent studies, for Shh pathway inhibition. This study demonstrates an integrated approach for leveraging multiple high-throughput datasets to identify potential birth defect risk factors.

As expected, high concordance (73%) was observed between compounds selected from the literature and hits in the Shh pathway signal transduction co-culture. These compounds were generally identified in more than one study, and Shh signaling disruption was often assessed through multiple endpoints. Curcumin and resveratrol, which did not surpass the 20% reduction threshold set for this study, were trending such that an additional higher concentration may have resolved the apparent discordance (Fig. S1). Genistein, by contrast, showed no clear concentration-dependency.

Concordance was lower when comparing our co-culture assay against the "active antagonists" identified from the Tox21 Shh pathway antagonism screen (57%). The limited concentration range utilized for hit-calling in the co-culture assay may again account for some of the inconsistent results, but this discordance also underscores the need for follow-up characterization and validation. The value of independent assessment of high-throughput screening data is also apparent among the compounds categorized as inconclusive antagonists in the Tox21 screen. Notably, only 3 of 10 inconclusive antagonists inhibited Shh pathway activity in the Shh pathway signal transduction co-culture assay. The utility of tractable follow-up evaluations is clear here given that these compounds would be missed if only "active antagonists" were considered for further assessment. Conversely, investing time and resources into testing all inconclusive antagonists in more complex biological models would be highly inefficient given the relatively low confirmation rate.

The disruption of jaw and/or snout development in zebrafish embryos was the least predictive of Shh pathway antagonism. However, because the zebrafish screen was not targeted to a specific mechanism of action, it is likely that a portion of the compounds tested alter craniofacial development through Shh signaling-independent mechanisms. Depending on the goals of future screening approaches, compound prioritization must weigh the biological relevance of phenotypic data against the increased proportion of negative hits likely to arise due to distinct mechanisms that converge on the morphologic feature(s) considered. An alternative approach to mitigate this challenge would be to select compounds for validation based only on mechanistic studies and utilize the phenotypic data to prioritize compounds for *in vivo* developmental toxicity experiments.

The SHH-autonomous nature of the co-culture assay, which makes it capable of identifying Shh pathway inhibitors that act throughout the signaling cascade, has potential benefits for use in screening. However, in this study, the lack of hits among compounds that altered craniofacial development in zebrafish but had no effect in the Tox21 screen suggests that no upstream inhibitors were present among the 44 compounds tested. Given that the majority of small molecule Shh inhibitors are purported to target the Shh pathway downstream of SHH ligand secretion, a larger screen may be required to fully realize the benefits of this pathway-competent assay.

Several trends among compound classes emerge based on the concordance or discordance of their activity across the assays considered in this study. Eight phytochemicals were tested in this screen, of which seven were hits or trending in the Shh pathway signal transduction assay. Furthermore, all five phytochemicals which were included in the Tox21 Shh antagonism screen were categorized as active antagonists. While genistein was the only compound among these phytochemicals to be included in the zebrafish screen, it did not alter jaw or snout development. In animal models, teratogenic effects have been described for berberine (Martini et al., 2020), curcumin (Wu et al., 2007), and an essential oil containing zerumbone (Thitinarongwate et al., 2021), though the reported effects were not linked to disruption of Hedgehog signaling. Despite inhibiting Shh signaling in the Tox21 screen, genistein did not demonstrate antagonistic effects in the current Shh pathway signal transduction assay and had limited effects in a previous chemical screen (Lipinski & Bushman, 2010). Genistein has independently been found to act as a teratogen in zebrafish (Kim et al., 2009) and in a rat whole embryo culture model, though its impacts on mammalian development are

proposed to be mitigated through biotransformation (Zou et al., 2012). Conversely, EGCG and curcumin are noted to be protective of Down Syndrome-associated craniofacial phenotypes (McElyea et al., 2016; Rueda et al., 2020), and there is evidence that curcumin, resveratrol, and sulforaphane attenuate the embryotoxicity and teratogenicity of developmental alcohol exposure in zebrafish (Małkowska et al., 2024; Wang et al., 2019; Wu et al., 2024). Previous reports also suggest that genistein and sulforaphane may be protective against hypospadias (Amato et al., 2022; Shi et al., 2024). Tomatidine, a natural plant alkaloid that is structurally related to cyclopamine, was shown to act as a weak inhibitor of Shh signaling but is considered non-teratogenic (Keeler, 1978; Lipinski et al., 2007). The disparate reports on the actions of phytochemicals on early development highlight the importance of conducting targeted studies informed by known mechanisms of teratogenicity to ensure that adverse effects do not occur at doses that are considered safe or even beneficial. If overlap exists between the recommended usage for supplements containing these phytochemicals and their adverse developmental impacts, then the benefits of such supplements should be carefully weighed against possible risks during pregnancy.

Additional compound classes are of potential interest. Three pyrethroid insecticides altered craniofacial development in the zebrafish screen, and esfenvalerate reduced pathway activity in the Tox21 screen as well as the Shh pathway signal transduction assay. Notably, pyrethroid pesticide formulations often contain the additive piperonyl butoxide (PBO), a compound that is known to inhibit Shh signaling and cause Shh-associated malformations in mice and zebrafish (Everson et al., 2020; Everson et al., 2019; Wang et al., 2012). In addition, we recently reported on the ability of PBO to synergistically

interact with other Shh pathway antagonists to reduce signaling activity (Beames et al., submitted). While evidence for pyrethroid-mediated inhibition of Shh signaling is very limited (Chaklader & Law, 2015; Uggini et al., 2012), the potential for interaction with PBO may warrant further investigation, even if separate mechanisms underlie the craniofacial effects of these pyrethroids and PBO. The benzimidazole fungicides benomyl, carbendazim, and thiophanate-methyl altered zebrafish craniofacial development and were categorized as inconclusive antagonists in the Tox21 screen. Although only benomyl reduced signaling activity in the Shh pathway signal transduction co-culture system, benzimidazoles have been hypothesized to target Shh signaling by disrupting the primary cilium, the site of SMO-mediated signal transduction (Larsen et al., 2015).

A potential limitation of the prioritization strategy used in this study is that the highest priority compounds identified in the Tox21 Shh pathway antagonism screen may not have been included in the smaller zebrafish screen. To address this concern, we scrutinized the top 30 AC_{50}-ranked compounds that were not included in the zebrafish assay and that were not excluded based on our viability criterion. Because many of the remaining compounds were screened in far fewer than 1000 of the ToxCast assays, the 15% pan-assay activity cut-off was modified to a flat value of 150 assays. Among these compounds (listed in Table S1), 15 were chemotherapeutics that would have been excluded from testing based on limited exposure potential in pregnant women. An additional 6 compounds were ionic liquids, a related group of chemicals with some industrial uses that exhibit variable properties based on structural differences (Gonçalves et al., 2021). The overrepresentation of ionic liquids in this grouping may suggest an unreported mechanism of toxicity, but it may also reflect non-specific effects given the broader

overrepresentation of this class of compound among Tox21 antagonists—49 hits, or ~3% of all Tox21 active and inconclusive antagonists. Rather than missing the most relevant compounds by limiting our prioritization to zebrafish-tested hits, it appears likely that many of the most potent compounds identified in the Tox21 screen are of limited environmental relevance. Based on the results of this study, an expanded screen is warranted to evaluate compounds that were not included in the zebrafish screen as well as additional chemicals that were negative in the Tox21 screen to more robustly evaluate differences in the performance of these *in vitro* approaches.

Taken together, these findings support the prioritization of chemicals for developmental toxicology testing by integrating publicly available toxicity screening data and highlight the benefits of validation studies following high-throughput chemical screens. Specifically, our results suggest that the use of phenotypic data in prioritization may be more effective following mechanistic validation studies than as a means for refinement early in prioritization. Additional studies should be conducted to investigate the developmental toxicity of the high-priority compounds identified in this study and to elucidate whether the combination of phenotypic and mechanistic data correlate with a targeted assessment of Shh-mediated craniofacial malformation. Furthermore, based on our recent report of synergistic interactions among Shh pathway inhibitors and a previous study investigating additive interactions among natural Hedgehog inhibitors, co-exposure testing using validated Shh pathway inhibitors could improve our understanding of environmental birth defect risk factors (Beames et al., submitted; Lipinski et al., 2007). Refined approaches to compound prioritization and testing as

described herein will help to further define the impacts of prenatal exposures and support the prevention of etiologically complex birth defects.

DECLARATIONS

Funding: This work was supported by the National Institutes of Environmental Health Sciences under awards R01ES026819, F31ES034632, and T32ES007015.

Conflict of interest: The authors declare that they have no conflict of interest.

Data Availability Statement: The datasets generated during the current study are available from the corresponding author on reasonable request.

TABLES

Table 1. Prioritized chemicals for in-house testing

CASRN	Chemical Name	Activity Source	AC50 range (μM)	References
6846-50-0	2,2,4-Trimethyl-1,3-pentanediol diisobutyrate	zebrafish	34-65	
135-19-3	2-Naphthalenol	*in vitro*/zebrafish	7.9-34	
121-33-5	4-Hydroxy-3-methoxybenzaldehyde	zebrafish	28-31	
17804-35-2	Benomyl	*in vitro*/zebrafish	41-47	
633-65-8	Berberine Cl	*in vitro*/literature search	0.1-7.5[b]	Sun et al., 2022; Wang et al., 2015
94-26-8	Butylparaben	zebrafish	20-23	
10605-21-7	Carbendazim	*in vitro*/zebrafish	8.7-25	
128639-02-1	Carfentrazone-ethyl	zebrafish	2.0-4.1	
101-21-3	Chlorpropham	*in vitro*/zebrafish	27-31	
5598-13-0	Chlorpyrifos-methyl	*in vitro*/zebrafish	41-78	
458-37-7	Curcumin	*in vitro*/literature search	10[c]-40[d]	Du et al., 2013; Elamin et al., 2010; Lian et al., 2015; Slusarz et al., 2010
4449-51-8	***Cyclopamine***[a]	***in vitro*/ zebrafish**	***0.17-27***	
57966-95-7	Cymoxanil	zebrafish	14-26	
52315-07-8	Cypermethrin	zebrafish	3.4-10	
94361-06-5	Cyproconazole	*in vitro*/zebrafish	9.3-23	
2392-39-4	Dexamethasone sodium phosphate	*in vitro*/zebrafish	0.34-2.8	
84-69-5	Diisobutyl phthalate	zebrafish	40-48	
110488-70-5	Dimethomorph	*in vitro*/zebrafish	0.07-37	
147-24-0	Diphenhydramine hydrochloride	*in vitro*/zebrafish	7.1-36	
122-39-4	Diphenylamine	zebrafish	19-29	

Table 1. (Continued)

CASRN	Chemical Name	Activity Source	AC50 range (μM)	References
989-51-5	Epigallocatechin gallate	*in vitro*/literature search	10[c]-25[b]	Ding & Yang, 2021; Mayer et al., 2023; Slusarz et al., 2010; Tang et al., 2012
66230-04-4	Esfenvalerate	*in vitro*/zebrafish	0.96-34	
120-47-8	Ethylparaben	zebrafish	16	
66332-96-5	Flutolanil	*in vitro*/zebrafish	5.7-47	
446-72-0	Genistein	*in vitro*/literature search	3[c]-15[b]	Fan et al., 2013; Slusarz et al., 2010; Zhang et al., 2012
35212-22-7	Ipriflavone	literature search	1.2	Lipinski & Bushman, 2010
1634-78-2	Malaoxon	*in vitro*/zebrafish	8.8	
121-75-5	Malathion	*in vitro*/zebrafish	26-34	
16752-77-5	Methomyl	zebrafish	38	
76738-62-0	Paclobutrazol	zebrafish	10	
110-62-3	Pentanal	zebrafish	32-34	
51-03-6	***Piperonyl butoxide***[a]	***in vitro/ zebrafish***	***3.2-6.5***	
709-98-8	Propanil	*in vitro*/zebrafish	7.9-34	
94-13-3	Propylparaben	zebrafish	10-12	
4478-93-7	Sulforaphane	literature search	4[b]-5[b]	Rodova et al., 2012; Wang et al., 2022
77-59-8	Tomatidine	literature search	2-3	Lipinski & Bushman, 2010; Lipinski et al., 2007
79538-32-2	Tefluthrin	zebrafish	3.4-10	
98-06-6	tert-Butylbenzene	zebrafish	3.1-3.7	
23564-05-8	Thiophanate-methyl	*in vitro*/zebrafish	43-49	
2398-96-1	Tolnaftate	*in vitro*/literature search	4-28	Lipinski & Bushman, 2010
501-36-0	Resveratrol	*in vitro*/literature search	10[c]-55[d]	Gao et al., 2015; Mo et al., 2011; Slusarz et al., 2010

Table 1. (Continued)

CASRN	Chemical Name	Activity Source	AC50 range (μM)	References
43121-43-3	Triadimefon	zebrafish	28	
55219-65-3	Triadimenol	*in vitro*/zebrafish	25	
124-94-7	Triamcinolone	*in vitro*/zebrafish	0.069-33	
67-97-0	Vitamin D3	*in vitro*/literature search	10[d]-19	Tang et al., 2011
471-05-6	Zerumbone	literature search	7.1	Hosoya et al., 2008

[a] Well-characterized Shh pathway antagonists demonstrated to cause Shh signaling-mediated craniofacial malformations

[b] Lowest concentration at which significant changes in Shh-related mRNA or protein levels were observed

[c] Lowest concentration at which luminescence was significantly decreased in Shh-LIGHT2 cells

[d] Single concentration assessed for changes in Shh-related mRNA or protein levels

Table 2. Shh pathway signal transduction assay activity by compound group

Prioritization Group	Number of Compounds by Group	Active in Co-culture Assay (≥20% inhibition)	Concordance
Zebrafish craniofacial phenotype hits only	16	0	0%
All zebrafish craniofacial phenotype hits	35	7	20%
Tox21 Shh antagonists (active) + zebrafish craniofacial phenotype hits	7	4	57%
Tox21 Shh antagonists (inconclusive) + zebrafish craniofacial phenotype hits	10	3	30%
Literature-reported Shh antagonists	11	8	73%
All screened compounds	44	15	34%

Table 3. Compounds ranked by composite potency-efficacy score

Compound	Concentration causing 50% Reduction (μM)	Maximum Efficacy (%)	Composite score
Ipriflavone	1.45	116	80.00
Flutolanil	1.59	105	66.04
Sulforaphane	1.43	90.5	63.29
Berberine Cl	3.92	88.4	22.55
Diphenhydramine HCl	9.03	102	11.30
Tolnaftate	9.47	99.2	10.48
Zerumbone	13.15	74.1	5.63
Vitamin D3	11.15	53.3	4.78
2-naphthalenol	25.6	82.6	3.23
Chlorpyrifos methyl	30.5	75.3	2.47
Benomyl	95.4	92.7	0.97
Esfenvalerate	n.d.[a]	47.3	n.d.
EGCG	n.d.	41.9	n.d.

Table S1. Top 30 AC_{50}-ranked compounds that were not included in zebrafish testing

CASRN	Chemical Name	Notes	AC50 (μM)
50-76-0	Actinomycin D	Chemotherapeutic[a]	0.0019
204005-46-9	Semaxanib	Chemotherapeutic[a]	0.0040
363-24-6	Dinoprostone	Medication to induce labor[a]	0.0050
108852-90-0	Nemorubicin	Chemotherapeutic[a]	0.0057
50-23-7	Hydrocortisone	Corticosteroid	0.0110
518-28-5	Podofilox	Genital wart medication	0.0110
316-42-7	Emetine dihydrochloride	Emetic, plant alkaloid	0.0122
244193-56-4	1-Decyl-3-methylimidazolium tetrafluoroborate	Ionic liquid	0.0125
433337-23-6	1-Decyl-3-methylimidazolium bis(trifluoromethylsulfonyl)imide	Ionic liquid	0.0131
483-18-1	Emetine	Emetic, plant alkaloid	0.0136
114977-28-5	Docetaxel	Chemotherapeutic[a]	0.0157
72496-41-4	Pirarubicin	Chemotherapeutic[a]	0.0163
362043-46-7	1-Decyl-3-methylimidazolium hexafluorophosphate	Ionic liquid	0.0182
66575-29-9	Colforsin	Cardiovascular medication	0.0201
868540-17-4	Carfilzomib	Chemotherapeutic[a]	0.0202
292618-32-7	Gimatecan	Chemotherapeutic[a]	0.0253
70476-82-3	Mitoxantrone dihydrochloride	Chemotherapeutic[a]	0.0275
123-03-5	Cetylpyridinium chloride	Quaternary ammonium compound[a]	0.0283
125317-39-7	Vinorelbine tartrate	Chemotherapeutic[a]	0.0322
20830-81-3	Daunorubicin	Chemotherapeutic[a]	0.0395

Supplemental Table S1. (Continued)

CASRN	Chemical Name	Notes	AC50 (μM)
57852-57-0	Idarubicin hydrochloride	Chemotherapeutic[a]	0.0407
905-97-5	3,3'-Diethylthiacarbocyanine iodide	Fluorescent dye	0.0488
188589-32-4	1-Decyl-3-methylimidazolium bromide	Ionic liquid	0.0576
412009-62-2	1-Decyl-3-methylimidazolium trifluoromethanesulfonate	Ionic liquid	0.0683
81995-09-7	1-Dodecyl-3-methylimidazolium iodide	Ionic liquid	0.0778
18556-44-0	Vinrosidine sulfate (1:x)	Chemotherapeutic[a]	0.0780
149647-78-9	Suberoylanilide hydroxamic acid	Chemotherapeutic[a]	0.0806
84878-61-5	Maduramicin ammonium	Veterinary drug	0.0809
131740-09-5	Flavopiridol hydrochloride	Chemotherapeutic[a]	0.0811
1032350-13-2	MK-2206	Chemotherapeutic[a]	0.0914

[a] Excluded based on low potential for unintentional exposure during gestation

FIGURES

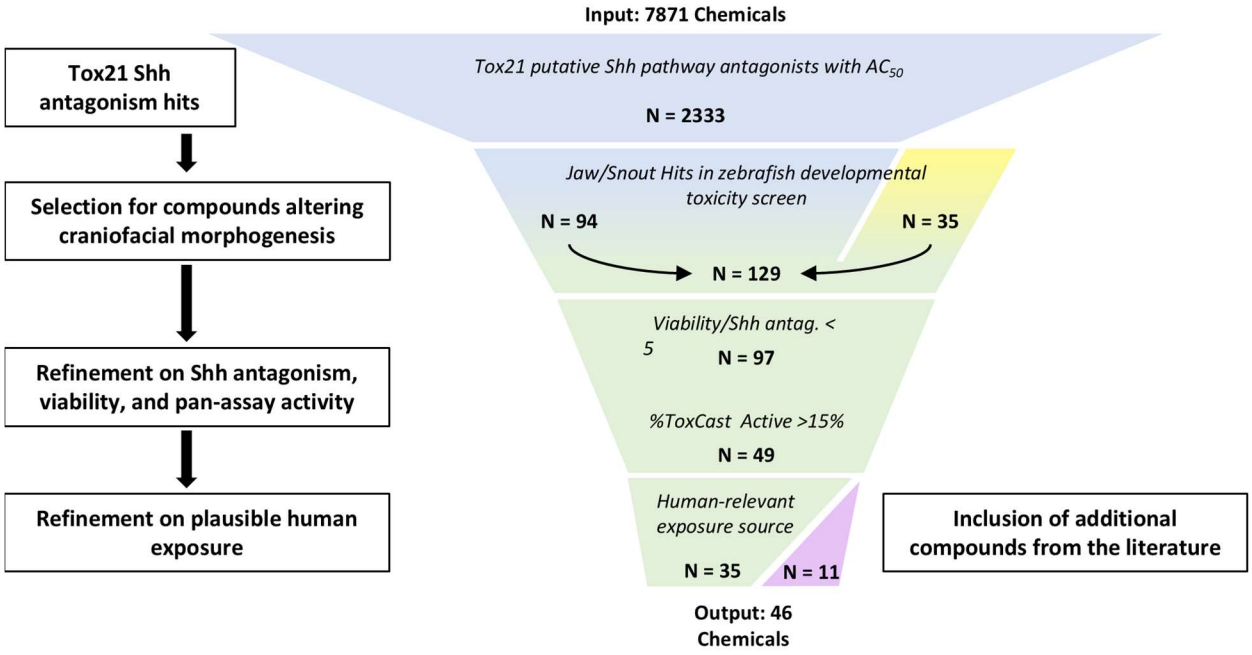

Figure 1. Prioritization of possible Shh signaling antagonists using an integrated approach. 7,871 chemicals were screened in a high-throughput Shh pathway antagonism assay, of which 2,333 were categorized as "active antagonists" or "inconclusive antagonists. A developmental toxicity screen in zebrafish enabled us to refine this list based on each compound's ability to alter craniofacial development in an organism and include 35 compounds that were not active in the Tox21 Shh pathway antagonism screen but may act upstream in the Shh signaling pathway. Additional compounds were excluded from in-house testing on the basis of potential cytotoxic and non-specific effects that may produce false positives. Finally, the list was curated to focus on chemicals with plausible human exposure sources, and 11 chemicals were included from the literature to compare activity of prioritized compounds against those which were previously validated.

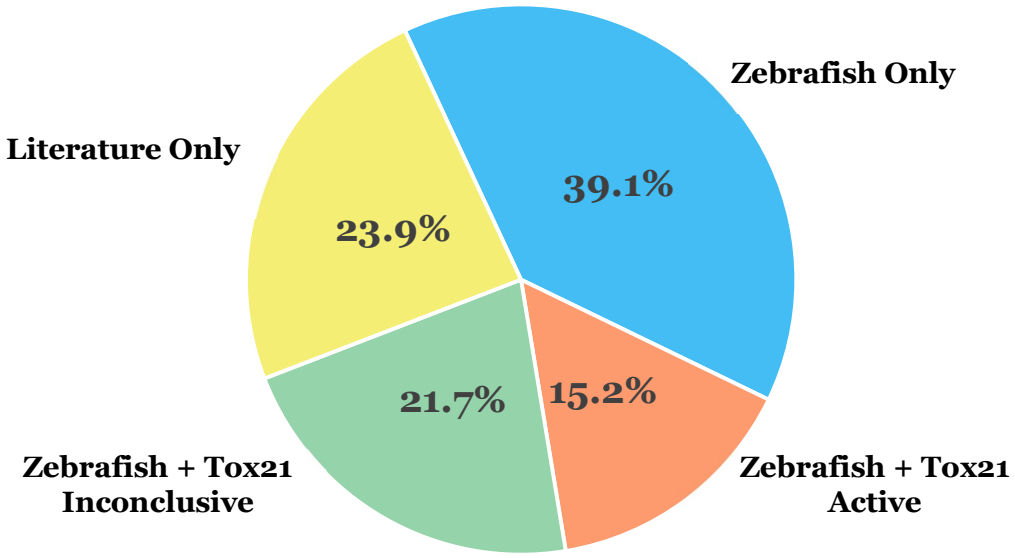

Figure 2. Breakdown of prioritized compounds by assay source. Chemical selection was based on the disruption of craniofacial development in zebrafish, activity in the Tox21 Shh antagonism assay, and independent reports of Shh pathway inhibition in the literature. The proportion of compounds identified from individual sources or across multiple sources is summarized in this chart.

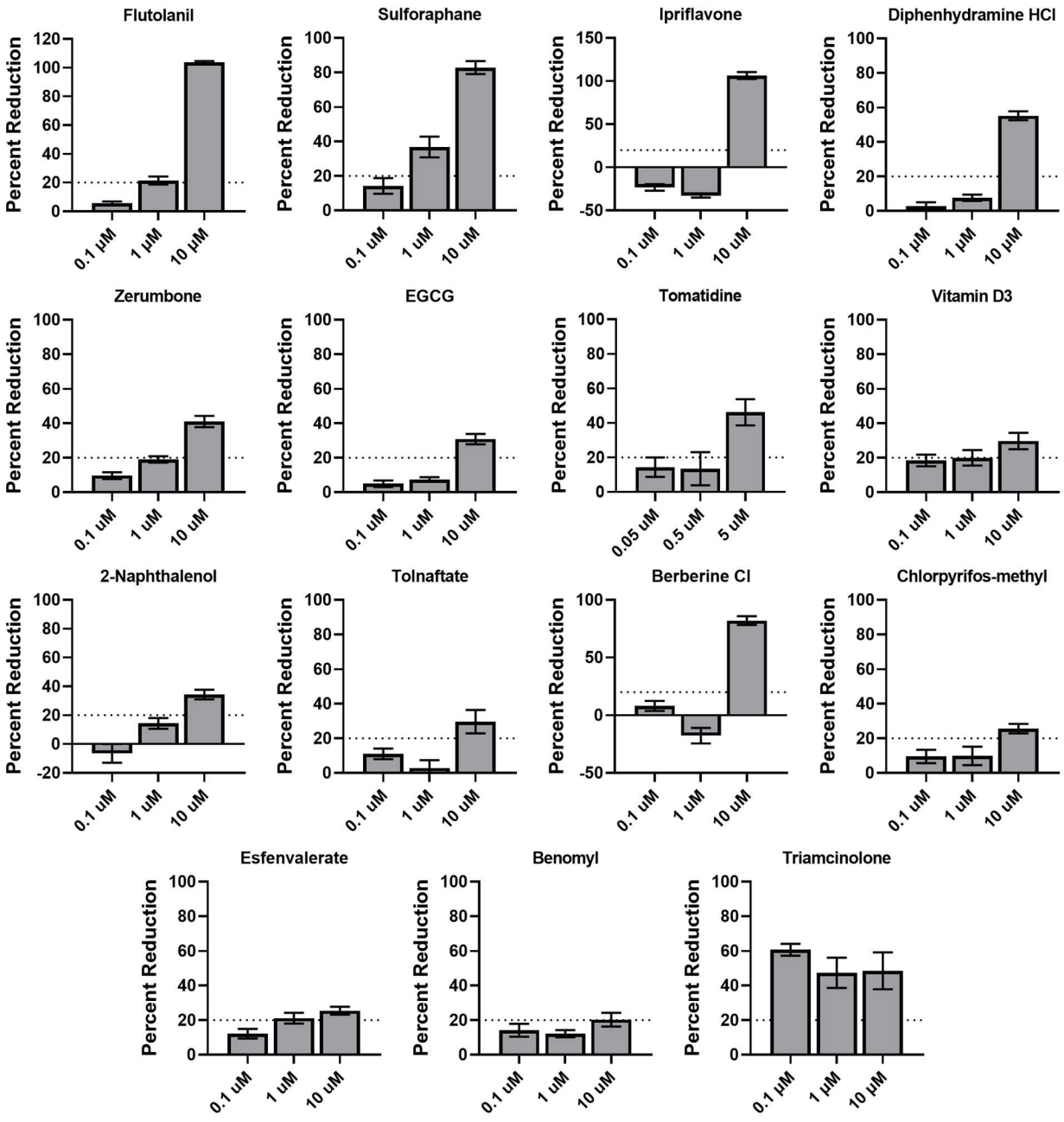

Figure 3. Environmental chemicals reduced pathway activity in a cell-based model of Shh signal transduction. A co-culture of CAL2 and Shh-LIGHT2 cells was treated with graded concentrations of putative Shh pathway antagonists. Normalized luminescence was used to evaluate Shh pathway activity, and percent reduction in luminescence was defined based on luminescence in vehicle controls (0%) and cells

treated with 10 μM cyclopamine. (100%) Bars show the mean ± SEM of five replicates. A cutoff of 20% reduction (dotted line) was used to select compounds for further investigation.

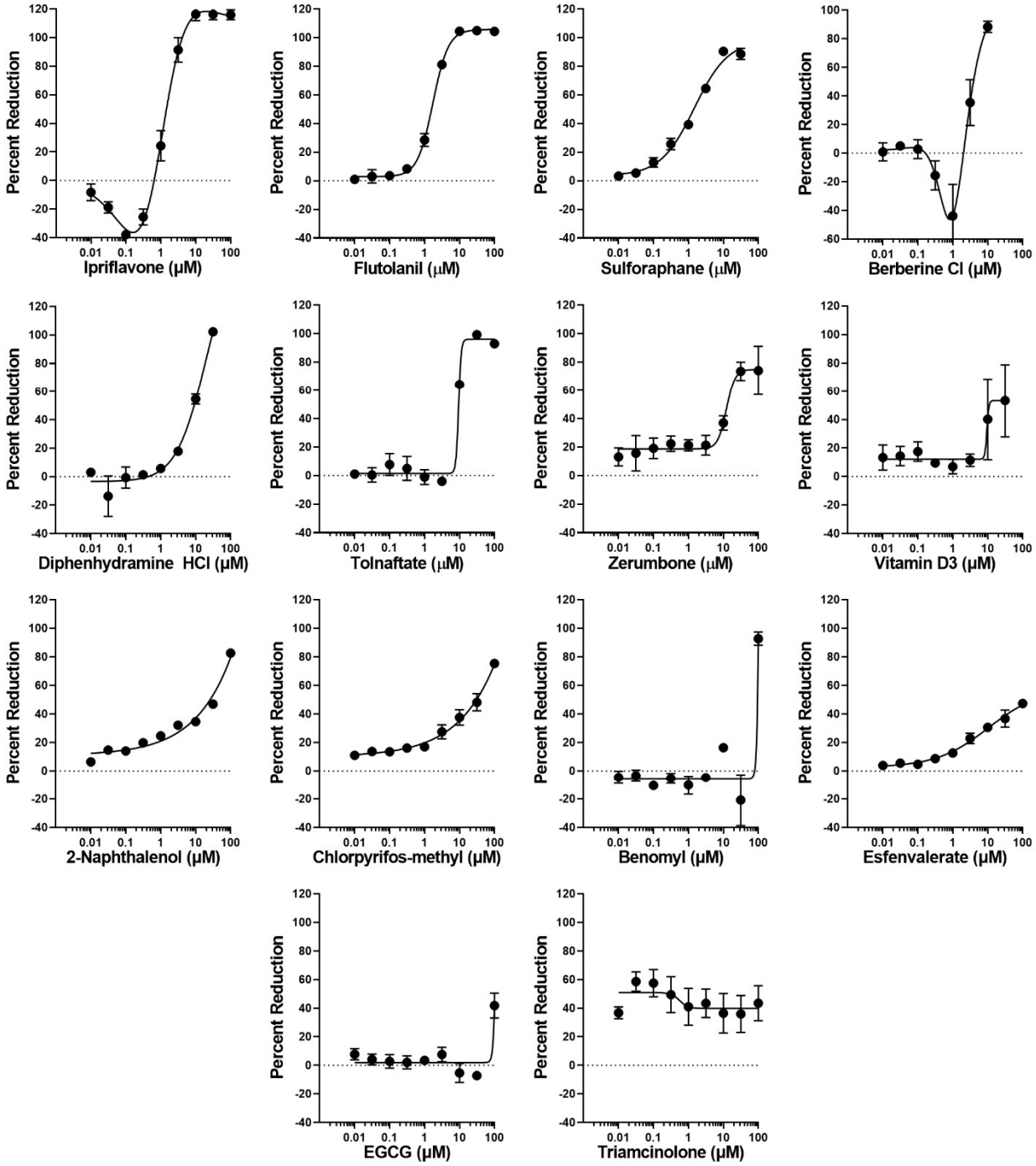

Figure 4. Prioritizing compounds for additional characterization by composite potency-efficacy score. The Shh pathway signal transduction co-culture was treated with nine-point, half-log concentration series of the indicated compounds.

The top concentration was excluded from analysis for compounds which disrupted cell monolayers upon visual inspection. Compounds are rank-ordered by composite potency-efficacy score.

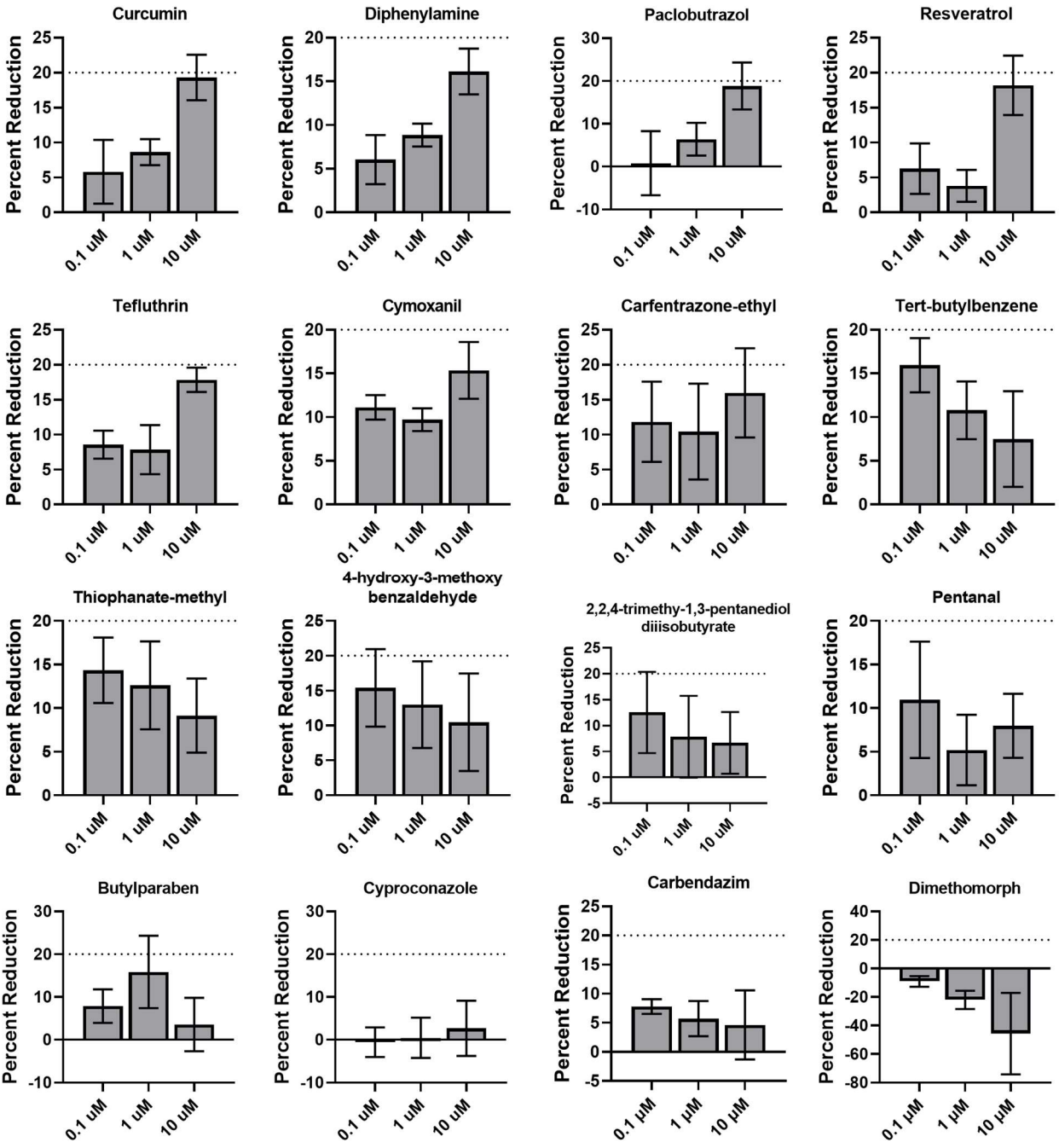

Figure S1. Additional Shh pathway signal transduction co-culture responses (continued on page 90).

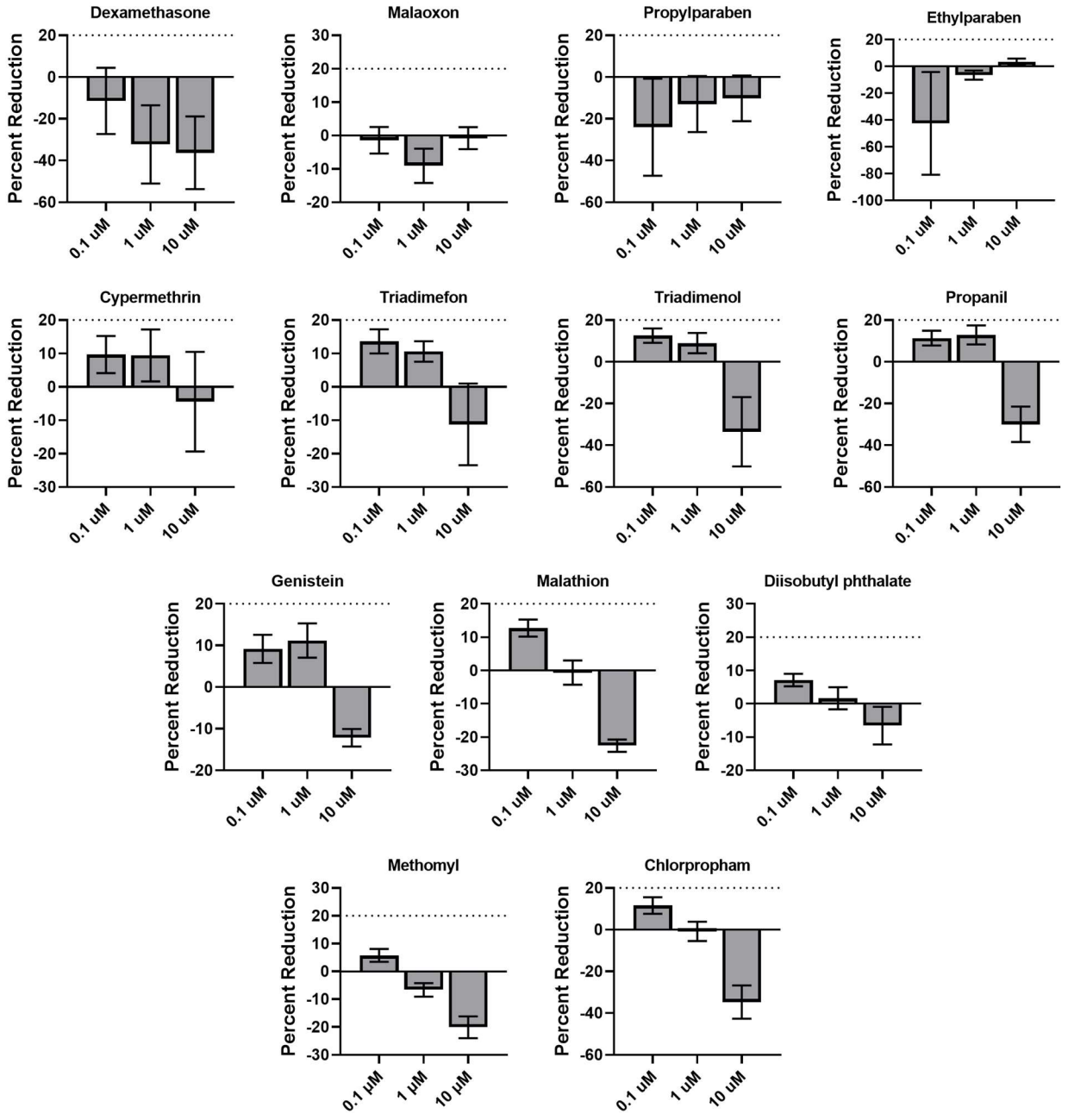

Figure S1. Additional Shh pathway signal transduction co-culture responses. A co-culture of CAL2 and Shh-LIGHT2 cells was treated with graded concentrations of putative Shh pathway antagonists. Normalized luminescence was used to evaluate Shh pathway activity, and percent reduction in luminescence was defined based on

luminescence in vehicle controls (0%) and cells treated with 10 μM cyclopamine. (100%) Bars show the mean ± SEM of five replicates. The compounds included in this supplemental figure failed to exceed the cutoff of 20% reduction (dotted line) that was used to select compounds for further investigation.

CHAPTER IV

This manuscript was published in Birth Defects Research (2025 Apr;117(4):e2466. doi: 10.1002/bdr2.2466/dev.191064). TGB, RJL, JBP designed studies; TGB, MYS, JBP conducted experiments and acquired data; TGB, MYS, RBW, JBP analyzed data; TGB, MYS, RJL wrote the manuscript; all authors read and approved the final manuscript.

CHAPTER IV: EXAMINING THE NEURODEVELOPMENTAL IMPACT OF SONIC HEDGEHOG PATHWAY INHIBITION IN MICE

Tyler G. Beames[1], Megan Y. Stewart[1], Rachel B. Walkup[1], Jules B. Panksepp[1], Robert J. Lipinski[1,*]

[1]Department of Comparative Biosciences, School of Veterinary Medicine, University of Wisconsin-Madison, Madison, Wisconsin, USA

[2]Waisman Center, University of Wisconsin-Madison, Madison, Wisconsin, USA

[*]Author for correspondence (robert.lipinski@wisc.edu)

ABSTRACT

Background: Neurodevelopmental disorders (NDDs) are common, highly variable, and etiologically complex. Identifying environmental factors that adversely impact prenatal brain development is a direct path to NDD prevention. Small molecule disruption of the Sonic hedgehog (Shh) signaling pathway, a key regulator of craniofacial morphogenesis, can lead to overt face and forebrain malformations that produce profound neurological deficits. However, whether environmental disruption of Shh signaling can cause subtle neurodevelopmental outcomes in the absence of overt facial malformations was unknown.

Methods: We developed a dietary model of Shh signaling inhibition using the specific Shh pathway antagonist vismodegib. C57BL/6J mice were fed control chow or chow containing 25, 75, or 225 ppm vismodegib from gestational day (GD)4 through GD12 to target Shh signaling during craniofacial morphogenesis. Impacts of Shh pathway disruption on face and forebrain development were examined in exposed embryos and fetuses, and behavioral characteristics were assessed in adult mice.

Results: Exposure to chow containing 225 ppm vismodegib resulted in abnormal forebrain patterning at GD11, face and brain malformations at GD17, and early postnatal mortality, while lower treatment groups appeared phenotypically normal. Adult mice exposed to 25 and 75 ppm vismodegib outperformed control mice on repeated rotarod sessions, but treated mice did not significantly differ from control animals in open field exploration, marble burying, olfactory discrimination and detection, or fear conditioning assays.

Conclusions: Under the examined conditions, prenatal Shh disruption did not produce robust neurobehavioral differences in the absence of craniofacial malformations.

INTRODUCTION

As increased awareness and improved diagnostic criteria have revealed higher incidences of neurodevelopmental disorders (NDDs) such as autism, attention-deficit/hyperactivity disorder, and intellectual disabilities, efforts to prevent these conditions have met with substantial challenges. A growing body of epidemiological and experimental evidence underscores the role of the environment in NDD occurrence, and reducing exposure to environmental toxicants remains the most effective path to prevention (De Felice et al., 2015; Lan et al., 2017; Lyall et al., 2017; Wagner et al., 2006). However, identifying individual risk factors is complicated by the etiologically complex nature of most common NDDs. Moreover, it is not feasible to assess the neurobehavioral impacts of all chemicals and mixtures that make up the exposome. Focusing instead on elucidating environmentally sensitive signaling pathways that contribute to NDDs presents a more direct approach to characterizing risk based on common mechanisms of toxicity.

The Sonic hedgehog (Shh) signaling pathway is a key regulator of craniofacial morphogenesis that is sensitive to both genetic and environmental perturbation (Chen, 2016; Everson et al., 2019; Roessler et al., 1996; Solomon et al., 2012). During embryogenesis, this paracrine factor plays a role in early neurospecification, promoting a ventral identity along the length of the neural tube and within the developing forebrain by counterbalancing dorsalizing factors such as BMPs and Wnt ligands (Ericson et al., 1995; Furuta et al., 1997; Roelink et al., 1995). Shh is also required for the development of the medial ganglionic eminence (MGE), a transient forebrain structure that gives rise to GABAergic cortical interneurons (Butt et al., 2005; Fuccillo et al., 2004; Wichterle et al., 2001; Xu et al., 2004), as well as for the expansion of the ventromedial forebrain

(Britto et al., 2002; Chiang et al., 1996). In addition to its role in forebrain morphogenesis, Shh drives the growth of the cranial neural crest-derived mesenchyme that gives rise to the connective tissue of the face (Jeong et al., 2004).

Disruption of the Shh pathway by both genetic and environmental factors causes craniofacial malformations including holoprosencephaly (HPE), a condition defined by medial forebrain deficiency and commonly co-occurring with midfacial dysmorphology (Addissie et al., 2021; Chiang et al., 1996; Dubourg et al., 2018; Everson et al., 2019; Richieri-Costa & Ribeiro, 2010; Solomon et al., 2012). While severe (i.e., alobar) HPE is rarely compatible with postnatal survival, moderately affected individuals may survive with significant cognitive impairments, and individuals with microform HPE can appear phenotypically normal (Tekendo-Ngongang et al., 2020). This variability in individuals with HPE supports a multifactorial model of pathogenesis in which environmental factors act together or in concert with genetic predispositions to modulate disease severity (Addissie et al., 2021; Everson et al., 2019; Hong & Krauss, 2012, 2018; Petryk et al., 2015). Moreover, the inherent sensitivity of Shh signaling to small molecule disruption highlights the potential for environmental Shh pathway antagonists to contribute to HPE incidence and severity. Recently, a study in mice demonstrated that chemical disruption of Shh can alter brain development at doses that cause only subtle craniofacial dysmorphology (Everson et al., 2019). This observation supports a model of environmental Shh pathway inhibition in which neurological function is altered in the absence of overt structural malformations.

To test the hypothesis that Shh signaling-mediated neurobehavioral deficits can be induced in mice without causing overt facial dysmorphology, we developed a dietary

model of Shh pathway inhibition. As a surrogate for the dozens of small molecule pathway inhibitors that have been described, pregnant mice were exposed to the potent and specific Shh pathway inhibitor vismodegib throughout the critical window for HPE. After determining an overtly teratogenic dose based on craniofacial morphology, lower doses were assessed for impacts on early forebrain patterning, face and brain morphology later in development, and behavior in adult mice.

MATERIALS AND METHODS

1–Materials

Vismodegib (Catalog No. V-4050; LC Labs) used in diet formulation was manually pulverized to achieve a uniform powder and suspended in soybean oil (Catalog N. S0255; Spectrum Chemical Mfg. Corp) prior to inclusion in rodent chow pellets.

2–Animals

Animal studies were conducted in strict accordance with the recommendations in the *Guide for the Care and Use of Laboratory Animals* of the National Institutes of Health. Studies followed procedures approved by the Institutional Animal Care and Use Committees of the University of Wisconsin School of Veterinary Medicine (protocol V005396) and Letters and Sciences and Vice Chancellor for Research Centers (protocol G005373). C57BL/6J mice (Strain No. 00664, Jackson Laboratories) were housed in rooms maintained at 22°C ± 2°C and 30% to 70% humidity on a 12 h light, 12 h dark cycle. Mice were fed Irradiated Soy Protein-Free Extruded Rodent Diet (Catalog No. 2920x; Envigo Teklad Global) until a copulation plug was detected, at which point dams received Irradiated Teklad Global 19% Protein Extruded Rodent Diet (breeder chow, Catalog No.

2919; Envigo Teklad Global) except when on experimental diets. Dams were euthanized via carbon dioxide asphyxiation followed by cervical dislocation at GD11 for embryo collection, GD17 for fetal collection, and after weaning for behavioral studies.

3–Dietary Exposure Procedure

Precision timed-matings were achieved by placing one to two nulliparous C57BL/6J wild-type female mice with a single C57BL/6J male mouse for 1–2 h (Heyne, Plisch, et al., 2015). Following the mating period, females were examined for the presence of a copulation plug, and the initiation of the mating period was designated as gestational day (GD)0. Vismodegib suspended in soybean oil was used to generate vismodegib-containing diets that were prepared from Envigo base diet (Catalog No. 2919; Envigo Teklad). Control chow diet was prepared with soybean oil alone. Control and vismodegib treatment diets were introduced to pregnant female mice at GD4. Dams were placed back on standard breeder chow at GD12.

4–Facial Morphometrics and Fetal Brain Morphology

Pregnant dams were administered control chow or 25, 75, or 225 ppm vismodegib chow from GD4 through GD12. Following euthanasia at GD17, uterine horns were dissected. Resorptions, live fetuses, and crown-rump length were recorded, and gross morphological abnormalities were noted. For facial morphometric analyses, fetuses were fixed in 10% phosphate buffered formalin for at least 1 week before being imaged by light microscopy. To ensure the reliability of image-based measurements, consistent head and face orientation were maintained across all images. Light microscopic images were captured using an Olympus QImaging MicroPublisher 5.0 camera (QImaging) connected to an SZX-10 stereomicroscope (Olympus). ImageJ software was used to quantify

interocular distance (IOD) and upper lip length (ULL) from facial images as previously described (Everson et al., 2019). All measurements were taken by a single rater.

For qualitative assessment of correlative face and brain morphology, fetuses were fixed in Bouin's solution for at least 1 week before being imaged for facial morphology. Bouin's-fixed brains were then dissected out and imaged dorsally. Brains were washed in 70% ethanol until the ethanol ran clear before being paraffinized and paraffin-embedded for sectioning. Coronal sections through the cerebrum were stained using hematoxylin and eosin (H&E) prior to imaging. Light microscopic images of fetal faces, whole brains, and H&E-stained sections were captured using an Olympus QImaging MicroPublisher 5.0 camera connected to an SZX-10 stereomicroscope.

5–In Situ Hybridization

Following euthanasia of dams and uterine dissection at GD11, embryos were dehydrated in graded solutions of methanol until staining. In situ hybridization was performed using a high-throughput technique which allowed samples to be identically processed across treatment groups (Abler et al., 2011). Embryos were hemisected mid-sagittally prior to staining. Embryos were then incubated in proteinase K (10 μg/mL) with collagenase (1 mg/mL) for 2 min before initial washes. The primer sequences used for probe generation include a T7-polymerase recognition site and a 5-bp leader sequence on the reverse probe. RNA probe sequences, with recognition site and leader underlined, are as follows: *Gli1* [forward- CCCTCCTCCTCTCATTCCAC and reverse- CGATGTTAATACGACTCACTATAGGGTCCAGCTGAGTGTTGTCCAG], *Pax6* [forward- AGTGAATGGGCGGAGTTATG and reverse- CGATGTTAATACGACTCACTATAGGGAGTGTGTGTTGTCCCAGGTTC], and

Nkx2-1 [forward-CCGCAAAGACCACCATTC and reverse- CGATGTTAATACGACTCACTATAGGGGGGGTTATGCTGAAGACTTTCC].

Following staining, embryos were imaged by light microscopy using a QImaging MicroPublisher 6 camera connected to an Olympus SZX-10 stereomicroscope. Area measurements of the MGEs and head were made in ImageJ. Measurements were made by a single rater blinded to the treatment group.

6–Behavioral Assays

For behavioral testing, litters from vehicle- and vismodegib-treated dams were weaned at 3 weeks of age, and males and females were placed in separate home cages. Mice were selected for behavioral testing at random, and no more than three males and three females were chosen from a single litter for an average of 2 mice of each sex per litter per treatment group. Eight- to ten-week-old mice were transferred to the Waisman Center Behavioral Testing Service and given 1 week to acclimate. Assays were conducted in the order listed below, beginning with the least stressful test and finishing with the most stressful. Mice were placed on a cart and transported to the respective testing rooms for 30 min to acclimate before the start of each assay.

6.1–Open Field

Mice were placed in an arena (43 cm^3) and allowed to move freely through the environment for 30 min. A 16 × 16 photobeam array surrounding each arena was used to monitor the position, horizontal locomotion, vertical activity, and stereotypic movement of each mouse during the testing period using Fusion 6.5 SuperFlex software. Position was defined as the center of the mouse, and the proportion of time the mouse spent in the

center (internal 25% floor area) versus the periphery (external 75% floor area) of the chamber was determined.

6.2–Marble Burying

Twenty marbles were arranged in 4 rows (5 marbles/row) within a standard home cage (20 × 32 cm) containing fresh bedding at a depth of 4 cm. Mice were individually placed in the test cage covered with a top for 30 min. At the end of the testing period, mice were returned to their home cages, and the number of marbles buried was counted. Marbles were considered buried only if they were 100% covered by bedding.

6.3–Rotarod

Mice were placed on rotating drums of an accelerating rotarod (Med Associates Inc.) to evaluate motor coordination and balance. Rota-Rod 2 computer software was used. Over the course of the assay, the rotarod accelerated continuously from 4 to 40 rpm over a 5 min period. Each mouse received 4 trials with ~20 min between each trial. Latency to fall and rotation speed upon falling were recorded. For mice that remained on the rotarod for the duration of the test, the maximum possible latency (300 s) is reported.

6.4–Olfactory Discrimination and Detection

The olfactory discrimination assay consisted of two sessions. In the first session, two cotton-tipped swabs (Dukal) were inserted into the home cage through a Plexiglas cover. The swabs were equally spaced from the walls of the cage and each other, with each swab tip located ~8 cm above the bedding. One swab was dampened with 2 μL water (familiar scent) and the other with 2 μL of either lemon or mint extract (both novel scents). The use of lemon or mint as the novel scent, as well as their placement in the cages, was

pseudo-randomized and counter-balanced across groups. Time spent investigating each swab was recorded over a 3-min period, followed by a 3-min rest period. For the second session, the mice were provided one swab with mint extract and one swab with lemon extract. Placement of each swab was randomized. In this session, each mouse had access to a familiar scent and a novel scent. Time spent investigating each swab was again recorded for 3 min.

To assess olfactory detection, mice were first familiarized with a novel food item (TestDiet, LabTab, Sucrose Choc, 45 mg pellet, ~10 pellets per mouse) in their home cage. Next, mice were housed singly and deprived of food for 24 h. Testing commenced once a single food pellet was buried in a corner of the home cage at a depth of 1 cm below the bedding. Mice were given 5 min to explore the cage, and the latency to find the buried food was recorded.

6.5–Fear Conditioning

Fear conditioning tests consisted of one training session and two testing sessions, and freezing was measured throughout each session. ANY-maze software (v4.1) was used to monitor freezing and control stimulus delivery. For training, a single mouse was placed in a fear conditioning chamber (Ugo Basile) cleaned with 70% ethanol. After a 120 s acclimation period, mice were exposed to a 30 s, 87 dB noise cue (conditioned stimulus, CS). During the last 2 s of the cue presentation, mice were delivered a scrambled, 0.7 mA shock (unconditioned stimulus, US) from the floor of the test cage. After 120 s, mice were exposed to another 30 s, 87 dB white noise cue co-terminating with a 0.7 mA shock. Mice were monitored for an additional 60 s after the second CS-US pairing before being returned to their home cages.

Twenty-two hours post-training, mice were placed back in the 70% ethanol-cleaned chambers for contextual fear recall testing. Freezing was again measured as mice explored the chamber for 360 s in the absence of an auditory cue or shock delivery. Mice were then returned to their home cages for 2 h. For cued fear recall testing, mice were placed in the fear conditioning chamber, now altered with gray plastic floor panels covering the shock grid, checkered wall inserts, and cleaned with 30% isopropyl alcohol instead of 70% ethanol. Mice were introduced to this altered context for a 120 s acclimation period before being exposed to the 30 s CS only. Mice were then able to free-roam for 120 s before another CS event. Mice remained in test cages for an additional 60 s before being returned to their home cages.

7–Statistical Analysis

Statistical analyses were performed using GraphPad Prism 9 for morphometric assessments and MGE size. One-way ANOVA with Tukey's post hoc test was used to analyze IOD and ULL in GD17 mice and MGE area in GD11 mice. Behavioral endpoints were analyzed in R (Version 4.4.0). Normality of the data was assessed using Shapiro–Wilk test. Normal and log-normal data were evaluated for treatment- and sex-dependent effects using two-way ANOVA and Tukey's post hoc test. Data that failed normality testing were analyzed using aligned-rank transform ANOVA with post hoc test for multiple comparisons (Elkin et al., 2021; Wobbrock et al., 2011). An alpha value of 0.05 was maintained for the determination of statistical significance.

RESULTS

1–Dose-Dependent Impacts of Shh Inhibition on Face and Brain Morphogenesis

Vismodegib, a therapeutic drug designed to treat Shh-active cancers, was previously shown to inhibit the Shh pathway in vitro and cause a variety of craniofacial and limb defects following an acute prenatal dose in animal models (Heyne, Melberg, et al., 2015; Robarge et al., 2009). A pilot study demonstrated that prenatal exposure to a diet of 225 ppm vismodegib induced robust craniofacial malformations consistent with Shh pathway inhibition. In the present study, two lower-dose diets separated by three-fold intervals (i.e., 25 and 75 ppm) were included with the goal of achieving exposures that did not produce overt dysmorphology.

Pregnant mice were provided vehicle- or vismodegib-containing chow between GD4 and GD12 to encompass key critical periods of Shh-mediated craniofacial morphogenesis. No significant differences in chow consumption were observed between treatment groups from GD4 to GD12 (Figure S1). For fetal endpoints, dams were euthanized at GD17, and litters were assessed for live fetuses, resorptions, and crown-rump length. Fetuses were fixed in formalin for facial morphometric analysis or Bouin's solution for assessment of brain phenotypes. Relative to vehicle-treated litters, there were fewer live fetuses and more resorptions following exposure to 225 ppm vismodegib, though crown-rump length in live fetuses was not significantly impacted by treatment (Table 1).

1.1–Impacts on Craniofacial Morphogenesis

Previous mouse models of HPE demonstrate that IOD and ULL are sensitive predictors of underlying changes in brain morphology that reflect the midline deficiency that defines

this disorder (Everson et al., 2019; Heyne et al., 2016). Fetal mice were imaged at GD17, and IOD and ULL measurements were taken (Figure 1, additional annotated images in Figure S2). Litters exposed to 225 ppm vismodegib exhibited dysmorphic facial features consistent with HPE, such as decreased IOD and increased ULL, relative to all other treatment groups. Of note, while many fetuses within the 225 ppm treatment group exhibited severe phenotypes (i.e., overt midfacial hypoplasia and microcephaly in Figure 1E), a subset of samples exhibited mild forms of HPE (i.e., a shallow upper lip notch in Figure 1D). Mean values indicated no differences between vehicle-exposed fetuses and the 25 and 75 ppm treatment groups, though moderate HPE phenotypes were observed in single samples from these lower treatment groups (Figure S3). Additional Shh-associated limb defects were observed only in the 225 ppm treatment group (Figure S4). No craniofacial or limb defects were observed within the vehicle control group.

1.2–Impacts on Brain Morphogenesis

Consistent with the results of the morphometric analysis, facial images showed no overt differences between vehicle-treated and 25 or 75 ppm vismodegib-treated fetuses, while the 225 ppm vismodegib diet induced HPE-like phenotypes with high penetrance (Figure 2A–E). Severe midfacial hypoplasia frequently co-occurred with microcephaly in the most affected animals (Figure 2E). One animal in the 225 ppm vismodegib group exhibited micrognathia without any obvious microcephaly (Figure 2D), again displaying a spectrum of phenotypic severity in the highest dose group. Disruption of Shh signaling during early neurodevelopment in mice causes various brain dysmorphologies, including hypoplasia or agenesis of the olfactory bulbs and incomplete forebrain division (Heyne et al., 2016; Heyne, Melberg, et al., 2015). In dissected brains, olfactory bulbs were

comparable in size and position among vehicle and 25 and 75 ppm vismodegib treatment groups but diminished, unseparated, or even absent in the 225 ppm vismodegib group (Figure 2A′–E′). Incomplete cortical division was apparent in whole brains from severely affected animals in the 225 ppm vismodegib group. Coronal sections revealed that only treatment with 225 ppm vismodegib was sufficient to induce true HPE, with loss of forebrain division apparent in mice with overt midfacial hypoplasia (Figure 2A″–E″). Severity of forebrain and olfactory bulb abnormalities generally correlated with facial dysmorphology.

2–Embryonic Forebrain Patterning Following Gestational Shh Pathway Antagonist Exposure

To test whether Shh pathway inhibition alters early forebrain patterning even at doses that do not produce overt craniofacial dysmorphology, embryos from dams provided control or 25, 75, or 225 ppm vismodegib diets were collected at GD11 for facial imaging and ISH. Although resorptions were similar between treatment groups, litter size was reduced in the 25 ppm group but increased in the 75 ppm group. Embryos in the 75 and 225 ppm vismodegib groups were slightly smaller than the control embryos (Table 2).

Prior to staining, the rostral portion of each sample was imaged and hemisected along the sagittal plane to reveal early forebrain structures. ISH was used to visualize *Gli1*, a marker of Shh pathway activity, *Pax6*, a dorsal marker within the central nervous system, and *Nkx2-1*, a marker strongly expressed in the Shh-dependent MGE. Facial images showed no overt differences between the control group and the 25 and 75 ppm vismodegib groups, while embryos in the 225 ppm vismodegib group displayed phenotypes ranging from apparently normal to severely hypoplastic (Figure 3A–E). The same pattern was observed

by ISH, with domains of localization for each marker remaining unchanged in the 25 ppm and 75 ppm vismodegib groups. Relative to the other groups, severely affected embryos from the 225 ppm vismodegib group exhibited reduced *Gli1* expression within the ventral forebrain and facial processes (Figure 3F–J), expanded *Pax6* expression into the ventral aspect of the forebrain (Figure 3K–O), and a greatly diminished or absent MGE based on *Nkx2-1* expression (Figure 3P–T). Measurements of the MGE, normalized to head size, revealed a significant decrease in the size of this structure in the 225 ppm vismodegib group (Figure 3U,V). As at later developmental stages, phenotypic variability was observed in facial images and ISH patterns among embryos in the 225 ppm vismodegib treatment group with a subset of samples exhibiting apparently normal facial features (Figure 3D) and intermediate differences in rostral *Gli1* and *Nkx2-1* patterning (Figure 3I,S). The domain of *Pax6* expression, however, was not clearly altered in the most normal individuals of the highest dose group (Figure 3N).

3–Impact of Gestational Shh Pathway Antagonist Exposure on Behavior

We next examined the impact of prenatal vismodegib exposure on postnatal behavior using a battery of established assays. Viable litters could not be raised from the 225 ppm vismodegib group, so behavioral assays were conducted only in the vehicle and 25 and 75 ppm vismodegib groups. One to three male and female mice were taken from each litter, and six to seven litters were produced to attain the final sample size. The number of viable pups in each litter was consistent across treatment groups, as was the number of perinatal losses (Table 3). A treatment-dependent decrease in pup weight at the time of weaning was observed across all weaned mice. This trend remained when considering only mice that underwent testing, though the difference in the 25 ppm vismodegib treatment group

was no longer significant. In total, 11 female and 12 male mice from the vehicle group underwent behavioral testing, and 12 females and 12 males underwent behavioral testing from both vismodegib-treated groups.

3.1–Open Field

Following a week-long period of acclimation, adult mice were placed in an enclosed arena and allowed 30 min to move freely around the open field. A photobeam array was used to assess horizontal movement within the arena as well as vertical activity and stereotypic activity. Horizontal movement through the cage was used to assess total distance traveled and the proportion of times pent near the center of the cage versus the peripheries. Stereotypic activity was evaluated as repeated breaking of a single photobeam, and vertical movements were similarly tallied. No significant changes were observed in the total distance traveled, percent of time spent in the center of the arena, stereotypic behavior, or vertical activity when comparing treatment groups (Figure 4). A sex-dependent difference was seen only in vertical activity, with males engaging in more vertical activity than females (Figure S5).

3.2–Marble Burying

In the marble burying assay, individual mice were placed in an arena with 20 marbles arrayed over a thick layer of bedding. After 30 min, mice were removed from the arena, and the number of fully buried marbles was counted. There were no treatment-dependent differences in the number of marbles buried (Figure 5), though there was a significant difference in marble burying between males and females (Figure S6).

3.3–Rotarod

Four sessions of rotarod testing were performed to investigate motor coordination and memory acquisition across treatment groups. Mice were placed on a rotating rod that increased from 4 rpm to 40 rpm over the 5-min test. Significant effects of treatment, sex, and session, as well as their interactions, were observed. Session 4 was found to significantly differ from session 1, indicating that assay performance improved with repetition (Figure 6). Treatment-related effects were observed only in the third and fourth sessions, with vismodegib-treated mice outperforming the vehicle-exposed mice (Figure 6). Of note, C57BL/6J mice have a high baseline performance in the rotarod assay, consistent with the results of the first session in which mice across all treatment groups remained on the rotarod for an average of 273.3 s of the 300-s assay. The improvement in rotarod performance observed in the vismodegib-exposed animals did not align with expectations. However, given the limited variability observed within this assay (i.e., the majority of mice tested remained on the rotarod for the entire duration of each session) and the modest nominal increase in latency to fall, this finding should be interpreted with caution. Across all treatment groups and sessions, males remained on the rotarod for 289.7 ± 2.7 s compared to 284.9 ± 3.6 s for females (Figure S7).

3.4–Olfactory Discrimination and Detection

Olfactory discrimination was probed over two phases by comparing time spent investigating a novel scent versus a familiar scent. In the first session, mice were placed in a cage containing swabs dampened with water (familiar scent) or either mint or lemon extract (novel scent). During the second session, the swabs were dampened with each of the extracts, one familiarized during the first session and the other novel. Time spent

investigating each swab was again recorded. Surprisingly, though there were no sex- or treatment-dependent effects, mice showed a preference for water (4.0 ± 0.6 s) over the novel scents (2.1 ± 0.2 s) in the first phase of testing (Figure 7A). No treatment-dependent differences in preference for the novel or familiar scents were observed in the second phase, nor were there sex-dependent effects (Figure S8A). To test whether these unexpected responses to novel scents indicated a general dysfunction in olfaction, the mice were also evaluated for their ability to detect an object buried under cage bedding. The ability of treated mice to detect odors was evaluated as the latency to find the scented object. No differences were observed between treatment groups in the olfactory detection assay, though all but one mouse was able to find the buried object during the 300 s testing window (Figure 7B). Additionally, there were no differences between sexes in olfactory detection (Figure S8B).

3.5–Fear Conditioning

Finally, the fear conditioning assay was employed as a well-established test of memory and learning. Following a training session in which mice experienced two CS-US pairings that induced freezing, contextual fear recall and cued fear recall tests were administered. No treatment-dependent differences in time spent freezing were observed when mice were placed into the fear conditioning chamber to assess contextual fear recall (Figure 8A). In the cued fear recall test, the fear conditioning chamber was modified to create a novel visual and olfactory context for the subjects. During cued fear recall testing sessions, the CS alone was administered twice and freezing during each 30-s event was recorded. All groups exhibited elevated freezing during the second CS event relative to the first. During the first CS event, the 25 ppm vismodegib treatment group froze for significantly

longer than the 75 ppm vismodegib treatment group, though neither treatment resulted in significant differences relative to the vehicle control mice (Figure 8B). No treatment-dependent differences were observed during the second CS event, and there was no effect of sex on fear conditioning (Figure S9).

DISCUSSION

Defining the molecular pathways that drive NDD pathogenesis is critical for preventing these etiologically complex diseases. To our knowledge, the study reported herein is the first to investigate neurobehavioral effects following low-dose Shh signaling disruption spanning the critical period for craniofacial morphogenesis. The pharmacological hedgehog pathway inhibitor vismodegib was selected for this study due to its specificity, potency, and short half-life, allowing for selective inhibition of the Shh pathway between GD4 and GD12 with minimal off-target toxic effects (Robarge et al., 2009; Wong et al., 2011; Wong et al., 2009). Gestational exposure to the 225 ppm vismodegib diet produced a spectrum of face and forebrain phenotypes of varying severity and was incompatible with postnatal survival. Surprisingly, consumption of chow containing 25 or 75 ppm vismodegib had no apparent impact on early forebrain patterning at GD11 or gross morphology of the face or forebrain at GD17. Adult mice that were prenatally exposed to 25 or 75 ppm vismodegib were phenotypically normal and did not exhibit robust behavioral differences in the battery of assays conducted in this study.

The potential for small molecule Shh pathway inhibitors to disrupt neurodevelopment without producing overt external dysmorphologies has critical implications for our understanding of NDD pathogenesis, broadening the spectrum of adverse outcomes that may otherwise go unnoticed due to a focus primarily on external anomalies. The

expansion of fetal alcohol spectrum disorders (FASD) to include individuals with neurobehavioral symptoms who lack external dysmorphologies provides a salient comparison. Studies in recent decades reveal a more substantial role of prenatal alcohol exposure in neurodevelopment than was previously recognized by identifying adverse neurobehavioral outcomes in children who appear phenotypically normal (Coles et al., 2020; Hoyme et al., 2016; Hoyme et al., 2005).

A role for low-dose Shh signaling inhibition in the disruption of early neurodevelopment was previously posited. One notable study investigated the capacity for piperonyl butoxide (PBO), a pesticide synergist and Shh pathway inhibitor (Rivera-González et al., 2021; Wang et al., 2012), to cause Shh-associated malformations in mice. The authors found that the MGE and septal region of the forebrain were diminished following doses of PBO that caused only subtle facial dysmorphology (Everson et al., 2019). Extrapolating to a human population in which normal face shape variation may mask subtle abnormalities, these results suggest that low levels of Shh signaling disruption may impact neurodevelopment without overtly altering facial morphogenesis (Hammond & Suttie, 2012; Hoyme et al., 2015). Under the experimental conditions examined in this study, brain anomalies were not observed in the absence of robust craniofacial anomalies. Several factors, such as the use of a dietary model of inhibition rather than an acute oral dose or differences in the specificity and potency of vismodegib and PBO as Shh pathway antagonists, may explain the seemingly disparate results between these studies.

Research from a separate lab demonstrated neurobehavioral changes in mice following gestational and lactational exposure to PBO through modified diets (Tanaka, 2003; Tanaka & Inomata, 2015, 2016; Tanaka et al., 2009). Significant changes in offspring mice

were observed in measures of motor coordination, exploratory behavior, spontaneous behavior, and olfaction, though treatment paradigms and neurobehavioral results were not consistent across all studies. Furthermore, the studies were not designed to interrogate underlying mechanisms. The exposure models presented by Tanaka and colleagues most closely match the dietary vismodegib model utilized herein (Tanaka, 2003; Tanaka & Inomata, 2015, 2016; Tanaka et al., 2009). However, that PBO exposure in each study spanned, at minimum, gestation and lactation may explain the subtler phenotypes observed by Tanaka et al. Furthermore, PBO's impacts are not limited solely to Shh pathway inhibition, and additional studies using specific antagonists, such as vismodegib, over a broader period of development will clarify whether Shh signaling disruption alone can induce neurobehavioral deficits in the absence of overt dysmorphology.

We designed this study to expose mice over a period spanning the critical period for HPE, providing vismodegib-laced diets from GD4 to GD12 (Heyne, Melberg, et al., 2015), roughly corresponding to the first 6 weeks in human gestation. This developmental period is highly dynamic and encompasses several, but not all, key roles of Shh signaling in brain morphogenesis and CNS development. For example, Shh is implicated in oligodendrogenesis in both the ventral and dorsal forebrain after GD12 in mice (Machold et al., 2003; Winkler et al., 2018; Zhou et al., 2020). In addition, oligodendrocyte and astrocyte differentiation were modulated based on Shh pathway activity in primary rodent neural cell culture models of gliogenesis (Araújo et al., 2014; Wang & Almazan, 2016). Whether targeted disruption of Shh during later stages in neurodevelopment can induce behavioral changes through altered gliogenesis or other mechanisms in the

absence of overt malformations remains unknown. Similarly, future studies investigating low-dose Shh signaling disruption may extend the window of treatment to encompass the murine equivalents of neurodevelopment during the second and third trimesters in humans, which extends into the early postnatal period in mice (Almeida et al., 2020; Parnell et al., 2014).

This study was constrained by several limitations. To reduce variability in the experimental design, litters were generated for each treatment group and endpoint concurrently. Therefore, additional treatment groups could not be added without potentially introducing a group-specific bias. The absence of a treatment group that consistently induced HPE with low penetrance prevented the assessment of neurobehavioral changes in apparently normal littermates of overtly affected individuals. Whether the treatment paradigm employed herein can induce mild or low-penetrance facial dysmorphology requires additional study. Furthermore, practical considerations limited the number of neurobehavioral tests that were conducted. The behavioral assays utilized, though not comprehensive in scope, were selected for their breadth due to limited reports of neurobehavioral impacts of gestational Shh pathway disruption. The finding of diminished MGE size in the 225 ppm vismodegib group can inform future studies on behavioral impacts of Shh disruption. The MGE, a transient forebrain structure, gives rise to cortical interneurons. This subset of neurons is implicated in diseases such as epilepsy, schizophrenia, and autism, as well as deficits in social behavior (reviewed in Ansen-Wilson & Lipinski, 2017; Katsarou et al., 2017). In addition to effects on the MGE, research has also found altered Shh levels in neurological conditions including autism spectrum disorder, Parkinson's Disease, epilepsy, and demyelinating

diseases such as multiple sclerosis (Al-Ayadhi, 2012; Dhekne et al., 2018; Fang et al., 2011; Feng et al., 2016; Mastronardi et al., 2003). A role for Shh in the pathogenesis of these disorders has not been fully elucidated, but future efforts may leverage behavioral and functional assays targeting specific disease outcomes to support a causative or predisposing effect of prenatal Shh disruption in NDD pathogenesis.

The dietary model of Shh pathway inhibition presented herein also possesses strengths. In both the human population and animal models, HPE presents with incomplete penetrance and phenotypic variability (Tekendo-Ngongang et al., 2020). Although HPE is most often embryonic lethal (Matsunaga & Shiota, 1977; Orioli & Castilla, 2010), individuals living with HPE-associated variants span the spectrum from phenotypically normal to mild midfacial hypoplasia (i.e., a single central top incisor) to more moderate and severe midfacial and forebrain hypoplasia (i.e., hypotelorism, microcephaly). HPE-related neurobehavioral impacts cover a similarly broad spectrum from normal brain function to cognitive delay to substantial impairment. Generally, the severity of facial and brain defects is closely correlated, inspiring the aphorism “the face predicts the brain” (DeMyer et al., 1964). The dietary Shh disruption model presented in this study recapitulates this phenotypic variability as well as the established correlation between face and forebrain outcomes. Leveraging this phenotypic variability and the low-stress exposure paradigm, the dietary vismodegib model is suitable for study of multifactorial insult including gene–environment and environment–environment interactions. Combining simultaneous environmental insult or predisposing genetic variations with the vismodegib diet can inform the impact of Shh modulation on multifactorial NDDs.

This model has the potential to be a powerful tool for exploring etiologically complex developmental disorders.

This study was designed to address whether Shh signaling pathway disruption alters neurodevelopment in the absence of overt facial dysmorphology. Resolving this question is critical to the informed assessment of health hazards in the context of environmental Shh pathway inhibition. The current study did not support a model of NDD pathogenesis in which Shh pathway disruption can significantly impact neurodevelopment without altering craniofacial or limb morphogenesis, though future research may further clarify the impact of low-dose Shh disruption on NDD outcomes by examining more intermediate doses of vismodegib, a broader spectrum of behavioral endpoints, or expanding the period of Shh pathway disruption to target additional critical periods of development.

DECLARATIONS

Funding: This work was supported by the National Institute of Child Health and Human Development; National Institutes of Health under awards R01ES026819, F31ES034632, P50HD105353, and T32ES007015; National Institute of Environmental Health Sciences; University of Wisconsin-Madison.

Acknowledgments: The authors acknowledge the Biomedical Research Model Services at the University of Wisconsin-Madison for careful management of our mouse colonies. The authors also thank Dr. Michael Cahill for thoughtful discussion of the behavioral approaches employed in this study.

Conflicts of Interest: The authors declare no conflicts of interest.

Data Availability Statement: The data that support the findings of this study are available from the corresponding author upon reasonable request.

TABLES

Table 1. Litter statistics for fetuses at GD17

Treatment	Litters collected [*n*]	Live fetuses [*n* (mean)]	Resorptions [*n* (mean)]	Crown-rump [mean ± SD mm]
Vehicle	7	47 (6.7)	9 (1.3)	17.23 ± 0.95
25 ppm Vis.	8	49 (6.1)	12 (1.5)	16.92 ± 1.12
75 ppm Vis.	8	55 (6.9)	14 (1.8)	16.95 ± 0.81
225 ppm Vis.	8	36 (4.5)*	22 (2.8)*	16.74 ± 0.79

*$p<0.05$

Table 2. Litter statistics for GD11 embryos

Treatment	Litters collected [*n*]	Viable embryos [*n* (mean)]	Resorptions [*n* (mean)]	Crown-rump [mean ± SD mm]
Vehicle	4	24 (6.0)	9 (2.3)	5.92 ± 0.24
25 ppm Vis.	3	12 (4.0)*	11 (3.7)	5.92 ± 0.29
75 ppm Vis.	3	26 (8.7)*	3 (1.0)	5.19 ± 0.65*
225 ppm Vis.	3	19 (6.3)	6 (2.0)	4.87 ± 1.05*

*$p<0.05$

Table 3. Population parameters for behavioral testing

Treatment	Litters [*n*]	Viable pups [*n* (mean)]	Pups lost [*n* (mean)]	Mass at weaning [mean ± SD g]
Vehicle	6	34 (5.67)	4 (0.67)	10.86 ± 2.06
25 ppm Vis.	7	41 (5.86)	4 (0.57)	9.64 ± 1.51*
75 ppm Vis.	7	38 (5.43)	9 (1.29)	8.83 ± 2.06*

*$p<0.05$

FIGURES

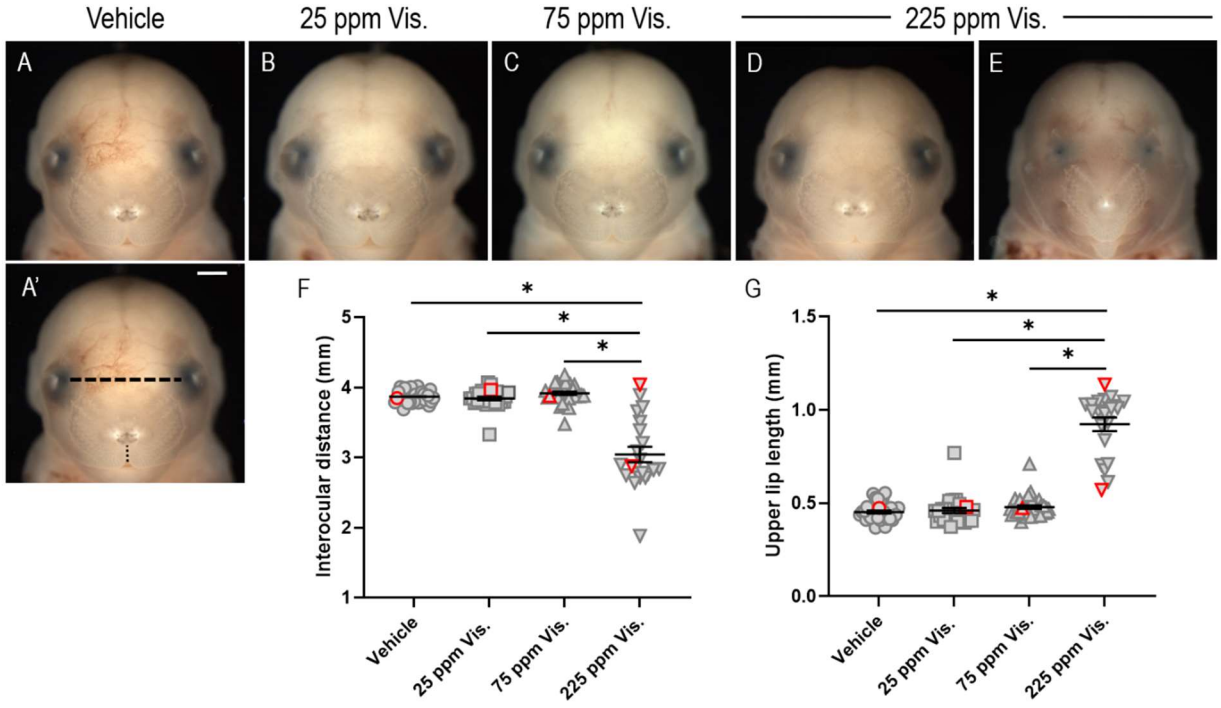

FIGURE 1. Facial morphometric assessment in a dietary model of Shh pathway inhibition. (A–E) GD17 fetuses from dams fed vehicle- or vismodegib-containing chow at the indicated concentrations. Interocular distance (IOD) and upper lip length (ULL) measurements are represented visually in A′ by dashed and dotted lines, respectively. (F, G) Plots of IOD and ULL measurements in fetuses of dams fed vehicle chow (n = 35) or chow containing 25 ppm (n = 28), 75 ppm (n = 36), or 225 ppm (n = 21) vismodegib. Individual data points are plotted along with bars representing mean ± SEM. IOD and ULL measurements for the fetuses shown in panels A–E are indicated by red borders. One-way ANOVA with Tukey's post hoc test was used to compare the statistical significance of IOD and ULL measurements between treatment groups. *$p < 0.05$. Scale bar: 1 mm.

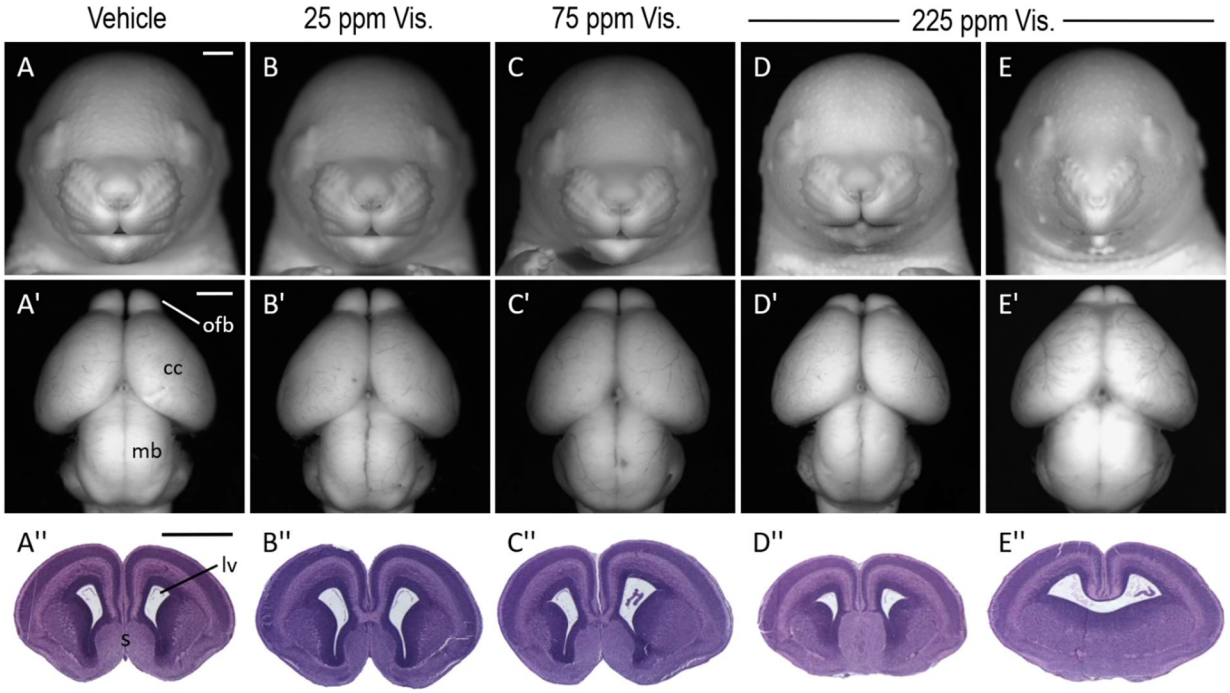

FIGURE 2. Evaluation of face and brain morphology in fetal mice exposed to vismodegib. (A–E) Facial images of GD17 fetuses from dams fed diets containing vehicle (n = 12) or 25 ppm (n = 20), 75 ppm (n = 19), or 225 ppm (n = 15) vismodegib. Midfacial hypoplasia was apparent in most individuals from the highest exposure group. (A′–E′) Dorsal view of brains from the same individuals shown in A–E. Olfactory bulbs (ofb) were hypoplastic and partially unseparated following high vismodegib exposure, and the cerebral cortices (cc) showed only shallow divisions in the most severely affected samples. (A″–E″) H&E staining of coronal sections through the forebrain of the individuals in A–E. The 225 ppm vismodegib diet altered the size and shape of the lateral ventricles (lv) and septal region (s) in moderately affected samples (D″) and induced true HPE (incomplete separation of the forebrain) in severely affected samples (E″). mb, midbrain. Scale bars: 1 mm.

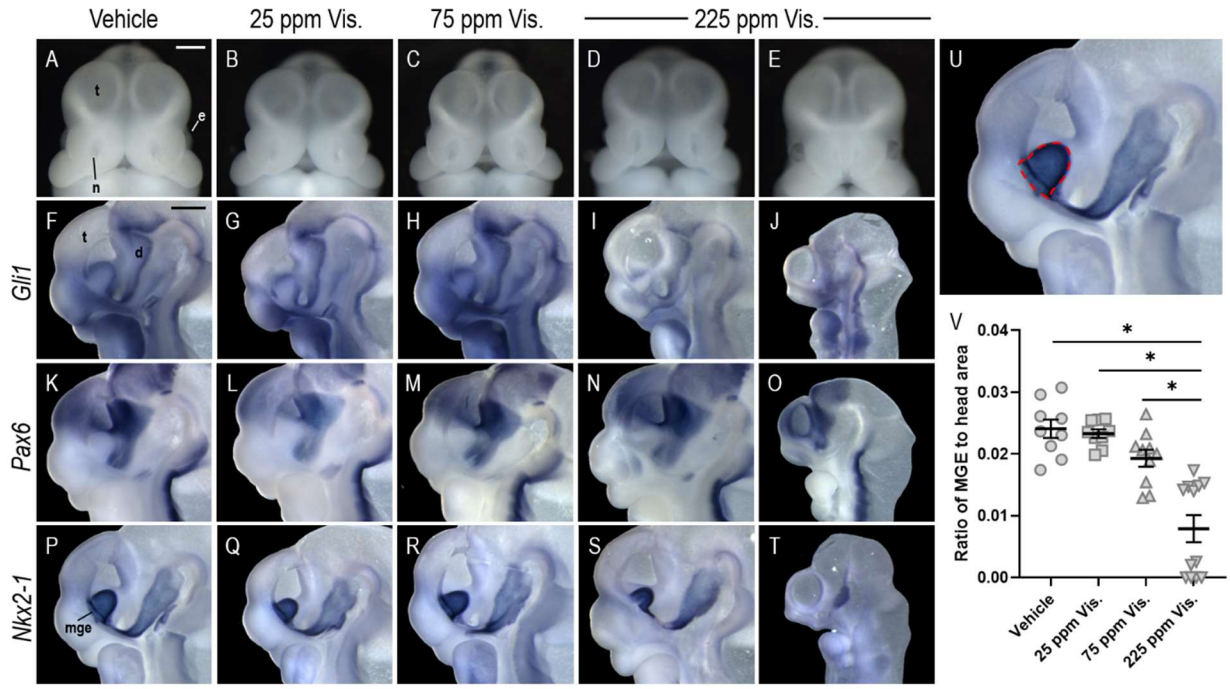

FIGURE 3. Expression pattern of select genes within the forebrain of vismodegib-exposed embryos. (A–E) Representative frontal images of GD11 embryos from dams provided chow containing vehicle (n = 24) or 25 ppm (n = 12), 75 ppm (n = 26), or 225 ppm (n = 19) vismodegib. The 225 ppm vismodegib group showed varying degrees of midfacial hypoplasia resulting in closely approximated facial processes, eyes (e), nostrils (n), and telencephalic vesicles (t). (F–T) Embryos were bisected sagittally and stained using in situ hybridization for the genes indicated. In control samples, *Gli1* was most strongly expressed in the inferior aspect of the facial processes and dorsally into the diencephalon (d). *Pax6* was expressed dorsally within the telencephalon and diencephalon. *Nkx2-1* was expressed in the medial ganglionic eminence (mge) and the ventral diencephalon. (U) An enlarged view of panel Q with the measured area of the MGE outlined with a dashed red line. (V) Plot of MGE area normalized to head area for a subset of embryos from each litter; vehicle (n = 9), 25 ppm vismodegib (n = 9), 75 ppm vismodegib (n = 10), and 225 ppm vismodegib (n = 12).

Individual samples are plotted, and bars represent the mean ± SEM. One-way ANOVA with Tukey's post hoc test was used to assess the statistical significance in MGE area. *$p < 0.05$. Scale bars: 500 μm.

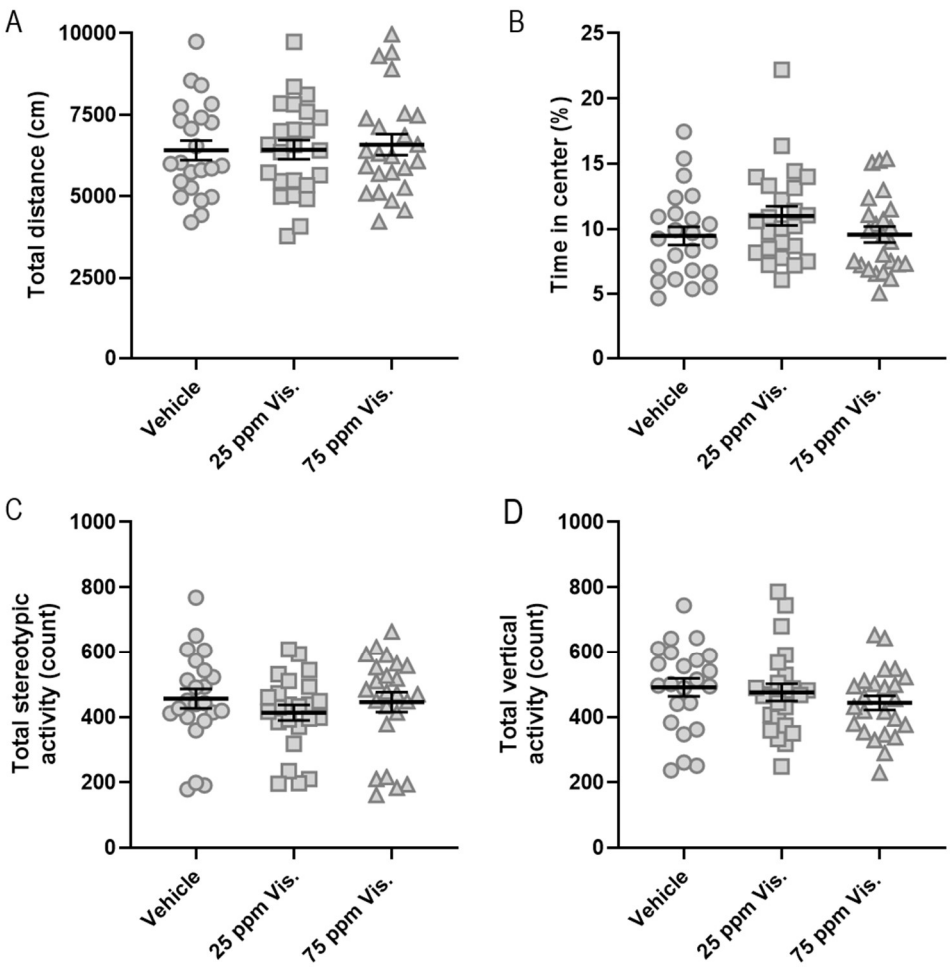

FIGURE 4. Evaluation of open field exploration in adult mice with prenatal vismodegib exposure. (A–D) Plots of total distance traveled, the percentage of time spent in the center of the arena versus the peripheries, and counts of stereotypic behavior and vertical activity in mice from dams provided chow containing vehicle (n = 23) or 25 ppm (n = 24) or 75 ppm (n = 24) vismodegib. The 225 ppm vismodegib group was excluded from behavioral testing due to low litter viability. Data are presented as mean ± SEM. For statistical testing, time in center data were log-transformed to achieve a normal distribution. Stereotypic activity results failed Shapiro-Wilk normality testing, so a nonparametric aligned rank transform was performed prior to analysis. Two-way ANOVA with Tukey's post hoc test was used to assess differences by treatment and sex.

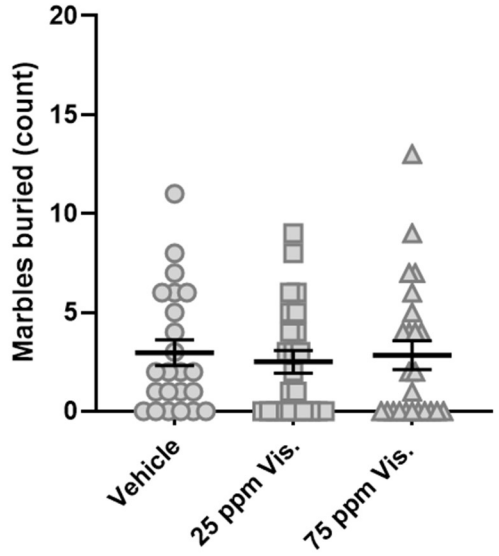

FIGURE 5. Marble burying behavior in adult mice with prenatal vismodegib exposure. The number of marbles buried by mice prenatally exposed to diets containing vehicle (n = 23) or 25 ppm (n = 24) or 75 ppm (n = 24) vismodegib. Data are presented as mean ± SEM. The data failed Shapiro–Wilk normality testing, so a nonparametric aligned rank transform two-way ANOVA with post hoc test was used to assess differences by treatment and sex.

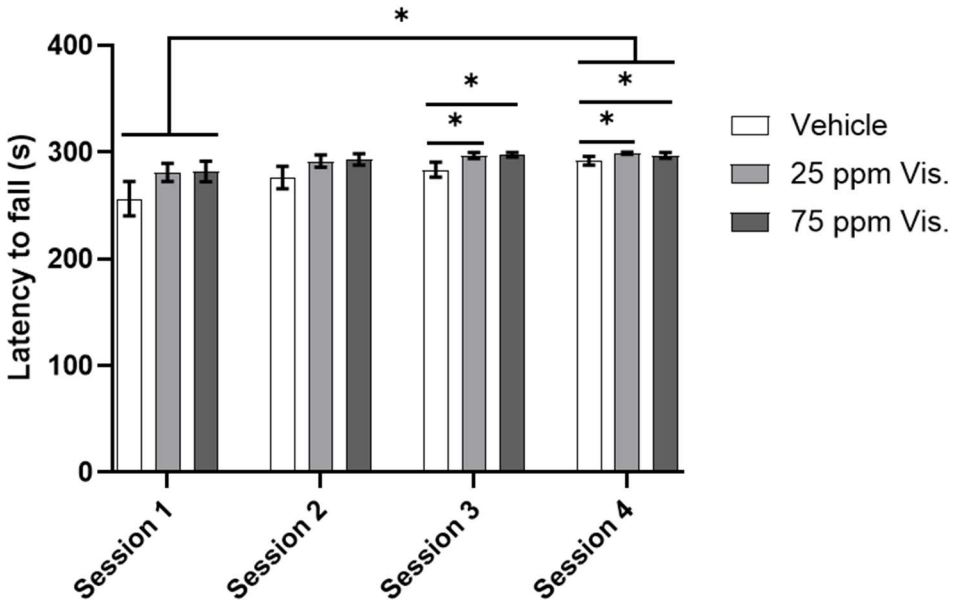

FIGURE 6. Rotarod performance in adult mice with prenatal vismodegib exposure. Mice prenatally exposed to diets containing vehicle (n = 23) or 25 ppm (n = 24) or 75 ppm (n = 24) vismodegib were placed on a rotarod apparatus for four sessions, and the time it took for mice to fall from the apparatus was recorded. Many mice from each treatment group successfully remained on the rotarod for the full duration of each 300-s session. Values represent the mean ± SEM for each treatment and session. The data failed Shapiro–Wilk normality testing, so a nonparametric aligned rank transform ANOVA with post hoc test was used to compare differences between treatment groups, sexes, and sessions. Treatment- dependent changes are indicated within sessions, and a session-dependent difference was observed between the first and fourth sessions. *$p < 0.05$.

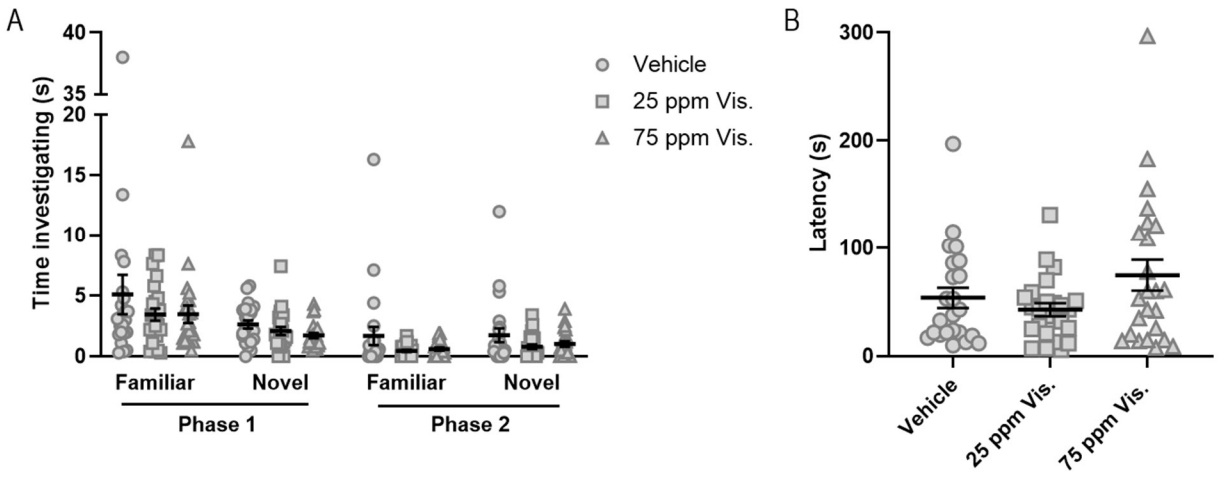

FIGURE 7. Assessment of olfactory detection and discrimination in adult mice exposed prenatally to vismodegib. (A) Olfactory discrimination in mice prenatally exposed to diets containing vehicle (n = 23) or 25 ppm (n = 24) or 75 ppm (n = 24) vismodegib was evaluated in two phases. In the first phase, the amount of time mice spent investigating a swab scented with water (familiar) or a swab scented with either lemon or mint (novel) was recorded. During the second phase, mice were provided with two scented swabs, one with the now familiar scent from phase one and the other with a novel scent. The amount of time spent investigating each swab was again recorded. (B) The latency to find a scented object buried beneath bedding was used to evaluate the ability of treated mice to detect odors. Data are presented as mean ± SEM. For olfactory discrimination, the data failed Shapiro–Wilk normality testing, so a nonparametric aligned rank transform ANOVA with post hoc test was used to compare differences by treatment group, sexes, and scent within each session. Olfactory detection data were log-normalized to achieve a normal distribution, and two-way ANOVA with Tukey's post hoc test was used to assess differences by treatment and sex.

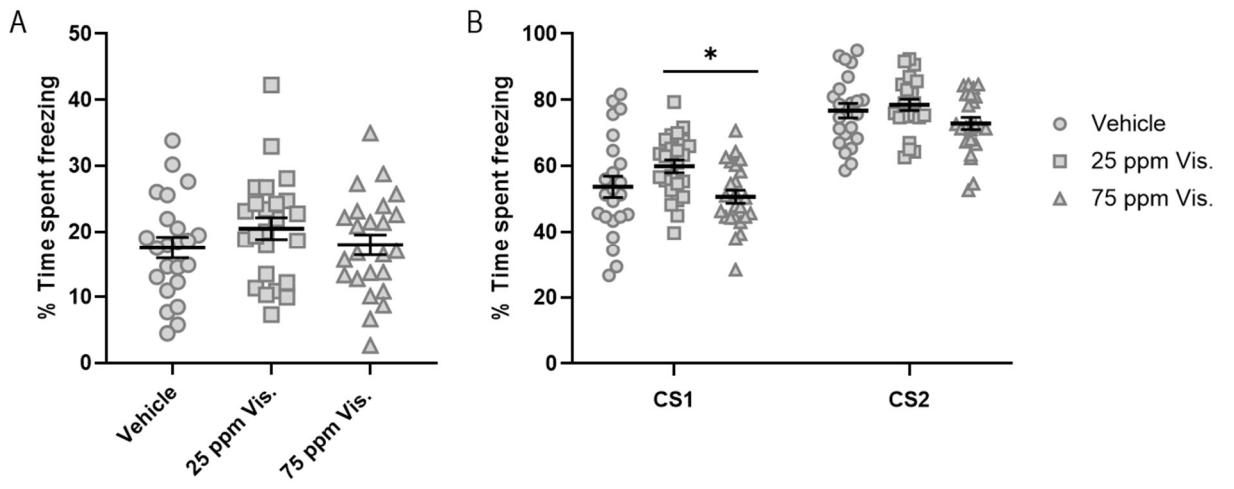

FIGURE 8. Fear conditioning behavior in adult mice exposed prenatally to vismodegib. (A) To test contextual fear recall, mice prenatally exposed to diets of vehicle (n = 23) or 25 ppm (n = 24) or 75 ppm (n = 24) vismodegib were placed in the same fear conditioning chamber in which they first experienced the CS-US pairing 22 h prior, and time spent freezing was recorded over a 360-s period. (B) Cued fear recall was assessed by administering the CS only to mice in a novel context 24 h after the CS-US training. Time spent freezing during each 30 s CS event was recorded. Bars represent mean ± SEM. Two-way ANOVA with Tukey's post hoc test was used to assess differences by treatment and sex. *$p<0.05$.

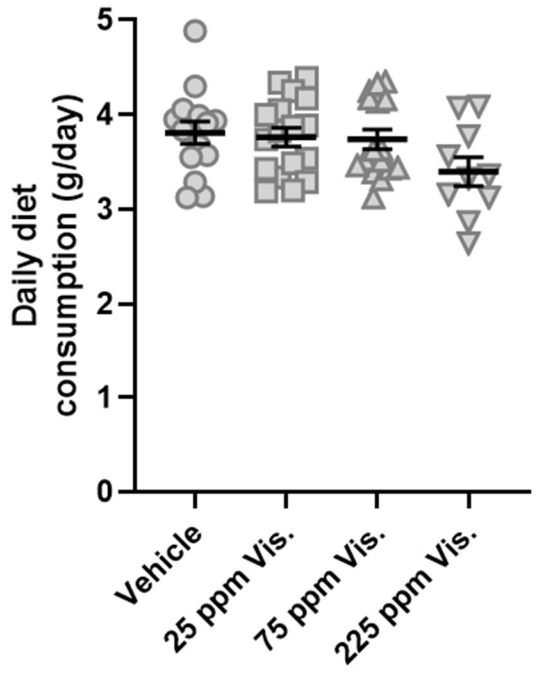

Supplemental Figure 1. Daily chow consumption in pregnant dams. Chow was weighed at the beginning (GD4) and end (GD11 or GD12) of the treatment period to calculate an estimate of daily consumption. No significant differences were observed between treatment groups, though the 225 ppm vismodegib group trended toward slightly lower consumption on average.

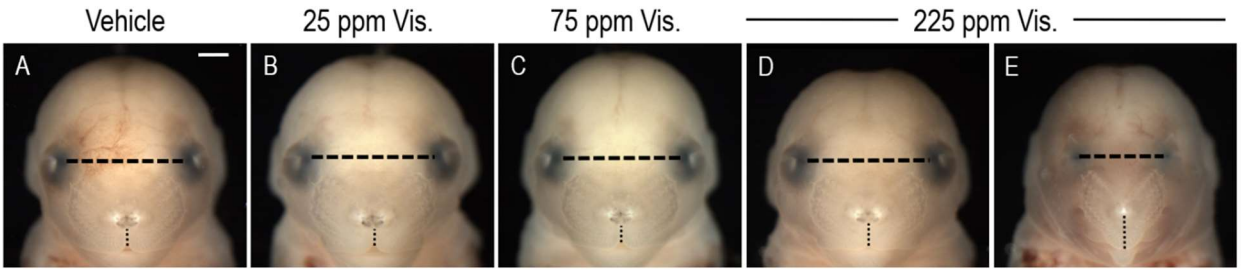

Supplemental Figure 2. Quantitative morphometric measurements of interocular distance (IOD) and upper lip length (ULL) in GD17 fetuses. (A-E) IOD (broken line) and ULL (dotted line) measurements are shown for each image in Figure 1. IOD reflects the minimum distance between the dark pigmented portion of the eyes, and ULL is the distance from the center of the upper lip (notched in normal and moderately affected animals) to the pigmented portion of the nose. In severely affected animals lacking pigment on the nose (i.e. panel E), upper lip length is measured from the center of the upper lip to the bright, single nostril.

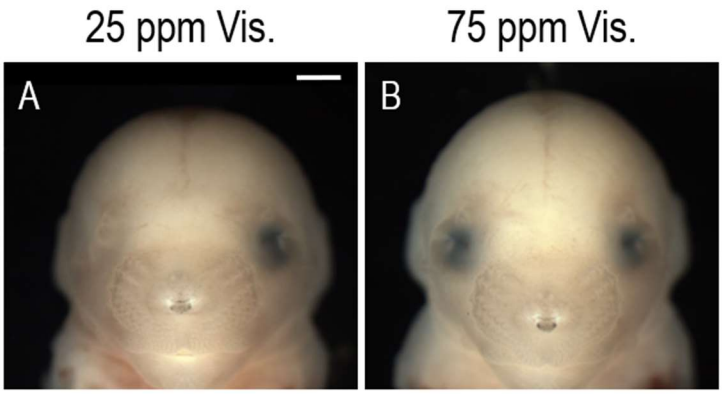

Supplemental Figure 3. HPE phenotypes in 25 ppm and 75 ppm vismodegib treatment groups. A single fetus each from the 25 ppm (A) and 75 ppm (B) treatment groups exhibited facial features consistent with HPE, such as decreased interocular distance (Figure 1F), increased upper lip length (Figure 1G), shallow upper lip notch, and narrow snout. Unilateral microphthalmia/anophthalmia was also observed in the apparently affected fetus from the 25 ppm treatment group. Scale bar: 1 mm

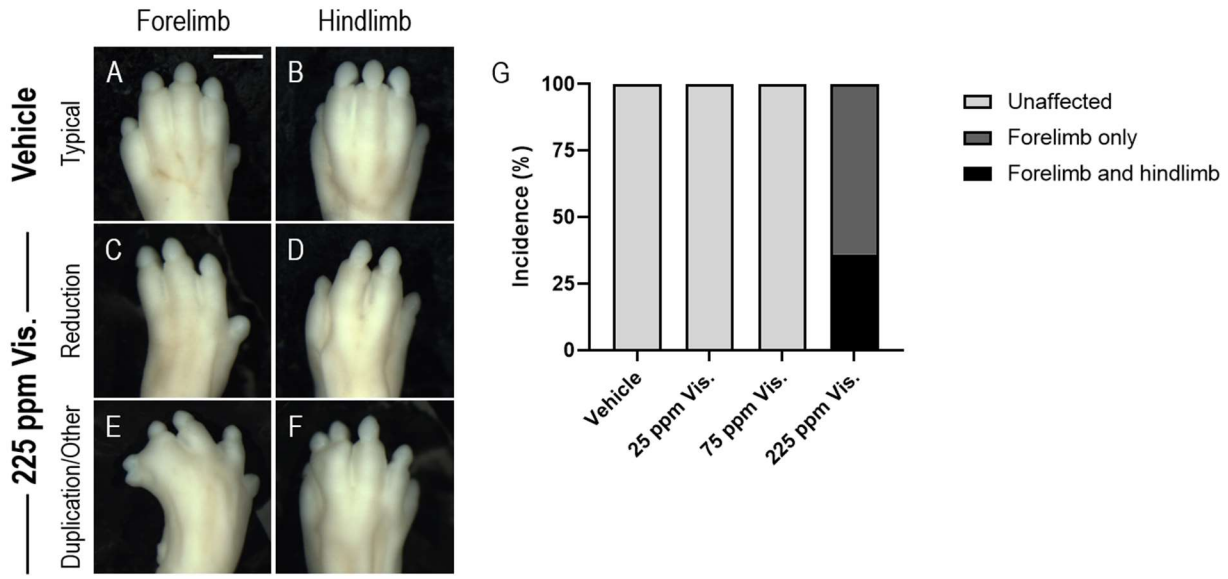

Supplemental Figure 4. Forelimb and hindlimb malformations were observed in the 225 ppm vismodegib treatment group. (A-B) Typical forelimb and hindlimb morphology from the vehicle-treated group are shown for reference. (C-D) In the 225 ppm vismodegib treatment group, digit reductions occurred in both forelimbs and hindlimbs. (E-F) Digit duplications, fusions, and other complex malformations were observed in both forelimbs and hindlimbs following prenatal exposure to the 225 ppm vismodegib diet. (G) Plot of incidence of limb malformations. Limb malformations were not observed in the vehicle or 25 ppm or 75 ppm vismodegib treatment groups. All 225 ppm vismodegib pups exhibited at least one forelimb malformation, and co-occurring hindlimb malformations were observed in 36% of pups. Scale bar: 1 mm

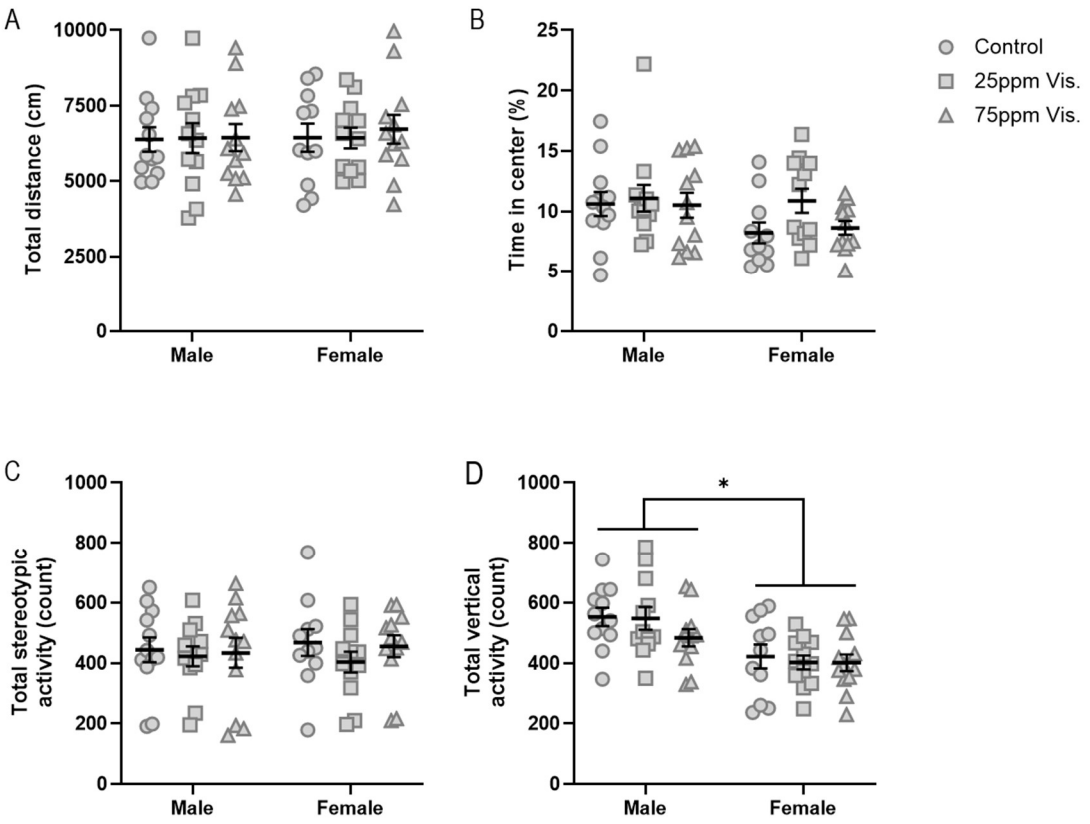

Supplemental Figure 5. Evaluation of open field exploration in adult mice with prenatal vismodegib exposure by sex. (A-D) Plots of total distance traveled, the percentage of time spent in the center of the arena versus the peripheries, and counts of stereotypic behavior and vertical activity separated by sex. Sex-dependent differences were only observed for total vertical activity (D). A total of twenty-three vehicle-treated mice (12 male, 11 female), twenty-four 25 ppm vismodegib-treated mice (12 male, 12 female), and twenty-four 75 ppm vismodegib-treated mice (12 male, 12 female) were evaluated. Data are presented as mean ± SEM. For statistical testing, time in center data were log-transformed to achieve a normal distribution. Stereotypic activity results failed Shapiro-Wilk normality testing, so a nonparametric aligned rank transform was performed prior to analysis. Two-way ANOVA with Tukey's post hoc test was used to assess differences by treatment and sex. * $p < 0.05$

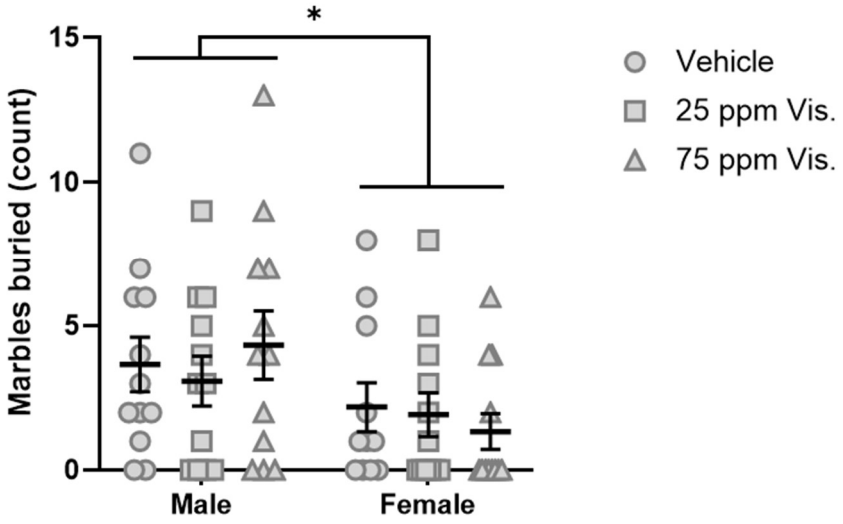

Supplemental Figure 6. Marble burying behavior in adult mice with prenatal vismodegib exposure evaluated by sex. The number of marbles buried by each mouse, separated by sex. A total of twenty-three vehicle-treated mice (12 male, 11 female), twenty-four 25 ppm vismodegib-treated mice (12 male, 12 female), and twenty-four 75 ppm vismodegib-treated mice (12 male, 12 female) were evaluated. Data are presented as mean ± SEM. The data failed Shapiro-Wilk normality testing, so a nonparametric aligned rank transform two-way ANOVA with post hoc test was used to assess differences by treatment and sex. * $p < 0.05$

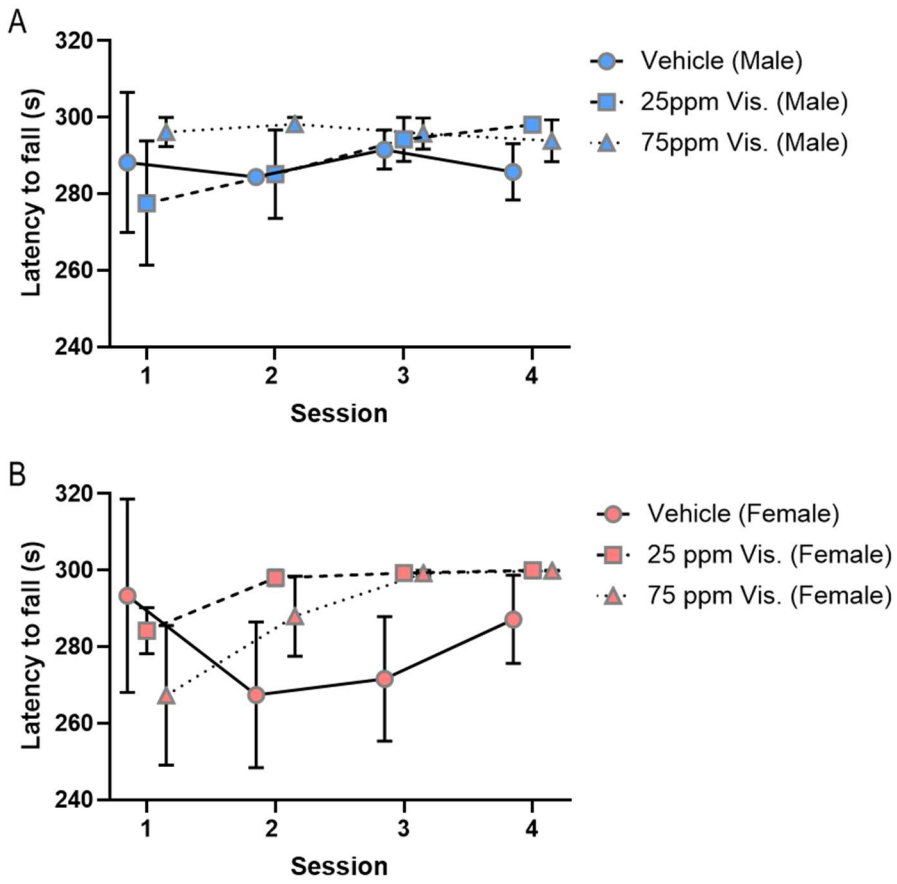

Supplemental Figure 7. Rotarod performance in adult male and female mice with prenatal vismodegib exposure. (A-B) Male and female mice were placed on a rotarod apparatus for four sessions, and the time it took for mice to fall from the apparatus was recorded. A total of twenty-three vehicle-treated mice (12 male, 11 female), twenty-four 25 ppm vismodegib-treated mice (12 male, 12 female), and twenty-four 75 ppm vismodegib-treated mice (12 male, 12 female) were evaluated. Values are offset for clarity and represent the mean ± SEM for each treatment and session. The data failed Shapiro-Wilk normality testing, so a nonparametric aligned rank transform ANOVA with post hoc test was used to compare differences between treatment groups, sexes, and sessions. Across all treatment groups and sessions, males remained on the rotarod for significantly more time, 289.7 ± 2.7 s compared to 284.9 ± 3.6 s for females. * $p < 0.05$

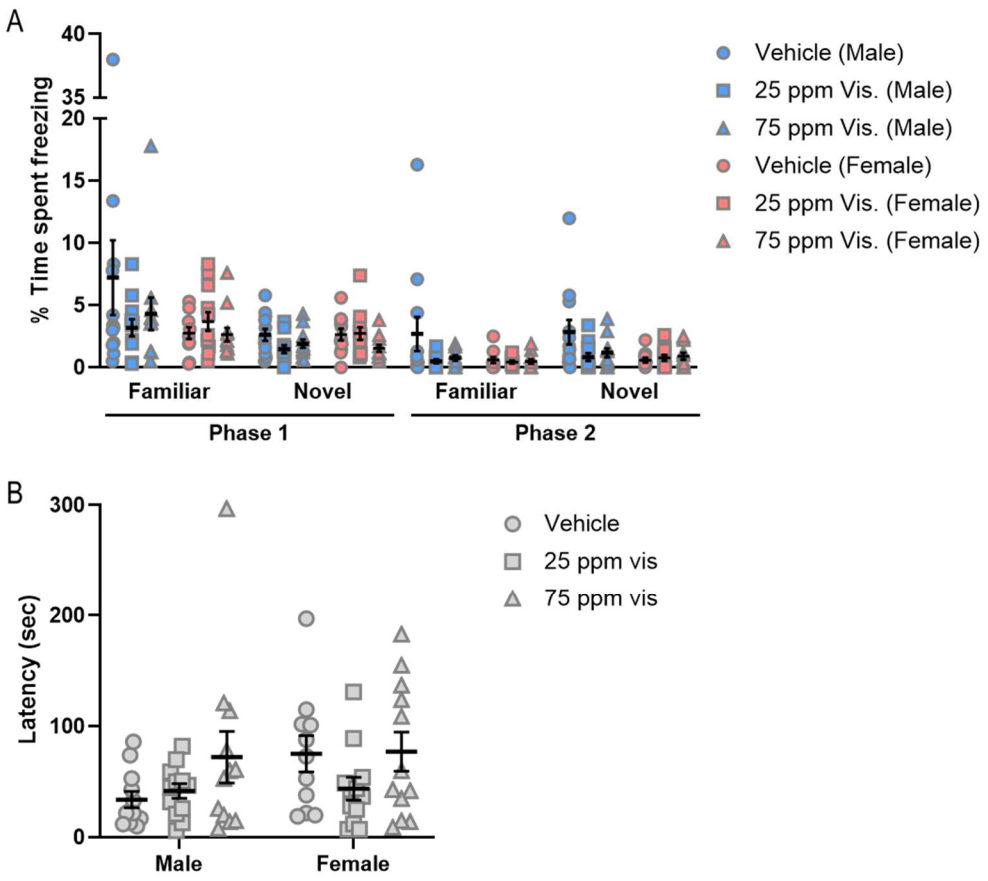

Supplemental Figure 8. Assessment of olfactory detection and discrimination in adult male and female mice exposed prenatally to vismodegib. (A) Olfactory discrimination in mice was evaluated in two phases. In the first phase, the amount of time mice spent investigating a swab scented with water (familiar) or a swab scented with either lemon or mint (novel) was recorded. During the second phase, mice were provided with two scented swabs, one with the now familiar scent from phase one and the other with a novel scent. The amount of time spent investigating each swab was again recorded. (B) The latency to find a scented object buried beneath bedding was used evaluate the ability of treated mice to detect odors. A total of twenty-three vehicle-treated mice (12 male, 11 female), twenty-four 25 ppm vismodegib-treated mice (12 male, 12 female), and twenty-four 75 ppm vismodegib-

treated mice (12 male, 12 female) were evaluated. Data are presented as mean ± SEM. For olfactory discrimination, the data failed ShapiroWilk normality testing, so a nonparametric aligned rank transform ANOVA with post hoc test was used to compare differences by treatment group, sexes, and scent within each session. Olfactory detection data were log-normalized to achieve a normal distribution, and two-way ANOVA with Tukey's post hoc test was used to assess differences by treatment and sex.

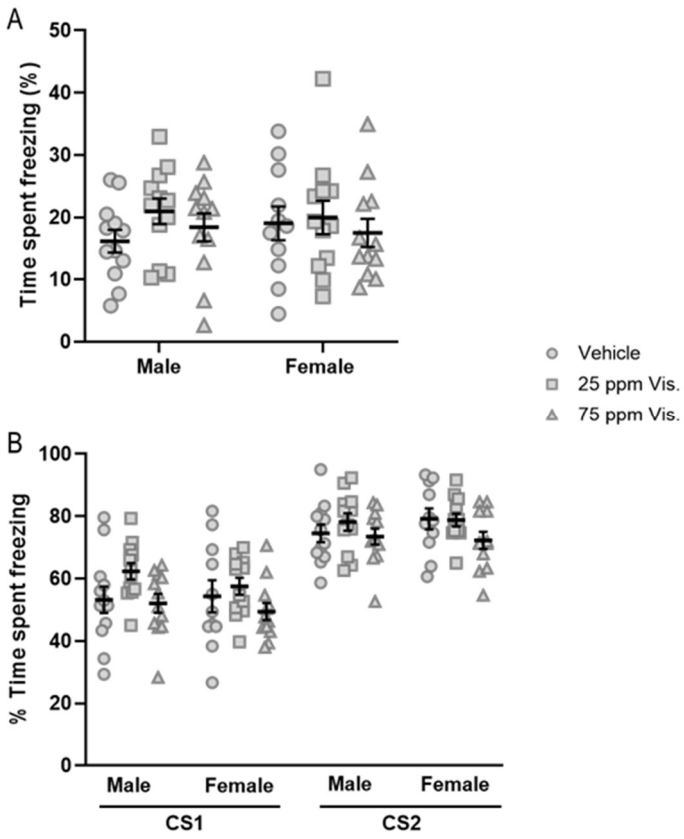

Supplemental Figure 9. Fear conditioning behavior in adult mice exposed prenatally to vismodegib evaluated by sex. (A) To test contextual fear recall, mice prenatally exposed to diets of vehicle (n=23) or 25 ppm (n=24) or 75 ppm (n=24) vismodegib were placed in the same fear conditioning chamber in which they first experienced the CS-US pairing 22 h prior, and time spent freezing was recorded over a 360 s period. (B) Cued fear recall was assessed by administering the CS only to mice in a novel context 24 h after the CS-US training. Time spent freezing during each 30 s CS event was recorded. A total of twenty-three vehicle-treated mice (12 male, 11 female), twenty-four 25 ppm vismodegib-treated mice (12 male, 12 female), and twenty-four 75 ppm vismodegib-treated mice (12 male, 12 female) were evaluated. Bars represent mean ± SEM. Two-way ANOVA with Tukey's post hoc test was used to assess differences by treatment and sex.

CHAPTER V: FUTURE DIRECTIONS

Tyler G. Beames

ABSTRACT

Defining the role of environmental risk in etiologically complex birth defects is an important step in developing effective prevention strategies. In this work, we investigated the impacts of chemical modulation of the Sonic hedgehog (Shh) signaling pathway, an integral developmental regulator that is associated with etiologically complex congenital malformations and is susceptible to disruption by diverse small molecules. To identify and characterize environmental risk factors in the context of etiologically complex birth defects, we utilized *in vitro* and *in vivo* models to examine the dynamics of chemical interactions, the potency and efficacy of human-relevant toxicants, and low-dose effects during gestation with a focus on Shh signaling-mediated outcomes. These studies demonstrated synergistic disruption of the Shh pathway *in vitro* and potentiation of teratogenesis in a zebrafish embryo model, characterized putative Shh pathway inhibitors with probable sources of human exposure, and investigated neurodevelopmental changes following dietary Shh signaling inhibition during early gestation. These results advance our understanding of environmental contributions to Shh signaling pathway disruption, but additional questions follow from the results of these studies. In this chapter, we propose additional avenues of research that will further clarify how environmental risk contributes to the overall prevalence and severity of birth defects.

Investigating the induction of Shh signaling-related malformations by environmental chemicals and mixtures

In chapters two and three of this work, we demonstrated that Shh signaling inhibitors can interact to synergistically reduce pathway activity and that human-relevant chemicals can disrupt Shh signaling. The next logical step is to confirm that the observed reduction in pathway activity using environmental chemicals translates to abnormal development. This approach was previously taken with the pesticide synergist piperonyl butoxide (PBO), which was found to inhibit Shh signaling in 2012 and subsequently demonstrated to cause HPE, cleft palate, and limb malformations (Everson et al., 2019; Rivera-González et al., 2024; Wang et al., 2012). Treating pregnant mice with the high-priority environmental compounds identified in chapter three during the critical period for craniofacial is an important step in validating the potential risk posed by these compounds. In addition to single-compound treatments, mixtures of Shh pathway antagonists can be established for dosing based on exposure estimates. Even when individual compounds are at concentrations below their lowest observed effect level (LOEL), mixtures have been shown to induce biological effects in accordance with the principles of dose addition (Kortenkamp et al., 2007; Silva et al., 2002). Exposure studies using mixtures of Shh pathway antagonists could provide the clearest demonstration of the risk posed by environmental factors in the development of etiologically complex, Shh signaling-mediated birth defects.

Elucidating mechanisms of synergism among Shh pathway inhibitors

The greatest mystery to arise over the course of the studies presented in this work is the mechanism by which PBO synergistically interacts with other SMO inhibitors such as

cyclopamine and vismodegib. Before beginning co-exposure testing with Shh pathway inhibitors, we hypothesized that similarly acting chemicals would interact additively, and dissimilar chemicals would have a higher probability to interact synergistically. To our surprise, PBO, which has been reported to competitively bind to the same region of SMO as cyclopamine (Wang et al., 2012), synergized with the highly studied SMO inhibitors cyclopamine and vismodegib. Following this observation, we utilized Shh pathway-modified cell lines to reveal that PBO likely has a SMO-independent mechanism that occurs further downstream in the pathway. One possibility we investigated was that PBO increased the activity of cyclopamine through its inhibition of cytochromes P450. To test this, we treated our Shh pathway-autonomous cell culture system with cyclopamine or PBO in the presence of SKF-525a, a pan-cytochrome P450 inhibitor. SKF-525a co-treatment increased the ability of these inhibitors to reduce Shh signaling activity (Fig. 1). Given that SKF-525a similarly increased the inhibitory effects of both PBO and cyclopamine, we do not believe that PBO is able to effectively inhibit cytochromes P450 at the concentrations that produce synergy. PBO's SMO-independent mechanism may belong to another signaling pathway that interacts with the Shh pathway, and this can be evaluated by assessing the GLI proteins. The GLI transcription factors are modified by phosphorylation and ubiquitination to regulate their stability and activity (reviewed in Yoshida & Yoshida, 2025). Changes in the amount of GLI proteins or the extent of phosphorylation and ubiquitination would support a non-canonical mechanism of Shh pathway inhibition. Another approach for distinguishing mechanisms between additive and synergistic interactions is to perform RNA-seq on samples treated with each of the inhibitors employed in chapter two. Differentially expressed genes across treatment groups may shed light on the mechanisms governing synergistic interactions and help

reveal additional mechanistic targets among compounds known to inhibit Shh signaling. Resolving the mystery of mechanisms of synergy would improve our ability to predict the types of interactions that occur within the Shh signaling pathway.

Incorporating advanced cell culture models to characterize environmental risk factors in birth defect etiology

Shh signaling in its native context during craniofacial development involves a spatially graded response (Dessaud et al., 2007; Kurosaka, 2015; Lan & Jiang, 2009; Stamataki et al., 2005), and alterations to the post-translational modification of the SHH ligand can impact its distribution throughout the extracellular space (Dawber et al., 2005). Multiple models have been reported to recapitulate this gradient of Shh signaling *in vitro*. In a microphysiological approach, the tissue architecture of the facial growth centers is recapitulated by seeding a thin layer of epithelial cells adjacent to a dense mesenchyme (Johnson et al., 2021). By overexpressing *SHH* in the epithelial cells, a gradient of Shh signaling activity was achieved within the mesenchymal cell population. This medium-throughput method could be leveraged to assess the impacts of chemicals that alter cholesterol availability on gradient formation, as well as to investigate co-exposures involving chemicals that disrupt the gradient. Another approach that incorporates gradient formation involves forebrain organoids (Cederquist et al., 2019). In the forebrain organoid model, a small population of cells capable of producing SHH ligand is embedded at one end of the organoid, becoming a point source of Shh activation. This model does not recapitulate the craniofacial tissue architecture, but it was shown to specify several unique cell populations within the organoid based on the extent of Shh signaling within those populations. These models could be leveraged to better understand how

environmental Shh pathway antagonists disrupt signaling across the gradient (i.e., are the cell populations with the lowest Shh signaling the most sensitive to inhibition?).

Assessing the impacts of coordinated disruption of critical developmental pathways on craniofacial development

Although the focus of this body of work is on the Shh signaling pathway, numerous other pathways regulate aspects of craniofacial development independently or through crosstalk (Neben & Merrill, 2015). Maintenance and specification of cranial neural crest cells within the developing facial processes requires interactions between the Shh, Wnt, FGF, TGF-β, and BMP signaling families (Roth et al., 2021; Xu et al., 2023). Within this complex network of pathways, small perturbations across distinct targets may add up to produce adverse effects. Testing this hypothesis can again leverage *in vitro* and *in vivo* models. Crosstalk with Shh signaling could be assessed in Shh-LIGHT2 cells through co-exposure to chemicals targeting different pathways or by reducing the activity of pathways that intersect with Shh signaling using CRISPR gene-editing. Gene editing is an especially promising approach since it enables the evaluation of human-relevant genetic variants. Once specific cross-pathway interactions are identified in cells, these methods can be brought to more biologically relevant models that better recapitulate tissue architecture and the full breadth of the signaling network. The proposed studies would support the identification of risk factors with disparate mechanisms within the etiology of multifactorial birth defects.

Impaired neurodevelopment resulting from second and third trimester Shh signaling disruption

In the fourth chapter of this work, we utilized a dietary model of low-dose Shh pathway inhibition to test whether we could induce neurodevelopmental deficits in the absence of overt craniofacial malformations. We provided mice with vismodegib-laced chow from gestational day (GD)4 through GD12 to target the critical periods for holoprosencephaly (HPE) and cleft palate (Heyne, Melberg, et al., 2015) and assessed early forebrain patterning at GD11 and behavior in adults. Vismodegib-exposed mice that appeared normal by facial phenotype showed no signs of abnormal neurodevelopment within the parameters of our investigation. This unexpected result may be explained by the selection of doses, the specific behavioral assays employed, or the incomplete penetrance of Shh pathway disruption reducing the power of our analyses by introducing high levels of variability. However, we favor the hypothesis that the exposure window did not align with a critical period during which neurodevelopment could be altered without modulating face shape. Relative to most organs, the development of the brain is prolonged, extending into the early postnatal period in mice. Animal models of fetal alcohol spectrum disorders have demonstrated that gestational alcohol exposure induces craniofacial malformations during the equivalent of the first trimester, whereas effects are primarily neurological when administration is delayed to the second and third trimester equivalents (Almeida et al., 2020). Robust disruption of the Shh signaling pathway subsequent to craniofacial morphogenesis may similarly induce neurobehavioral deficits without producing external malformations. There is also a functional basis for this hypothesis. Shh signaling plays a role in oligodendrogenesis later than GD 12 in mice, and rodent neural cell culture models exhibit altered oligodendrocyte and astrocyte differentiation following modulation of Shh

signaling (Araújo et al., 2014; Machold et al., 2003; Wang & Almazan, 2016; Winkler et al., 2018). This hypothesis is readily addressable using our dietary model of Shh pathway inhibition. Pregnant dams can be maintained on modified diets from approximately GD12 through weaning of pups, and behavior can be similarly assessed in adults. The identification of a later critical period for Shh-associated neurobehavioral disorders would support the expansion of diagnostic criteria for diseases associated with prenatal Shh pathway disruption.

FIGURES

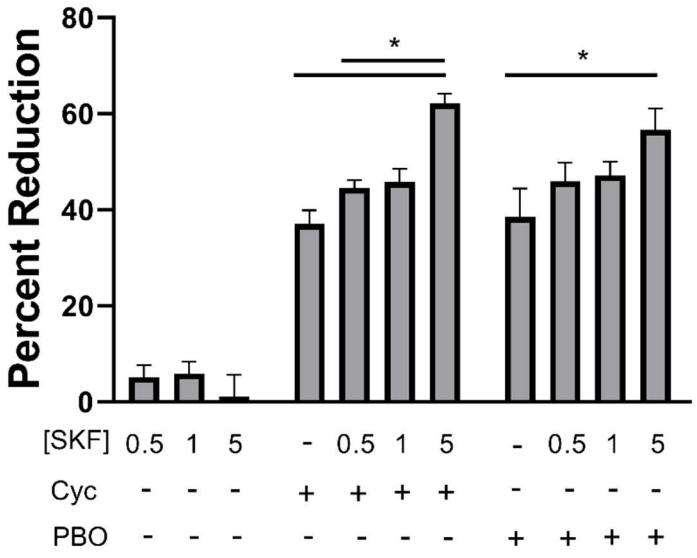

FIGURE 1. Inhibition of cytochrome P450 enzymes enhances the efficacy of cyclopamine and PBO. The Shh pathway signal transduction model was treated with graded concentrations of the non-selective cytochrome P450 inhibitor SKF-525A alone or in combination with cyclopamine or PBO. Following 48 h of treatment, the reduction in GLI1-driven luminescence was assessed. Bars represent the mean and SEM. One-way ANOVA with Dunnett's post-hoc was used to compare the co-exposed groups against singe cyclopamine or PBO exposure. Bars represent the mean ± SEM (n = 3). * $p<0.05$

WORKS CITED

Abler, L. L., Mehta, V., Keil, K. P., Joshi, P. S., Flucus, C. L., Hardin, H. A.,...Vezina, C. M. (2011). A high throughput in situ hybridization method to characterize mRNA expression patterns in the fetal mouse lower urogenital tract. *J Vis Exp*(54). https://doi.org/10.3791/2912

Addissie, Y. A., Troia, A., Wong, Z. C., Everson, J. L., Kozel, B. A., Muenke, M.,...Kruszka, P. (2021). Identifying environmental risk factors and gene–environment interactions in holoprosencephaly [https://doi.org/10.1002/bdr2.1834]. *Birth Defects Research*, *113*(1), 63-76. https://doi.org/https://doi.org/10.1002/bdr2.1834

Ahlborg, U. G., & Hanberg, A. (1994). Toxic equivalency factors for dioxin-like PCBs. *Environ Sci Pollut Res Int*, *1*(2), 67-68. https://doi.org/10.1007/bf02986503

Al-Ayadhi, L. Y. (2012). Relationship Between Sonic Hedgehog Protein, Brain-Derived Neurotrophic Factor and Oxidative Stress in Autism Spectrum Disorders. *Neurochemical Research*, *37*(2), 394-400. https://doi.org/10.1007/s11064-011-0624-x

Almeida, L., Andreu-Fernández, V., Navarro-Tapia, E., Aras-López, R., Serra-Delgado, M., Martínez, L.,...Gómez-Roig, M. D. (2020). Murine Models for the Study of Fetal Alcohol Spectrum Disorders: An Overview [Review]. *Frontiers in Pediatrics*, *8*.

Amato, C. M., Fricke, A., Marella, S., Mogus, J. P., Bereman, M., & McCoy, K. A. (2022). An experimental evaluation of the efficacy of perinatal sulforaphane supplementation to decrease the incidence and severity of vinclozolin-induced hypospadias in the mouse model. *Toxicol Appl Pharmacol*, *451*, 116177. https://doi.org/10.1016/j.taap.2022.116177

Ansen-Wilson, L. J., & Lipinski, R. J. (2017). Gene-environment interactions in cortical interneuron development and dysfunction: A review of preclinical studies. *NeuroToxicology*, *58*, 120-129.

Araújo, G. L., Araújo, J. A., Schroeder, T., Tort, A. B., & Costa, M. R. (2014). Sonic hedgehog signaling regulates mode of cell division of early cerebral cortex progenitors and increases astrogliogenesis [Original Research]. *Frontiers in Cellular Neuroscience*, *8*.

Arora, N., Imran Alsous, J., Guggenheim, J. W., Mak, M., Munera, J., Wells, J. M.,...Griffith, L. G. (2017). A process engineering approach to increase organoid yield. *Development*, *144*(6), 1128. https://doi.org/10.1242/dev.142919

Balik-Meisner, M., Truong, L., Scholl Elizabeth, H., La Du Jane, K., Tanguay Robert, L., & Reif David, M. (2018). Elucidating Gene-by-Environment Interactions Associated with Differential Susceptibility to Chemical Exposure. *Environmental Health Perspectives*, *126*(6), 067010. https://doi.org/10.1289/EHP2662

Barbieri, O., Ognio, E., Rossi, O., Astigiano, S., & Rossi, L. (1986). Embryotoxicity of Benzo(a)pyrene and Some of Its Synthetic Derivatives in Swiss Mice1. *Cancer Research*, *46*(1), 94-98.

Barratt, K. S., Drover, K. A., Thomas, Z. M., & Arkell, R. M. (2022). Patterning of the antero-ventral mammalian brain: Lessons from holoprosencephaly comparative biology in man

and mouse. *WIREs Mechanisms of Disease*, *14*(4), e1552. https://doi.org/https://doi.org/10.1002/wsbm.1552

Beames, T. G., Everson, J. L., Desai, D. A, Perez, K. Y., Wu, E., Eberhart, J. K., & Lipinski, R. J. A cell-based Sonic hedgehog signaling transduction system to identify additive and synergistic chemical interactions. Submitted to *Arch of Tox*, 2025 Jun 04.

Beames, T. G., & Lipinski, R. J. (2020). Gene-environment interactions: aligning birth defects research with complex etiology. *Development*, *147*(21). https://doi.org/10.1242/dev.191064

Beaty, T. H., Marazita, M. L., & Leslie, E. J. (2016). Genetic factors influencing risk to orofacial clefts: today's challenges and tomorrow's opportunities. *F1000Research*, *5*, 2800-2800. https://doi.org/10.12688/f1000research.9503.1

Beauchamp, E. M., Ringer, L., Bulut, G., Sajwan, K. P., Hall, M. D., Lee, Y. C.,...Uren, A. (2011). Arsenic trioxide inhibits human cancer cell growth and tumor development in mice by blocking Hedgehog/GLI pathway. *J Clin Invest*, *121*(1), 148-160. https://doi.org/10.1172/jci42874

Belair, D. G., Wolf, C. J., Moorefield, S. D., Wood, C., Becker, C., & Abbott, B. D. (2018). A Three-Dimensional Organoid Culture Model to Assess the Influence of Chemicals on Morphogenetic Fusion. *Toxicological Sciences*, *166*(2), 394-408. https://doi.org/10.1093/toxsci/kfy207

Bell, J. C., Raynes-Greenow, C., Turner, R. M., Bower, C., Nassar, N., & O'Leary, C. M. (2014). Maternal Alcohol Consumption during Pregnancy and the Risk of Orofacial Clefts in Infants: a Systematic Review and Meta-Analysis. *Paediatric and Perinatal Epidemiology*, *28*(4), 322-332. https://doi.org/10.1111/ppe.12131

Biesecker, L. G. (2011). Polydactyly: how many disorders and how many genes? 2010 update. *Dev Dyn*, *240*(5), 931-942. https://doi.org/10.1002/dvdy.22609

Britto, J., Tannahill, D., & Keynes, R. (2002). A critical role for sonic hedgehog signaling in the early expansion of the developing brain. *Nature Neuroscience*, *5*(2), 103-110. https://doi.org/10.1038/nn797

Buglino, J. A., & Resh, M. D. (2008). Hhat Is a Palmitoylacyltransferase with Specificity for *N*-Palmitoylation of Sonic Hedgehog. *Journal of Biological Chemistry*, *283*(32), 22076-22088. https://doi.org/10.1074/jbc.M803901200

Bush, J. O., & Jiang, R. (2012). Palatogenesis: morphogenetic and molecular mechanisms of secondary palate development. *Development*, *139*(2), 231. https://doi.org/10.1242/dev.067082

Butt, S. J. B., Fuccillo, M., Nery, S., Noctor, S., Kriegstein, A., Corbin, J. G., & Fishell, G. (2005). The temporal and spatial origins of cortical interneurons predict their physiological subtype. *Neuron*, *48*(4), 591-604. https://doi.org/10.1016/j.neuron.2005.09.034

Cederquist, G. Y., Asciolla, J. J., Tchieu, J., Walsh, R. M., Cornacchia, D., Resh, M. D., & Studer, L. (2019). Specification of positional identity in forebrain organoids. *Nature biotechnology*, *37*(4), 436-444. https://doi.org/10.1038/s41587-019-0085-3

Cenedella, R. J. (2009). Cholesterol Synthesis Inhibitor U18666A and the Role of Sterol Metabolism and Trafficking in Numerous Pathophysiological Processes. *Lipids*, *44*(6), 477-487. https://doi.org/https://doi.org/10.1007/s11745-009-3305-7

Chaklader, M., & Law, S. (2015). Alteration of hedgehog signaling by chronic exposure to different pesticide formulations and unveiling the regenerative potential of recombinant sonic hedgehog in mouse model of bone marrow aplasia. *Molecular and Cellular Biochemistry*, *401*(1), 115-131. https://doi.org/10.1007/s11010-014-2299-5

Chapman, G., Moreau, J. L. M., Ip, E., Szot, J. O., Iyer, K. R., Shi, H.,...Dunwoodie, S. L. (2019). Functional genomics and gene-environment interaction highlight the complexity of Congenital Heart Disease caused by Notch pathway variants. *Human Molecular Genetics*. https://doi.org/10.1093/hmg/ddz270

Chen, J. K. (2016). I only have eye for ewe: the discovery of cyclopamine and development of Hedgehog pathway-targeting drugs. *Nat Prod Rep*, *33*(5), 595-601. https://doi.org/10.1039/c5np00153f

Chen, J. K., Taipale, J., Cooper, M. K., & Beachy, P. A. (2002). Inhibition of Hedgehog signaling by direct binding of cyclopamine to Smoothened. *Genes Dev*, *16*(21), 2743-2748. https://doi.org/10.1101/gad.1025302

Chen, M. H., Li, Y. J., Kawakami, T., Xu, S. M., & Chuang, P. T. (2004). Palmitoylation is required for the production of a soluble multimeric Hedgehog protein complex and long-range signaling in vertebrates. *Genes Dev*, *18*(6), 641-659. https://doi.org/10.1101/gad.1185804

Chiang, C., Litingtung, Y., Lee, E., Young, K. E., Corden, J. L., Westphal, H., & Beachy, P. A. (1996). Cyclopia and defective axial patterning in mice lacking Sonic hedgehog gene function. *Nature*, *383*(6599), 407-413. https://doi.org/10.1038/383407a0

Choudhry, Z., Rikani, A. A., Choudhry, A. M., Tariq, S., Zakaria, F., Asghar, M. W.,...Mobassarah, N. J. (2014). Sonic hedgehog signalling pathway: a complex network. *Ann Neurosci*, *21*(1), 28-31. https://doi.org/10.5214/ans.0972.7531.210109

Christianson, A., Howson, C. P., & Modell, B. (2006). March of Dimes global report on birth defects: the hidden toll of dying and disabled children. *The March of Dimes Birth Defects Foundations*. Retrieved 11 November 2021, from

Cohen, M. M. (2006). Holoprosencephaly: Clinical, anatomic, and molecular dimensions. *Birth Defects Research Part a-Clinical and Molecular Teratology*, *76*(9), 658-673. https://doi.org/Doi 10.1002/Bdra.20295

Coles, C. D., Kalberg, W., Kable, J. A., Tabachnick, B., May, P. A., & Chambers, C. D. (2020). Characterizing Alcohol-Related Neurodevelopmental Disorder: Prenatal Alcohol Exposure and the Spectrum of Outcomes. *Alcoholism: Clinical and Experimental Research*, *44*(6), 1245-1260. https://doi.org/https://doi.org/10.1111/acer.14325

Cooper, M. K., Porter, J. A., Young, K. E., & Beachy, P. A. (1998). Teratogen-mediated inhibition of target tissue response to Shh signaling. *Science*, *280*(5369), 1603-1607. https://doi.org/10.1126/science.280.5369.1603

Cuny, H., Rapadas, M., Gereis, J., Martin, E. M. M. A., Kirk, R. B., Shi, H., & Dunwoodie, S. L. (2020). NAD deficiency due to environmental factors or gene–environment interactions causes congenital malformations and miscarriage in mice. *Proceedings of the National Academy of Sciences*, *117*(7), 3738. https://doi.org/10.1073/pnas.1916588117

Dawber, R. J., Hebbes, S., Herpers, B., Docquier, F., & van den Heuvel, M. (2005). Differential range and activity of various forms of the Hedgehog protein. *BMC Dev Biol*, *5*, 21. https://doi.org/10.1186/1471-213x-5-21

De Felice, A., Ricceri, L., Venerosi, A., Chiarotti, F., & Calamandrei, G. (2015). Multifactorial Origin of Neurodevelopmental Disorders: Approaches to Understanding Complex Etiologies. *Toxics*, *3*(1), 89-129.

DeMyer, W., Zeman, W., & Palmer, C. G. (1964). The face predicts the brain: Diagnostic significance of median facial anomalies for holoprosencephaly (arhinencephaly). *Pediatrics*, *34*, 256-263.

Dessaud, E., Yang, L. L., Hill, K., Cox, B., Ulloa, F., Ribeiro, A.,...Briscoe, J. (2007). Interpretation of the sonic hedgehog morphogen gradient by a temporal adaptation mechanism. *Nature*, *450*(7170), 717-720. https://doi.org/10.1038/nature06347

Dhekne, H. S., Yanatori, I., Gomez, R. C., Tonelli, F., Diez, F., Schüle, B.,...Pfeffer, S. R. (2018). A pathway for Parkinson's Disease LRRK2 kinase to block primary cilia and Sonic hedgehog signaling in the brain. *eLife*, *7*, e40202. https://doi.org/10.7554/eLife.40202

Ding, F., & Yang, S. (2021). Epigallocatechin-3-gallate inhibits proliferation and triggers apoptosis in colon cancer via the hedgehog/phosphoinositide 3-kinase pathways. *Canadian Journal of Physiology and Pharmacology*, *99*(9), 910-920. https://doi.org/10.1139/cjpp-2020-0588

Dixon, M. J., Marazita, M. L., Beaty, T. H., & Murray, J. C. (2011). Cleft lip and palate: understanding genetic and environmental influences. *Nature Reviews Genetics*, *12*(3), 167-178.

Du, W.-Z., Feng, Y., Wang, X.-F., Piao, X.-Y., Cui, Y.-Q., Chen, L.-C.,...Jiang, C.-L. (2013). Curcumin suppresses malignant glioma cells growth and induces apoptosis by inhibition of SHH/GLI1 signaling pathway in vitro and vivo. *CNS neuroscience & therapeutics*, *19*(12), 926-936. https://doi.org/10.1111/cns.12163

Dubourg, C., Kim, A., Watrin, E., De Tayrac, M., Odent, S., David, V., & Dupé, V. (2018). Recent advances in understanding inheritance of Holoprosencephaly. *American Journal of Medical Genetics Part C Seminar in Medical Genetics*, *178*(2), 258-269. https://doi.org/10.1002/ajmg.c.31619 (Holoprosencephaly)

Eberhart, J. K., Swartz, M. E., Crump, J. G., & Kimmel, C. B. (2006). Early Hedgehog signaling from neural to oral epithelium organizes anterior craniofacial development. *Development*, *133*(6), 1069-1077. https://doi.org/10.1242/dev.02281

Elamin, M. H., Shinwari, Z., Hendrayani, S. F., Al-Hindi, H., Al-Shail, E., Khafaga, Y.,...Aboussekhra, A. (2010). Curcumin inhibits the Sonic Hedgehog signaling pathway and triggers apoptosis in medulloblastoma cells. *Mol Carcinog*, *49*(3), 302-314. https://doi.org/10.1002/mc.20604

Elkin, L. A., Kay, M., Higgins, J. J., & Wobbrock, J. O. (2021). *An Aligned Rank Transform Procedure for Multifactor Contrast Tests* The 34th Annual ACM Symposium on User Interface Software and Technology, Virtual Event, USA. https://doi.org/10.1145/3472749.3474784

Ericson, J., Muhr, J., Placzek, M., Lints, T., Jessel, T. M., & Edlund, T. (1995). Sonic hedgehog induces the differentiation of ventral forebrain neurons: A common signal for ventral patterning within the neural tube. *Cell*, *81*(5), 747-756. https://doi.org/https://doi.org/10.1016/0092-8674(95)90536-7

Escher, B. I., Hackermüller, J., Polte, T., Scholz, S., Aigner, A., Altenburger, R.,...Wambaugh, J. F. (2017). From the exposome to mechanistic understanding of chemical-induced adverse effects. *Environ Int*, *99*, 97-106. https://doi.org/10.1016/j.envint.2016.11.029

Everson, J. L., Batchu, R., & Eberhart, J. K. (2020). Multifactorial Genetic and Environmental Hedgehog Pathway Disruption Sensitizes Embryos to Alcohol-Induced Craniofacial Defects. *Alcohol Clin Exp Res*, *44*(10), 1988-1996. https://doi.org/10.1111/acer.14427

Everson, J. L., Fink, D. M., Yoon, J. W., Leslie, E. J., Kietzman, H. W., Ansen-Wilson, L. J.,...Lipinski, R. J. (2017). Sonic hedgehog regulation of Foxf2 promotes cranial neural crest mesenchyme proliferation and is disrupted in cleft lip morphogenesis. *Development*, *144*(11), 2082-2091. https://doi.org/10.1242/dev.149930

Everson, J. L., Sun, M. R., Fink, D. M., Heyne, G. W., Melberg, C. G., Nelson, K. F.,...Lipinski, R. J. (2019). Developmental Toxicity Assessment of Piperonyl Butoxide Exposure Targeting Sonic Hedgehog Signaling and Forebrain and Face Morphogenesis in the Mouse: An in Vitro and in Vivo Study. *Environmental Health Perspectives*, *127*(10), 107006. https://doi.org/10.1289/EHP5260

Everson, J. L., Tseng, Y. C., & Eberhart, J. K. (2023). High-throughput detection of craniofacial defects in fluorescent zebrafish. *Birth Defects Res*, *115*(3), 371-389. https://doi.org/10.1002/bdr2.2127

Fan, P., Fan, S., Wang, H., Mao, J., Shi, Y., Ibrahim, M. M.,...Li, L. (2013). Genistein decreases the breast cancer stem-like cell population through Hedgehog pathway. *Stem cell research & therapy*, *4*(6), 146-146. https://doi.org/10.1186/scrt357

Fang, M., Lu, Y., Chen, G. J., Shen, L., Pan, Y. M., & Wang, X. F. (2011). Increased expression of Sonic hedgehog in temporal lobe epileptic foci in humans and experimental rats. *Neuroscience*, *182*, 62-70. https://doi.org/https://doi.org/10.1016/j.neuroscience.2011.02.060

Feldkamp, M. L., Carey, J. C., Byrne, J. L. B., Krikov, S., & Botto, L. D. (2017). Etiology and clinical presentation of birth defects: population based study. *BMJ*, *357*, j2249. https://doi.org/10.1136/bmj.j2249

Feng, S., Ma, S., Jia, C., Su, Y., Yang, S., Zhou, K.,...Wang, Y. (2016). Sonic hedgehog is a regulator of extracellular glutamate levels and epilepsy. *EMBO reports*, *17*(5), 682-694-694. https://doi.org/https://doi.org/10.15252/embr.201541569

Finnell, R. H., Caiaffa, C. D., Kim, S. E., Lei, Y., Steele, J., Cao, X.,...Wlodarczyk, B. J. (2021). Gene Environment Interactions in the Etiology of Neural Tube Defects. *Front Genet*, *12*, 659612. https://doi.org/10.3389/fgene.2021.659612

Fraser, F. C. (2008). Of mice and children: Reminiscences of a teratogeneticist. *American Journal of Medical Genetics Part A*, *146A*(17), 2179-2202. https://doi.org/10.1002/ajmg.a.32372

Fraser, F. C., & Fainstat, T. D. (1951). PRODUCTION OF CONGENITAL DEFECTS IN THE OFFSPRING OF PREGNANT MICE TREATED WITH CORTISONE. *Pediatrics*, *8*(4), 527.

Fuccillo, M., Rallu, M., McMahon, A. P., & Fishell, G. (2004). Temporal requirement for hedgehog signaling in ventral telencephalic patterning. *Development*, *131*(20), 5031-5040.

Furuta, Y., Piston, D. W., & Hogan, B. L. M. (1997). Bone morphogenetic proteins (BMPs) as regulators of dorsal forebrain development. *Development*, *124*(11), 2203-2212. https://doi.org/10.1242/dev.124.11.2203

Gao, Q., Yuan, Y., Gan, H.-Z., & Peng, Q. (2015). Resveratrol inhibits the hedgehog signaling pathway and epithelial-mesenchymal transition and suppresses gastric cancer invasion and metastasis. *Oncology letters*, *9*(5), 2381-2387. https://doi.org/10.3892/ol.2015.2988

Gofflot, F., Gaoua, W., Bourguignon, L., Roux, C., & Picard, J. J. (2001). Expression of sonic hedgehog downstream genes is modified in rat embryos exposed in utero to a distal inhibitor of cholesterol biosynthesis. *Developmental Dynamics*, *220*(2), 99-111. https://doi.org/https://doi.org/10.1002/1097-0177(2000)9999:9999<::AID-DVDY1092>3.0.CO;2-G

Gonçalves, A. R. P., Paredes, X., Cristino, A. F., Santos, F. J. V., & Queirós, C. (2021). Ionic Liquids-A Review of Their Toxicity to Living Organisms. *Int J Mol Sci*, *22*(11). https://doi.org/10.3390/ijms22115612

Grabovsky, Y., & Tallarida, R. J. (2004). Isobolographic analysis for combinations of a full and partial agonist: curved isoboles. *J Pharmacol Exp Ther*, *310*(3), 981-986. https://doi.org/10.1124/jpet.104.067264

Grinblat, Y., & Lipinski, R. J. (2019). A forebrain undivided: Unleashing model organisms to solve the mysteries of holoprosencephaly. *Developmental Dynamics*, *248*(8), 626-633. https://doi.org/10.1002/dvdy.41

Hackshaw, A., Rodeck, C., & Boniface, S. (2011). Maternal smoking in pregnancy and birth defects: a systematic review based on 173 687 malformed cases and 11.7 million controls. *Human reproduction update*, *17*(5), 589-604. https://doi.org/10.1093/humupd/dmr022

Hammond, P., & Suttie, M. (2012). Large-scale objective phenotyping of 3D facial morphology. *Human mutation*. https://doi.org/10.1002/humu.22054

Heyne, G. W., Everson, J. L., Ansen-Wilson, L. J., Melberg, C. G., Fink, D. M., Parins, K. F.,...Lipinski, R. J. (2016). Gli2 gene-environment interactions contribute to the etiological complexity of holoprosencephaly: evidence from a mouse model. *Dis Model Mech*, *9*(11), 1307-1315. https://doi.org/10.1242/dmm.026328

Heyne, G. W., Melberg, C. G., Doroodchi, P., Parins, K. F., Kietzman, H. W., Everson, J. L.,...Lipinski, R. J. (2015). Definition of critical periods for Hedgehog pathway antagonist-induced holoprosencephaly, cleft lip, and cleft palate. *PLoS One*, *10*(3), e0120517. https://doi.org/10.1371/journal.pone.0120517

Heyne, G. W., Plisch, E. H., Melberg, C. G., Sandgren, E. P., Peter, J. A., & Lipinski, R. J. (2015). A Simple and Reliable Method for Early Pregnancy Detection in Inbred Mice. *J Am Assoc Lab Anim Sci*, *54*(4), 368-371. https://doi.org/n/a

Hong, M., Christ, A., Christa, A., Willnow, T. E., & Krauss, R. S. (2020). Mutation and fetal alcohol converge on Nodal signaling in a mouse model of holoprosencephaly. *Elife*, *9*. https://doi.org/10.7554/eLife.60351

Hong, M., & Krauss, R. S. (2012). Cdon mutation and fetal ethanol exposure synergize to produce midline signaling defects and holoprosencephaly spectrum disorders in mice. *PLoS Genet*, *8*(10), e1002999. https://doi.org/10.1371/journal.pgen.1002999

Hong, M., & Krauss, R. S. (2018). Modeling the complex etiology of holoprosencephaly in mice. *Am J Med Genet C Semin Med Genet*, *178*(2), 140-150. https://doi.org/10.1002/ajmg.c.31611

Hosoya, T., Arai, M. A., Koyano, T., Kowithayakorn, T., & Ishibashi, M. (2008). Naturally Occurring Small-Molecule Inhibitors of Hedgehog/GLI-Mediated Transcription. *ChemBioChem*, *9*(7), 1082-1092. https://doi.org/10.1002/cbic.200700511

Hoyme, H. E., Hoyme, D. B., Elliott, A. J., Blankenship, J., Kalberg, W. O., Buckley, D.,...May, P. A. (2015). A South African mixed race lip/philtrum guide for diagnosis of fetal alcohol spectrum disorders. *Am J Med Genet A*, *167a*(4), 752-755. https://doi.org/10.1002/ajmg.a.37023

Hoyme, H. E., Kalberg, W. O., Elliott, A. J., Blankenship, J., Buckley, D., Marais, A. S.,...May, P. A. (2016). Updated Clinical Guidelines for Diagnosing Fetal Alcohol Spectrum Disorders. *Pediatrics*, *138*(2). https://doi.org/10.1542/peds.2015-4256

Hoyme, H. E., May, P. A., Kalberg, W. O., Kodituwakku, P., Gossage, J. P., Trujillo, P. M.,...Robinson, L. K. (2005). A practical clinical approach to diagnosis of fetal alcohol spectrum disorders: clarification of the 1996 institute of medicine criteria [Research Support, Non-U.S. Gov't Research Support, U.S. Gov't, P.H.S.]. *Pediatrics*, *115*(1), 39-47. https://doi.org/10.1542/peds.2004-0259

Hu, D., Young, N. M., Li, X., Xu, Y., Hallgrímsson, B., & Marcucio, R. S. (2015). A dynamic Shh expression pattern, regulated by SHH and BMP signaling, coordinates fusion of

primordia in the amniote face. *Development*, *142*(3), 567-574. https://doi.org/10.1242/dev.114835

Huang, R.-Y., Pei, L., Liu, Q., Chen, S., Dou, H., Shu, G.,...Fu, H. (2019). Isobologram Analysis: A Comprehensive Review of Methodology and Current Research. *Frontiers in pharmacology*, *10*, 1222-1222. https://doi.org/10.3389/fphar.2019.01222

Hughes, J. J., Alkhunaizi, E., Kruszka, P., Pyle, L. C., Grange, D. K., Berger, S. I.,...Chitayat, D. (2020). Loss-of-Function Variants in PPP1R12A: From Isolated Sex Reversal to Holoprosencephaly Spectrum and Urogenital Malformations. *The American Journal of Human Genetics*, *106*(1), 121-128. https://doi.org/10.1016/j.ajhg.2019.12.004

Incardona, J. P., Gaffield, W., Kapur, R. P., & Roelink, H. (1998). The teratogenic Veratrum alkaloid cyclopamine inhibits sonic hedgehog signal transduction. *Development*, *125*(18), 3553.

Innes, A. M., & Lynch, D. C. (2021). Fifty years of recognizable patterns of human malformation: Insights and opportunities. *Am J Med Genet A*, *185*(9), 2653-2669. https://doi.org/10.1002/ajmg.a.62240

Jeong, J., Mao, J., Tenzen, T., Kottmann, A. H., & McMahon, A. P. (2004). Hedgehog signaling in the neural crest cells regulates the patterning and growth of facial primordia. *Genes Dev*, *18*(8), 937-951. https://doi.org/10.1101/gad.1190304 18/8/937 [pii]

Jeong, J., & McMahon, A. P. (2002). Cholesterol modification of Hedgehog family proteins. *J Clin Invest*, *110*(5), 591-596. https://doi.org/10.1172/JCI16506

Jiang, R., Bush, J. O., & Lidral, A. C. (2006). Development of the upper lip: morphogenetic and molecular mechanisms. *Dev Dyn*, *235*(5), 1152-1166. https://doi.org/10.1002/dvdy.20646

Johnson, B. P., Vitek, R. A., Morgan, M. M., Fink, D. M., Beames, T. G., Geiger, P. G.,...Lipinski, R. J. (2021). A Microphysiological Approach to Evaluate Effectors of Intercellular Hedgehog Signaling in Development. *Frontiers in cell and developmental biology*, *9*, 621442-621442. https://doi.org/10.3389/fcell.2021.621442

Jones, K. L., & Smith, D. W. (1975). The fetal alcohol syndrome. *Teratology*, *12*(1), 1-10. https://doi.org/https://doi.org/10.1002/tera.1420120102

Jones, K. L., Smith, D. W., Ulleland, C. N., & Streissguth, P. (1973). Pattern of malformation in offspring of chronic alcoholic mothers. *Lancet*, *1*(7815), 1267-1271. https://doi.org/10.1016/s0140-6736(73)91291-9

Judson, R., Richard, A., Dix, D. J., Houck, K., Martin, M., Kavlock, R.,...Smith, E. (2009). The toxicity data landscape for environmental chemicals. *Environ Health Perspect*, *117*(5), 685-695. https://doi.org/10.1289/ehp.0800168

Katsarou, A. M., Moshé, S. L., & Galanopoulou, A. S. (2017). INTERNEURONOPATHIES AND THEIR ROLE IN EARLY LIFE EPILEPSIES AND NEURODEVELOPMENTAL DISORDERS. *Epilepsia Open*, *2*(3), 284-306. https://doi.org/10.1002/epi4.12062

Keeler, R. F. (1978). Cyclopamine and related steroidal alkaloid teratogens: their occurrence, structural relationship, and biologic effects. *Lipids*, *13*(10), 708-715. https://doi.org/10.1007/BF02533750

Khaliullina, H., Bilgin, M., Sampaio, J. L., Shevchenko, A., & Eaton, S. (2015). Endocannabinoids are conserved inhibitors of the Hedgehog pathway. *Proceedings of the National Academy of Sciences*, *112*(11), 3415. https://doi.org/10.1073/pnas.1416463112

Khoury, M. J., Adams, M. J., Jr., & Flanders, W. D. (1988). An epidemiologic approach to ecogenetics. *American journal of human genetics*, *42*(1), 89-95.

Kietzman, H. W., Everson, J. L., Sulik, K. K., & Lipinski, R. J. (2014). The teratogenic effects of prenatal ethanol exposure are exacerbated by Sonic Hedgehog or GLI2 haploinsufficiency in the mouse. *PLoS One*, *9*(2), e89448. https://doi.org/10.1371/journal.pone.0089448

Kim, D. J., Seok, S. H., Baek, M. W., Lee, H. Y., Na, Y. R., Park, S. H.,...Park, J. H. (2009). Developmental toxicity and brain aromatase induction by high genistein concentrations in zebrafish embryos. *Toxicol Mech Methods*, *19*(3), 251-256. https://doi.org/10.1080/15376510802563330

Kimmel, C. B., Ballard, W. W., Kimmel, S. R., Ullmann, B., & Schilling, T. F. (1995). Stages of embryonic development of the zebrafish. *Dev Dyn*, *203*(3), 253-310. https://doi.org/10.1002/aja.1002030302

Knudsen, T. B., Kavlock, R. J., Daston, G. P., Stedman, D., Hixon, M., & Kim, J. H. (2011). Developmental toxicity testing for safety assessment: new approaches and technologies. *Birth Defects Research Part B: Developmental and Reproductive Toxicology*, *92*(5), 413-420. https://doi.org/https://doi.org/10.1002/bdrb.20315

Kortenkamp, A., Faust, M., Scholze, M., & Backhaus, T. (2007). Low-Level Exposure to Multiple Chemicals: Reason for Human Health Concerns? *Environmental Health Perspectives*, *115*(Suppl 1), 106-114. https://doi.org/10.1289/ehp.9358

Kraml, M., Bagli, J. F., & Dvornik, D. (1964). Inhibition of the conversion of 7-dehydrocholesterol to cholesterol by AY-9944. *Biochemical and Biophysical Research Communications*, *15*(5), 455-457. https://doi.org/https://doi.org/10.1016/0006-291X(64)90485-1

Kratz, S. R. A., Höll, G., Schuller, P., Ertl, P., & Rothbauer, M. (2019). Latest Trends in Biosensing for Microphysiological Organs-on-a-Chip and Body-on-a-Chip Systems. *Biosensors*, *9*(3), 110. https://doi.org/10.3390/bios9030110

Krauss, R. S., & Hong, M. (2016). Gene–Environment Interactions and the Etiology of Birth Defects. *Current Topics in Developmental Biology*, *116*, 569-580. https://doi.org/10.1016/bs.ctdb.2015.12.010

Krewski, D., Acosta, D., Jr., Andersen, M., Anderson, H., Bailar, J. C., 3rd, Boekelheide, K.,...Zeise, L. (2010). Toxicity testing in the 21st century: a vision and a strategy. *J*

Toxicol Environ Health B Crit Rev, *13*(2-4), 51-138. https://doi.org/10.1080/10937404.2010.483176

Kruszka, P., Berger, S. I., Casa, V., Dekker, M. R., Gaesser, J., Weiss, K.,...Muenke, M. (2019). Cohesin complex-associated holoprosencephaly. *Brain : a journal of neurology*, *142*(9), 2631-2643. https://doi.org/10.1093/brain/awz210

Kruszka, P., Berger, S. I., Weiss, K., Everson, J. L., Martinez, A. F., Hong, S.,...Muenke, M. (2019). A CCR4-NOT Transcription Complex, Subunit 1, CNOT1, Variant Associated with Holoprosencephaly. *American journal of human genetics*, *104*(5), 990-993. https://doi.org/10.1016/j.ajhg.2019.03.017

Kurosaka, H. (2015). The Roles of Hedgehog Signaling in Upper Lip Formation. *Biomed Res Int*, *2015*, 901041. https://doi.org/10.1155/2015/901041

Lan, A., Kalimian, M., Amram, B., & Kofman, O. (2017). Prenatal chlorpyrifos leads to autism-like deficits in C57Bl6/J mice. *Environmental Health*, *16*(1), 43. https://doi.org/10.1186/s12940-017-0251-3

Lan, Y., & Jiang, R. (2009). Sonic hedgehog signaling regulates reciprocal epithelial-mesenchymal interactions controlling palatal outgrowth. *Development*, *136*(8), 1387-1396. https://doi.org/136/8/1387 [pii] 10.1242/dev.028167

Larsen, A. R., Bai, R.-Y., Chung, J. H., Borodovsky, A., Rudin, C. M., Riggins, G. J., & Bunz, F. (2015). Repurposing the Antihelmintic Mebendazole as a Hedgehog Inhibitor. *Molecular Cancer Therapeutics*, *14*(1), 3-13. https://doi.org/10.1158/1535-7163.MCT-14-0755-T

Lauth, M., Bergström, A., Shimokawa, T., & Toftgård, R. (2007). Inhibition of GLI-mediated transcription and tumor cell growth by small-molecule antagonists. *Proc Natl Acad Sci U S A*, *104*(20), 8455-8460. https://doi.org/10.1073/pnas.0609699104

Leslie, E. J., & Marazita, M. L. (2013). Genetics of cleft lip and cleft palate. *American journal of medical genetics. Part C, Seminars in medical genetics*, *163C*(4), 246-258. https://doi.org/10.1002/ajmg.c.31381

Lian, N., Jiang, Y., Zhang, F., Jin, H., Lu, C., Wu, X.,...Zheng, S. (2015). Curcumin regulates cell fate and metabolism by inhibiting hedgehog signaling in hepatic stellate cells. *Laboratory Investigation*, *95*(7), 790-803. https://doi.org/https://doi.org/10.1038/labinvest.2015.59

Lipinski, R. J., Bijlsma, M. F., Gipp, J. J., Podhaizer, D. J., & Bushman, W. (2008). Establishment and characterization of immortalized Gli-null mouse embryonic fibroblast cell lines. *BMC Cell Biol*, *9*, 49. https://doi.org/1471-2121-9-49 [pii] 10.1186/1471-2121-9-49

Lipinski, R. J., & Bushman, W. (2010). Identification of Hedgehog signaling inhibitors with relevant human exposure by small molecule screening. *Toxicol In Vitro*, *24*(5), 1404-1409. https://doi.org/S0887-2333(10)00094-9 [pii] 10.1016/j.tiv.2010.04.011

Lipinski, R. J., Dengler, E., Kiehn, M., Peterson, R. E., & Bushman, W. (2007). Identification and characterization of several dietary alkaloids as weak inhibitors of hedgehog signaling. *Toxicol Sci*, *100*(2), 456-463. https://doi.org/10.1093/toxsci/kfm222

Lipinski, R. J., Hutson, P. R., Hannam, P. W., Nydza, R. J., Washington, I. M., Moore, R. W.,...Bushman, W. (2008). Dose-and route-dependent teratogenicity, toxicity, and pharmacokinetic profiles of the hedgehog signaling antagonist cyclopamine in the mouse. *Toxicological sciences*, *104*(1), 189-197.

Lipinski, R. J., & Krauss, R. S. (2023). Gene-environment interactions in birth defect etiology: Challenges and opportunities. *Curr Top Dev Biol*, *152*, 1-30. https://doi.org/10.1016/bs.ctdb.2022.10.001

Lo, H. F., Hong, M., Szutorisz, H., Hurd, Y. L., & Krauss, R. S. (2021). Δ9-Tetrahydrocannabinol inhibits Hedgehog-dependent patterning during development. *Development*, *148*(19). https://doi.org/10.1242/dev.199585

Lovely, C., Rampersad, M., Fernandes, Y., & Eberhart, J. (2017). Gene-environment interactions in development and disease. *Wiley Interdiscip Rev Dev Biol*, *6*(1). https://doi.org/10.1002/wdev.247

Luchetti, G., Sircar, R., Kong, J. H., Nachtergaele, S., Sagner, A., Byrne, E. F.,...Rohatgi, R. (2016). Cholesterol activates the G-protein coupled receptor Smoothened to promote Hedgehog signaling. *Elife*, *5*. https://doi.org/10.7554/eLife.20304

Lyall, K., Croen, L., Daniels, J., Fallin, M. D., Ladd-Acosta, C., Lee, B. K.,...Newschaffer, C. (2017). The Changing Epidemiology of Autism Spectrum Disorders. *Annual Review of Public Health*, *38*(Volume 38, 2017), 81-102. https://doi.org/https://doi.org/10.1146/annurev-publhealth-031816-044318

Machold, R., Hayashi, S., Rutlin, M., Muzumdar, M. D., Nery, S., Corbin, J. G.,...Fishell, G. (2003). Sonic Hedgehog Is Required for Progenitor Cell Maintenance in Telencephalic Stem Cell Niches. *Neuron*, *39*(6), 937-950. https://doi.org/https://doi.org/10.1016/S0896-6273(03)00561-0

Marazita, M. L. (2023). Gene×environment associations in orofacial clefting. *Curr Top Dev Biol*, *152*, 169-192. https://doi.org/10.1016/bs.ctdb.2022.10.006

Martini, D., Pucci, C., Gabellini, C., Pellegrino, M., & Andreazzoli, M. (2020). Exposure to the natural alkaloid Berberine affects cardiovascular system morphogenesis and functionality during zebrafish development. *Sci Rep*, *10*(1), 17358. https://doi.org/10.1038/s41598-020-73661-5

Mastronardi, F. G., daCruz, L. A. G., Wang, H., Boggs, J., & Moscarello, M. A. (2003). The amount of sonic hedgehog in multiple sclerosis white matter is decreased and cleavage to the signaling peptide is deficient. *Multiple Sclerosis Journal*, *9*(4), 362-371. https://doi.org/10.1191/1352458503ms924oa

Matsunaga, E., & Shiota, K. (1977). Holoprosencephaly in human embryos: epidemiologic studies of 150 cases. *Teratology*, *16*(3), 261-272. https://doi.org/10.1002/tera.1420160304

Mayer, B. F. B., Stagno, M. J., Fuchs, J., Warmann, S. W., & Schmid, E. V. I. (2023). Epigallocatechin Gallate Inhibits Cell Growth and Hedgehog Signalling in Human Rhabdomyosarcoma Cell Lines. *Anticancer Research*, *43*(3), 1025. https://doi.org/10.21873/anticanres.16247

Małkowska, A., Makarowa, K., Zawada, K., Grzelak, M., & Zmysłowska, A. (2024). Effect of curcumin on the embryotoxic effect of ethanol in a zebrafish model. *Toxicology in Vitro*, *101*, 105951. https://doi.org/https://doi.org/10.1016/j.tiv.2024.105951

McElyea, S. D., Starbuck, J. M., Tumbleson-Brink, D. M., Harrington, E., Blazek, J. D., Ghoneima, A.,...Roper, R. J. (2016). Influence of prenatal EGCG treatment and Dyrk1a dosage reduction on craniofacial features associated with Down syndrome. *Hum Mol Genet*, *25*(22), 4856-4869. https://doi.org/10.1093/hmg/ddw309

Mills, R. J., Parker, B. L., Quaife-Ryan, G. A., Voges, H. K., Needham, E. J., Bornot, A.,...Hudson, J. E. (2019). Drug Screening in Human PSC-Cardiac Organoids Identifies Pro-proliferative Compounds Acting via the Mevalonate Pathway. *Cell Stem Cell*, *24*(6), 895-907.e896. https://doi.org/https://doi.org/10.1016/j.stem.2019.03.009

Miyagawa, S., Matsumaru, D., Murashima, A., Omori, A., Satoh, Y., Haraguchi, R.,...Yamada, G. (2011). The role of sonic hedgehog-Gli2 pathway in the masculinization of external genitalia. *Endocrinology*, *152*(7), 2894-2903. https://doi.org/10.1210/en.2011-0263

Mo, R., Freer, A. M., Zinyk, D. L., Crackower, M. A., Michaud, J., Heng, H. H.,...Hui, C. (1997). Specific and redundant functions of Gli2 and Gli3 zinc finger genes in skeletal patterning and development. *Development*, *124*(1), 113-123.

Mo, W., Xu, X., Xu, L., Wang, F., Ke, A., Wang, X., & Guo, C. (2011). Resveratrol Inhibits Proliferation and Induces Apoptosis through the Hedgehog Signaling Pathway in Pancreatic Cancer Cell. *Pancreatology*, *11*(6), 601-609. https://doi.org/https://doi.org/10.1159/000333542

Moreau, J. L. M., Kesteven, S., Martin, E. M. M. A., Lau, K. S., Yam, M. X., O'Reilly, V. C.,...Dunwoodie, S. L. (2019). Gene-environment interaction impacts on heart development and embryo survival. *Development*, *146*(4). https://doi.org/10.1242/dev.172957

Neben, C. L., & Merrill, A. E. (2015). Signaling Pathways in Craniofacial Development: Insights from Rare Skeletal Disorders. *Curr Top Dev Biol*, *115*, 493-542. https://doi.org/10.1016/bs.ctdb.2015.09.005

Orioli, I. M., & Castilla, E. E. (2010). Epidemiology of holoprosencephaly: Prevalence and risk factors. *Am J Med Genet C Semin Med Genet*, *154C*(1), 13-21. https://doi.org/10.1002/ajmg.c.30233

Ornoy, A. (2009). Valproic acid in pregnancy: How much are we endangering the embryo and fetus? *Reproductive Toxicology*, *28*(1), 1-10. https://doi.org/https://doi.org/10.1016/j.reprotox.2009.02.014

Parnell, S. E., Holloway, H. E., Baker, L. K., Styner, M. A., & Sulik, K. K. (2014). Dysmorphogenic effects of first trimester-equivalent ethanol exposure in mice: a

magnetic resonance microscopy-based study. *Alcohol Clin Exp Res*, *38*(7), 2008-2014. https://doi.org/10.1111/acer.12464

Payne, J., Rajapakse, N., Wilkins, M., & Kortenkamp, A. (2000). Prediction and assessment of the effects of mixtures of four xenoestrogens. *Environmental Health Perspectives*, *108*(10), 983-987. https://doi.org/10.1289/ehp.00108983

Pepinsky, R. B., Zeng, C., Wen, D., Rayhorn, P., Baker, D. P., Williams, K. P.,...Galdes, A. (1998). Identification of a palmitic acid-modified form of human Sonic hedgehog. *J Biol Chem*, *273*(22), 14037-14045. https://doi.org/10.1074/jbc.273.22.14037

Petrova, E., Rios-Esteves, J., Ouerfelli, O., Glickman, J. F., & Resh, M. D. (2013). Inhibitors of Hedgehog acyltransferase block Sonic Hedgehog signaling. *Nat Chem Biol*, *9*(4), 247-249. https://doi.org/10.1038/nchembio.1184

Petryk, A., Graf, D., & Marcucio, R. (2015). Holoprosencephaly: signaling interactions between the brain and the face, the environment and the genes, and the phenotypic variability in animal models and humans. *Wiley Interdiscip Rev Dev Biol*, *4*(1), 17-32. https://doi.org/10.1002/wdev.161

Pietrobono, S., & Stecca, B. (2018). Targeting the Oncoprotein Smoothened by Small Molecules: Focus on Novel Acylguanidine Derivatives as Potent Smoothened Inhibitors. *Cells*, *7*(12). https://doi.org/10.3390/cells7120272

Richard, A. M., Huang, R., Waidyanatha, S., Shinn, P., Collins, B. J., Thillainadarajah, I.,...Tice, R. R. (2021). The Tox21 10K Compound Library: Collaborative Chemistry Advancing Toxicology. *Chemical Research in Toxicology*, *34*(2), 189-216. https://doi.org/10.1021/acs.chemrestox.0c00264

Richieri-Costa, A., & Ribeiro, L. A. (2010). Holoprosencephaly and holoprosencephaly-like phenotypes: Review of facial and molecular findings in patients from a craniofacial hospital in Brazil. *Am J Med Genet C Semin Med Genet*, *154C*(1), 149-157. https://doi.org/10.1002/ajmg.c.30247

Rimkus, T. K., Carpenter, R. L., Qasem, S., Chan, M., & Lo, H. W. (2016). Targeting the Sonic Hedgehog Signaling Pathway: Review of Smoothened and GLI Inhibitors. *Cancers (Basel)*, *8*(2). https://doi.org/10.3390/cancers8020022

Ritzefeld, M., Zhang, L., Xiao, Z., Andrei, S. A., Boyd, O., Masumoto, N.,...Tate, E. W. (2024). Design, Synthesis, and Evaluation of Inhibitors of Hedgehog Acyltransferase. *J Med Chem*, *67*(2), 1061-1078. https://doi.org/10.1021/acs.jmedchem.3c01363

Rivera-González, K. S., Beames, T. G., & Lipinski, R. J. (2021). Examining the developmental toxicity of piperonyl butoxide as a Sonic hedgehog pathway inhibitor. *Chemosphere*, *264*(Pt 1), 128414. https://doi.org/10.1016/j.chemosphere.2020.128414

Rivera-González, K. S., Reynolds, P. M., & Lipinski, R. J. (2024). Examination of piperonyl butoxide developmental toxicity as a Sonic hedgehog pathway inhibitor targeting limb and palate morphogenesis. *Reprod Toxicol*, *130*, 108716. https://doi.org/10.1016/j.reprotox.2024.108716

Robarge, K. D., Brunton, S. A., Castanedo, G. M., Cui, Y., Dina, M. S., Goldsmith, R.,...Xie, M. (2009). GDC-0449-a potent inhibitor of the hedgehog pathway. *Bioorg Med Chem Lett*, *19*(19), 5576-5581. https://doi.org/10.1016/j.bmcl.2009.08.049

Rodova, M., Fu, J., Watkins, D. N., Srivastava, R. K., & Shankar, S. (2012). Sonic hedgehog signaling inhibition provides opportunities for targeted therapy by sulforaphane in regulating pancreatic cancer stem cell self-renewal. *PloS one*, *7*(9), e46083-e46083. https://doi.org/10.1371/journal.pone.0046083

Roelink, H., Porter, J. A., Chiang, C., Tanabe, Y., Chang, D. T., Beachy, P. A., & Jessell, T. M. (1995). Floor plate and motor neuron induction by different concentrations of the amino-terminal cleavage product of sonic hedgehog autoproteolysis. *Cell*, *81*(3), 445-455. https://doi.org/https://doi.org/10.1016/0092-8674(95)90397-6

Roessler, E., Belloni, E., Gaudenz, K., Jay, P., Berta, P., Scherer, S. W.,...Muenke, M. (1996). Mutations in the human Sonic Hedgehog gene cause holoprosencephaly. *Nat Genet*, *14*(3), 357-360. https://doi.org/10.1038/ng1196-357

Roessler, E., Hu, P., & Muenke, M. (2018). Holoprosencephaly in the genomics era. *Am J Med Genet C Semin Med Genet*, *178*(2), 165-174. https://doi.org/10.1002/ajmg.c.31615

Roth, D. M., Bayona, F., Baddam, P., & Graf, D. (2021). Craniofacial Development: Neural Crest in Molecular Embryology. *Head Neck Pathol*, *15*(1), 1-15. https://doi.org/10.1007/s12105-021-01301-z

Roux, C., Wolf, C., Mulliez, N., Gaoua, W., Cormier, V., Chevy, F., & Citadelle, D. (2000). Role of cholesterol in embryonic development. *The American Journal of Clinical Nutrition*, *71*(5), 1270S-1279S. https://doi.org/https://doi.org/10.1093/ajcn/71.5.1270s

Rueda, N., Vidal, V., García-Cerro, S., Puente, A., Campa, V., Lantigua, S.,...Martínez-Cué, C. (2020). Prenatal, but not Postnatal, Curcumin Administration Rescues Neuromorphological and Cognitive Alterations in Ts65Dn Down Syndrome Mice. *J Nutr*, *150*(9), 2478-2489. https://doi.org/10.1093/jn/nxaa207

Shi, B., He, E., Chang, K., Xu, G., Meng, Q., Xu, H.,...Cui, H. (2024). Genistein prevents the production of hypospadias induced by Di-(2-ethylhexyl) phthalate through androgen signaling and antioxidant response in rats. *J Hazard Mater*, *466*, 133537. https://doi.org/10.1016/j.jhazmat.2024.133537

Shi, H., Enriquez, A., Rapadas, M., Martin, E. M. M. A., Wang, R., Moreau, J.,...Dunwoodie, S. L. (2017). NAD Deficiency, Congenital Malformations, and Niacin Supplementation. *New England Journal of Medicine*, *377*(6), 544-552. https://doi.org/10.1056/NEJMoa1616361

Sidik, A., Dixon, G., Buckley, D. M., Kirby, H. G., Sun, S., & Eberhart, J. K. (2021). Exposure to ethanol leads to midfacial hypoplasia in a zebrafish model of FASD via indirect interactions with the Shh pathway. *BMC Biol*, *19*(1), 134. https://doi.org/10.1186/s12915-021-01062-9

Silva, E., Rajapakse, N., & Kortenkamp, A. (2002). Something from "nothing"--eight weak estrogenic chemicals combined at concentrations below NOECs produce significant

mixture effects. *Environ Sci Technol*, *36*(8), 1751-1756. https://doi.org/10.1021/es0101227

Skardal, A., Aleman, J., Forsythe, S., Rajan, S., Murphy, S., Devarasetty, M.,...Atala, A. (2020). Drug compound screening in single and integrated multi-organoid body-on-a-chip systems. *Biofabrication*, *12*(2), 025017. https://doi.org/10.1088/1758-5090/ab6d36

Slusarz, A., Shenouda, N. S., Sakla, M. S., Drenkhahn, S. K., Narula, A. S., MacDonald, R. S.,...Lubahn, D. B. (2010). Common botanical compounds inhibit the hedgehog signaling pathway in prostate cancer. *Cancer Res*, *70*(8), 3382-3390. https://doi.org/70/8/3382 [pii] 10.1158/0008-5472.CAN-09-3012

Solomon, B. D., Bear, K. A., Wyllie, A., Keaton, A. A., Dubourg, C., David, V.,...Muenke, M. (2012). Genotypic and phenotypic analysis of 396 individuals with mutations in Sonic Hedgehog. *J Med Genet*, *49*(7), 473-479. https://doi.org/10.1136/jmedgenet-2012-101008

Sparrow, Duncan B., Chapman, G., Smith, Allanceson J., Mattar, Muhammad Z., Major, Joelene A., O'Reilly, Victoria C.,...Dunwoodie, Sally L. (2012). A Mechanism for Gene-Environment Interaction in the Etiology of Congenital Scoliosis. *Cell*, *149*(2), 295-306. https://doi.org/https://doi.org/10.1016/j.cell.2012.02.054

Stallings, E. B., Isenburg, J. L., Rutkowski, R. E., Kirby, R. S., Nembhard, W. N., Sandidge, T.,...for the National Birth Defects Prevention, N. (2024). National population-based estimates for major birth defects, 2016–2020. *Birth Defects Research*, *116*(1), e2301. https://doi.org/https://doi.org/10.1002/bdr2.2301

Stamataki, D., Ulloa, F., Tsoni, S. V., Mynett, A., & Briscoe, J. (2005). A gradient of Gli activity mediates graded Sonic Hedgehog signaling in the neural tube. *Genes & development*, *19*(5), 626-641. https://doi.org/10.1101/gad.325905

Sulik, K. K. (2005). Genesis of alcohol-induced craniofacial dysmorphism [Review]. *Experimental biology and medicine*, *230*(6), 366-375.

Sun, Q., Yang, H., Liu, M., Ren, S., Zhao, H., Ming, T.,...Xu, H. (2022). Berberine suppresses colorectal cancer by regulation of Hedgehog signaling pathway activity and gut microbiota. *Phytomedicine*, *103*, 154227. https://doi.org/https://doi.org/10.1016/j.phymed.2022.154227

Taipale, J., Chen, J. K., Cooper, M. K., Wang, B., Mann, R. K., Milenkovic, L.,...Beachy, P. A. (2000). Effects of oncogenic mutations in Smoothened and Patched can be reversed by cyclopamine. *Nature*, *406*(6799), 1005-1009. https://doi.org/10.1038/35023008

Takebe, T., Sekine, K., Enomura, M., Koike, H., Kimura, M., Ogaeri, T.,...Taniguchi, H. (2013). Vascularized and functional human liver from an iPSC-derived organ bud transplant. *Nature*, *499*(7459), 481-484. https://doi.org/10.1038/nature12271

Tallarida, R. J. (2016). Drug Combinations: Tests and Analysis with Isoboles. *Curr Protoc Pharmacol*, *72*, 9.19.11-19.19.19. https://doi.org/10.1002/0471141755.ph0919s72

Tanaka, T. (2003). Reproductive and neurobehavioural effects of piperonyl butoxide administered to mice in the diet. *Food Addit Contam*, *20*(3), 207-214. https://doi.org/10.1080/0265203021000050617

Tanaka, T., & Inomata, A. (2015). Effects of Maternal Exposure to Piperonyl Butoxide (PBO) on Behavioral Development in F1-Generation Mice. *Birth Defects Res B Dev Reprod Toxicol*, *104*(6), 227-237. https://doi.org/10.1002/bdrb.21163

Tanaka, T., & Inomata, A. (2016). Reproductive and neurobehavioral effects of maternal exposure to piperonyl butoxide (PBO) in F1-generation mice. *Birth Defects Res B Dev Reprod Toxicol*, *107*(4-5), 195-205. https://doi.org/10.1002/bdrb.21185

Tanaka, T., Takahashi, O., Oishi, S., & Ogata, A. (2009). Effects of piperonyl butoxide on spontaneous behavior in F1-generation mice. *Toxicol Ind Health*, *25*(7), 489-497. https://doi.org/10.1177/0748233709346756

Tang, J. Y., Xiao, T. Z., Oda, Y., Chang, K. S., Shpall, E., Wu, A.,...Epstein, E. H., Jr. (2011). Vitamin D3 Inhibits Hedgehog Signaling and Proliferation in Murine Basal Cell Carcinomas. *Cancer Prevention Research*, *4*(5), 744-751. https://doi.org/10.1158/1940-6207.CAPR-10-0285

Tang, S.-N., Fu, J., Nall, D., Rodova, M., Shankar, S., & Srivastava, R. K. (2012). Inhibition of sonic hedgehog pathway and pluripotency maintaining factors regulate human pancreatic cancer stem cell characteristics. *International journal of cancer*, *131*(1), 30-40. https://doi.org/10.1002/ijc.26323

Tekendo-Ngongang, C., Muenke, M., & Kruszka, P. (2020). Holoprosencephaly overview. In M. Adam, H. Ardinger, R. Pagon, S. Wallace, L. Bean, K. Stephens, & A. Amemiya (Eds.), *GeneReviews(R)*. University of Washington, Seattle.

Thitinarongwate, W., Mektrirat, R., Nimlamool, W., Khonsung, P., Pikulkaew, S., Okonogi, S., & Kunanusorn, P. (2021). Phytochemical and Safety Evaluations of Zingiber ottensii Valeton Essential Oil in Zebrafish Embryos and Rats. *Toxics*, *9*(5). https://doi.org/10.3390/toxics9050102

Tickle, C., & Towers, M. (2017). Sonic Hedgehog Signaling in Limb Development [10.3389/fcell.2017.00014]. *Frontiers in Cell and Developmental Biology*, *5*, 14.

Toufaily, M. H., Westgate, M. N., Lin, A. E., & Holmes, L. B. (2018). Causes of Congenital Malformations. *Birth Defects Res*, *110*(2), 87-91. https://doi.org/10.1002/bdr2.1105

Truong, L., Reif, D. M., St Mary, L., Geier, M. C., Truong, H. D., & Tanguay, R. L. (2014). Multidimensional in vivo hazard assessment using zebrafish. *Toxicological sciences : an official journal of the Society of Toxicology*, *137*(1), 212-233. https://doi.org/10.1093/toxsci/kft235

Truskey, G. A. (2018). Human Microphysiological Systems and Organoids as in Vitro Models for Toxicological Studies [Review]. *Frontiers in Public Health*, *6*(185). https://doi.org/10.3389/fpubh.2018.00185

Uggini, G. K., Patel, P. V., & Balakrishnan, S. (2012). Embryotoxic and teratogenic effects of pesticides in chick embryos: A comparative study using two commercial formulations. *Environmental Toxicology*, *27*(3), 166-174. https://doi.org/https://doi.org/10.1002/tox.20627

van der Zanden, L. F. M., Galesloot, T. E., Feitz, W. F. J., Brouwers, M. M., Shi, M., Knoers, N. V. A. M.,...van Rooij, I. A. L. M. (2012). Exploration of gene-environment interactions, maternal effects and parent of origin effects in the etiology of hypospadias. *The Journal of urology*, *188*(6), 2354-2360. https://doi.org/10.1016/j.juro.2012.08.033

Vargesson, N. (2015). Thalidomide-induced teratogenesis: history and mechanisms. *Birth Defects Res C Embryo Today*, *105*(2), 140-156. https://doi.org/10.1002/bdrc.21096

Voges, H. K., Mills, R. J., Elliott, D. A., Parton, R. G., Porrello, E. R., & Hudson, J. E. (2017). Development of a human cardiac organoid injury model reveals innate regenerative potential. *Development*, *144*(6), 1118. https://doi.org/10.1242/dev.143966

Wagner, G. C., Reuhl, K. R., Cheh, M., McRae, P., & Halladay, A. K. (2006). A New Neurobehavioral Model of Autism in Mice: Pre- and Postnatal Exposure to Sodium Valproate. *Journal of Autism and Developmental Disorders*, *36*(6), 779-793. https://doi.org/10.1007/s10803-006-0117-y

Wang, F., Huang, X., Sun, Y., Li, Z., Sun, R., Zhao, T.,...Liu, P. (2022). Sulforaphane regulates the proliferation of leukemia stem-like cells via Sonic Hedgehog signaling pathway. *European Journal of Pharmacology*, *919*, 174824. https://doi.org/https://doi.org/10.1016/j.ejphar.2022.174824

Wang, F., Lin, J., Jian, J., Wang, Y. H., Guo, N., & Li, Q. (2019). Protection role of resveratrol against alcohol-induced heart defect in zebrafish embryos. *Chin Med J (Engl)*, *132*(8), 990-993. https://doi.org/10.1097/cm9.0000000000000194

Wang, J., Lu, J., Mook, R., Zhang, M., Zhao, S., Barak, L.,...Chen, W. (2012). The insecticide synergist piperonyl butoxide inhibits Hedgehog signaling: assessing chemical risks. *Toxicological Sciences*, *128*(2), 517-523. https://doi.org/10.1093/toxsci/kfs165

Wang, J., Peng, Y., Liu, Y., Yang, J., Ding, N., & Tan, W. (2015). Berberine, a natural compound, suppresses Hedgehog signaling pathway activity and cancer growth. *BMC Cancer*, *15*, 595. https://doi.org/10.1186/s12885-015-1596-z

Wang, L.-C., & Almazan, G. (2016). Role of Sonic Hedgehog Signaling in Oligodendrocyte Differentiation. *Neurochemical Research*, *41*(12), 3289-3299. https://doi.org/10.1007/s11064-016-2061-3

Wang, Z., Walker, G. W., Muir, D. C. G., & Nagatani-Yoshida, K. (2020). Toward a Global Understanding of Chemical Pollution: A First Comprehensive Analysis of National and Regional Chemical Inventories. *Environ Sci Technol*, *54*(5), 2575-2584. https://doi.org/10.1021/acs.est.9b06379

Watkins, S. E., Meyer, R. E., Strauss, R. P., & Aylsworth, A. S. (2014). Classification, epidemiology, and genetics of orofacial clefts. *Clin Plast Surg*, *41*(2), 149-163. https://doi.org/10.1016/j.cps.2013.12.003

Westerfield, M. (1993). The Zebrafish Book: A Guide for the Laboratory Use of Zebrafish (*Brachydanio rerio*). In (5th ed. ed.). Eugene: Univ. of Oregon Press.

Wichterle, H., Turnbull, D. H., Nery, S., Fishell, G., & Alvarez-Buylla, A. (2001). In utero fate mapping reveals distinct migratory pathways and fates of neurons born in the mammalian basal forebrain. *Development*, *128*(19), 3759-3771.

Wild, C. P. (2005). Complementing the Genome with an "Exposome": The Outstanding Challenge of Environmental Exposure Measurement in Molecular Epidemiology. *Cancer Epidemiology Biomarkers & Prevention*, *14*(8), 1847. https://doi.org/10.1158/1055-9965.EPI-05-0456

Wild, C. P. (2011). Future research perspectives on environment and health: the requirement for a more expansive concept of translational cancer research. *Environmental health : a global access science source*, *10 Suppl 1*(Suppl 1), S15-S15. https://doi.org/10.1186/1476-069X-10-S1-S15

Wild, C. P. (2012). The exposome: from concept to utility. *International Journal of Epidemiology*, *41*(1), 24-32. https://doi.org/10.1093/ije/dyr236

Williams, A. J., Grulke, C. M., Edwards, J., McEachran, A. D., Mansouri, K., Baker, N. C.,...Richard, A. M. (2017). The CompTox Chemistry Dashboard: a community data resource for environmental chemistry. *J Cheminform*, *9*(1), 61. https://doi.org/10.1186/s13321-017-0247-6

Winkler, C. C., Yabut, O. R., Fregoso, S. P., Gomez, H. G., Dwyer, B. E., Pleasure, S. J., & Franco, S. J. (2018). The Dorsal Wave of Neocortical Oligodendrogenesis Begins Embryonically and Requires Multiple Sources of Sonic Hedgehog. *The Journal of Neuroscience*, *38*(23), 5237. https://doi.org/10.1523/JNEUROSCI.3392-17.2018

Wobbrock, J. O., Findlater, L., Gergle, D., & Higgins, J. J. (2011). *The aligned rank transform for nonparametric factorial analyses using only anova procedures* Proceedings of the SIGCHI Conference on Human Factors in Computing Systems, Vancouver, BC, Canada. https://doi.org/10.1145/1978942.1978963

Wolf, C. J., Belair, D. G., Becker, C. M., Das, K. P., Schmid, J. E., & Abbott, B. D. (2018). Development of an organotypic stem cell model for the study of human embryonic palatal fusion. *Birth defects research*, *110*(17), 1322-1334. https://doi.org/10.1002/bdr2.1394

Wong, H., Alicke, B., West, K. A., Pacheco, P., La, H., Januario, T.,...Gould, S. E. (2011). Pharmacokinetic-pharmacodynamic analysis of vismodegib in preclinical models of mutational and ligand-dependent Hedgehog pathway activation. *Clin Cancer Res*, *17*(14), 4682-4692. https://doi.org/10.1158/1078-0432.CCR-11-0975

Wong, H., Chen, J. Z., Chou, B., Halladay, J. S., Kenny, J. R., La, H.,...Khojasteh, S. C. (2009). Preclinical assessment of the absorption, distribution, metabolism and excretion of GDC-0449 (2-chloro-N-(4-chloro-3-(pyridin-2-yl)phenyl)-4-(methylsulfonyl)benzamide), an orally bioavailable systemic Hedgehog signalling pathway inhibitor. *Xenobiotica*, *39*(11), 850-861. https://doi.org/10.3109/00498250903180289

Wu, J. Y., Lin, C. Y., Lin, T. W., Ken, C. F., & Wen, Y. D. (2007). Curcumin affects development of zebrafish embryo. *Biol Pharm Bull*, *30*(7), 1336-1339. https://doi.org/10.1248/bpb.30.1336

Wu, Z., Chen, S. Y., & Zheng, L. (2024). Sulforaphane Attenuates Ethanol-Induced Teratogenesis and Dysangiogenesis in Zebrafish Embryos. *Int J Mol Sci*, *25*(21). https://doi.org/10.3390/ijms252111529

Xu, J., Iyyanar, P. P. R., Lan, Y., & Jiang, R. (2023). Sonic hedgehog signaling in craniofacial development. *Differentiation*, *133*, 60-76. https://doi.org/10.1016/j.diff.2023.07.002

Xu, Q., Cobos, I., De La Cruz, E., Rubenstein, J. L., & Anderson, S. A. (2004). Origins of cortical interneuron subtypes. *J Neurosci*, *24*(11), 2612-2622. https://doi.org/10.1523/jneurosci.5667-03.2004

Yi, Y., Park, J., Lim, J., Lee, C. J., & Lee, S.-H. (2015). Central Nervous System and its Disease Models on a Chip. *Trends in Biotechnology*, *33*(12), 762-776. https://doi.org/10.1016/j.tibtech.2015.09.007

Yoshida, S., & Yoshida, K. (2025). Regulatory mechanisms governing GLI proteins in hedgehog signaling. *Anat Sci Int*, *100*(2), 143-154. https://doi.org/10.1007/s12565-024-00814-1

Zhang, L., Li, L., Jiao, M., Wu, D., Wu, K., Li, X.,...He, D. (2012). Genistein inhibits the stemness properties of prostate cancer cells through targeting Hedgehog-Gli1 pathway. *Cancer Lett*, *323*(1), 48-57. https://doi.org/10.1016/j.canlet.2012.03.037

Zhou, Y., Sinnathamby, V., Yu, Y., Sikora, L., Johnson, C. Y., Mossey, P., & Little, J. (2020). Folate intake, markers of folate status and oral clefts: An updated set of systematic reviews and meta-analyses. *Birth Defects Res*, *112*(19), 1699-1719. https://doi.org/10.1002/bdr2.1827

Zou, P., Xing, L., Tang, Q., liu, R., & Hao, W. (2012). Comparative evaluation of the teratogenicity of genistein and genistin using rat whole embryo culture and limbud micromass culture methods. *Food and Chemical Toxicology*, *50*(8), 2831-2836. https://doi.org/https://doi.org/10.1016/j.fct.2012.05.009